12-2010

Radiation-Curable Adhesives for Wood Composites

Timothy H. Starr
University of Tennessee - Knoxville, tstarr@utk.edu

To the Graduate Council:

I am submitting herewith a thesis written by Timothy H. Starr entitled "Radiation-Curable Adhesives for Wood Composites." I have examined the final electronic copy of this thesis for form and content and recommend that it be accepted in partial fulfillment of the requirements for the degree of Master of Science, with a major in Chemical Engineering.

Tim G. Rials, Major Professor

We have read this thesis and recommend its acceptance:

David P. Harper, Paul D. Frymier

Accepted for the Council:
Carolyn R. Hodges

Vice Provost and Dean of the Graduate School

(Original signatures are on file with official student records.)

To the Graduate Council:

I am submitting herewith a thesis written by Timothy H. Starr entitled "Radiation-Curable Adhesives for Wood Composites." I have examined the final electronic copy of this thesis for form and content and recommend that it be accepted in partial fulfillment of the requirements for the degree of Master of Science, with a major in Chemical Engineering.

Timothy G. Rials

Major Professor

We have read this thesis and recommend its acceptance:

David P. Harper

Paul D. Frymier

Accepted for the Council:

Carolyn R. Hodges

Vice Provost and Dean of the Graduate School

(Original signatures are on file with official student records)

Radiation-Curable Adhesives for Wood Composites

A Thesis Presented for the

Masters of Science

Degree

The University of Tennessee, Knoxville

Timothy H. Starr

December 2010

DEDICATION

I would like to dedicate this work to my family – my wonderful wife, April, and our delightful daughter, Leila. I can't thank them enough for their patience and support while I finished my thesis, and I appreciate them putting up with all of the times that I had to come home from work only to lock myself away in the back room to work on my research. The completion of this paper I enthusiastically dedicate to making up for all of the family time that was forfeited while I was in school.

ACKNOWLEDGEMENTS

I would like to thank Dr. Rials for the opportunities that I was afforded to work and conduct research in the Forest Products Center; it truly was a privilege to work in such a resourceful facility. I would like to thank Bill Griffith at ORNL for his assistance in providing access to previous research, and for helping get the sample shipments to Sterigenics set up. Also, I would like to thank George Dorsey for the previous work he did in screening potential resins for radiation curable composites. I would like to thank Chris Helton for his assistance in the wood shop/lab where I did much of my sample preparation. I would like to thank Nikki Labbé for sharing her expertise in the area of multivariate analysis, and her advice regarding quality of work. I would like to thank Dr. Frymier for stepping in at the last moment to make up for the departures of Dr. Collier (now with Florida State University) and Dr. Petrovan (now retired). My biggest thanks, by far, are owed to Dr. Harper who dedicated countless hours to helping me with my research and providing much-needed guidance through the whole process of graduate school. He kept me on track and helped me stay focused, was very patient with me when I would get bogged down, and was very encouraging when I felt overwhelmed. I could not have done this without him.

ABSTRACT

Wood composites are widely used in construction applications because of their superior dimensional and structural attributes over raw wood products. However, current wood composite manufacturing practices, which rely on thermal-curing of adhesives, are expensive, energy intensive, time consuming and are prone to manufacturing defects. Use of radiation curable adhesives (RCAs) could potentially answer all of these issues.

Specifically, use of electron-beam (e-beam) radiation has been increasing in areas of research and industry where rapid, low-temperature polymerization is required and low energy consumption is desired. For e-beams to be used in wood composites, however, it must be determined whether or not the wood is structurally impacted by irradiation, and to what extent. Maple beams irradiated with a range of e-beam dosages were studied in three-point bend tests to assess the changes in bulk properties of the wood, and were further studied with infrared spectroscopy to identify chemical changes resulting from the radiation treatments. Also, dynamic mechanical analysis (DMA) was performed on maple veneers treated with the same doses of radiation to characterize changes in the viscoelastic properties.

Furthermore, while RCAs and their curing have been studied, it is important to understand if the presence of wood will impede the polymerization of these adhesives, and to what extent. Maple veneers impregnated with one of two resins were cured with the same e-beam dosages and investigated by means of DMA and FTIR spectroscopy. Swelling tests were conducted to detect interaction between the resins and the wood, which would indicate good interfacial bonding in the composite matrix.

Notable loss of strength was observed in the irradiated wood, especially at 180kGy. Monitoring the glass transition temperature (T_g) and activation energy (E_a) derived from DMA revealed that the most destructive trends in the wood began around 80kGy. Cure of resins in the composites was hindered by the presence of the wood, but both resins did eventually reach complete cure at

doses higher than what the neat resins required. Interaction between the resins and the wood was evident. In the end, results indicate that there is a range of radiation dosages in which the resin in a wood composite can be cured without destroying the structural integrity of the wood.

TABLE OF CONTENTS

LIST OF FIGURES

CHAPTER 1: INTRODUCTION

CHAPTER 1: INTRODUCTION

About half of the wood used today in structural applications is some form of glued-wood composite. These engineered composites have significant benefits over natural wood, including improved strength, toughness, resistance to moisture and the ability to produce them in shapes and dimensions that are simply not possible to obtain directly from cut lumber. However, the production of engineered wood products has several drawbacks, most of which result from the required process heat.

Most wood composites are made with thermally cured resins that require substantial amounts of energy to provide elevated temperatures for extended periods of time in order to obtain complete cure. Additionally, before the resin is even applied, heat is used to dry the parent wood in order to lower its moisture content, which must be then monitored and controlled carefully during the rest of the process (Griffith et al. 2006). Low moisture content could result in poor resin bonding, while high moisture content could lead to excessive steam pressure within the product that results in internal defects (Harper et al. n.d.). Either way, if the proper moisture content is not carefully maintained, damaged or substandard or otherwise unusable products result. This ultimately wastes time, money and resources. High process temperature also leads to emission of volatiles that can be hazardous and must be properly contained and controlled (Singh 2001).

Fortunately, the last several years have seen significant progress in the development of technology which would address all of these issues. Electron beam (e-beam) curable resin systems will provide alternatives to the currently used thermal-cured systems that can be manufactured faster, require drastically less energy because of lower temperature requirements, have lower volatiles emissions, and are not dependent on specific manufacturing conditions like moisture content (Stern 2000). The US wood-based paneling industry is expected to outgrow its current production capacity for thermosetting resin composites in the near future (White 1995),

which could give this new technology quite an opportunity for growth as new production facilities will make way for its implementation.

The goal of this research is to assist in the investigation of the feasibility of e-beam radiation technology as an economical, environmental, and efficient alternative to traditional thermal-cured resin composite systems. This work will look into the effect that electron beam radiation has on wood and wood components that are used as fillers or substrates for composite materials, study the cure of radiation-curable resins in the presence of wood, and investigate molecular interactions between these adhesives and wood that occur at the bond interface.

Electron Beam Technology

E-beam machines basically consist of an electron accelerator which generates fast electrons in the energy range of keV or MeV and at speeds approaching the speed of light, a conveyance system to bring the work pieces to the electron gun, and shielding to protect operators from the radiation and harmful x-rays that can be produced from electrons striking materials such as steel. The electron accelerator is much like what is found in tube-type televisions or computer monitors, only hundreds of thousands or millions of times more powerful. The electron beam is guided in the same way as it is in television or monitor applications, and is made to scan perpendicular to the direction which the conveyor belt brings the fabricated parts to the electron gun. Radiation doses are given in units called Grays where

$$1\text{Gy} = 1\text{J/kg} = 6.24\text{x}10^{15}\ \text{eV/g}.$$

Typically doses are of such magnitude that they are related in thousands of Grays, or kilograys (kGy).

E-beam Technology in Industry

High-energy electron beam technology has recently seen an increase in use in a large variety of industries and applications, providing many benefits and improvements over older methods wherever it is used. In the electronics industry, e-beam is used for crosslinking wire and cable insulation, producing heat shrinkable tubing, and making polymer devices such as resettable fuses for automotive and portable devices (Singh & Silverman 1992). In the automotive industry, e-beam is used to bond composites to metal substrates without the delamination that can happen during the cooling cycle of thermal-cure processes because of the differing thermal expansions of the bonded pieces (Goodman & Palmese 2001). In the aerospace industry, e-beam technology is used to replace thermally cured adhesives used to bond large, integrated structures in fewer steps and at lower cost than that of processes using an autoclave (Goodman & Palmese 2001). French aerospace and defense manufacturer, Aerospatiale, reported a reduced process time for the curing of rocket motors from about one week to less than eight hours, and with lower residual stresses in the part (Beziers et al. 1990). In the viscose industry, e-beam has been found to be a precise, reproducible substitute for the chemical aging step in the conventional viscose process, leading to superior process control and increased throughput, and saving a manufacturer several million dollars per year in chemical costs alone (Stepanik et al. 1998).

Other applications of electron beam radiation include the sterilization of medical products, strengthening of supermarket plastic bags, crosslinking of rubber in tires, and sterilization or pasteurization of foods and spices (Goodman & Palmese 2001; Scharf 1989; Wilson & Wilson 2001). Significant energy savings were found in many applications, including one example that showed that radiation-induced vulcanization of rubber would have an energy requirement of only 80J/g, while typical thermal vulcanization at 150^{o}C requires 281J/g (Stern 2000). Energy savings, money savings, a reduction of ruined and unusable products and higher throughput are all benefits that e-beam technology can provide for the wood composite industry.

Application and Benefits of E-beam Technology in the Wood Composite Industry

The advantages that electron beam technology could bring to the wood composite industry are many and well documented. Most benefits result from the lower process temperature required for e-beam curing. Curing at ambient or only slightly elevated temperatures significantly reduces energy requirements (Mehnert 1995; Lopata et al. 1999). In one study (Singh 2001), the energy use required for e-beam curing was estimated to be about a factor of five lower than that of thermal curing, and another reported that electron beam curing could save as much as 65 trillion Btu/yr in the wood composite industry (Griffith et al. 2006). These tremendous energy savings translate into reduction of process costs. In an aerospace application study of e-beam curable resins conducted by the Oak Ridge National Labs Y-12 facility and Lockheed Martin, they reported a reduction in production energy costs of 25-60% (Janke et al. 1998).

Lower temperature processing means that expensive high-temperature tooling is no longer required, and leads to money savings on peripheral items (Janke et al. 1998; Lopata et al. 1999; Mehnert 1995). Lower temperature curing also reduces thermal stresses in final products that result from the thermal expansion and contraction within the product itself during heating and cooling cycles (Goodman & Palmese 2001), or internal stresses that are produced when the tooling dimensions change to a different extent than the dimensions of the composite product during those same thermal cycles (Singh 2001; Mehnert 1995). Radiation-cured composites also have drastically lower volatile emissions than thermally cured composites, also because of the lower process temperature (Lopata et al. 1999). The aerospace application study mentioned previously also reported that volatile emissions were reduced by more than 90% with e-beam processing (Janke et al. 1998).

The benefits of e-beam cured composites extend beyond those related to the lower curing temperature. Radiation curing offers a degree of flexibility not available when using thermal-

cure processes. Autoclave processing requires that all resins of the products in one load have the same cure cycle, but radiation curing allows the fabrication of products using a variety of matrix resins, chosen by the desired final properties and not their thermal cure requirements (Singh 2001). Radiation-cured resins are also a lot more stable than thermally cured resins, which tend to auto-cure, leading to short shelf lives. So long as the radiation curable resins are stored in opaque containers, their shelf lives are virtually limitless (Singh 2001; Janke et al. 1998; Mehnert 1995; Lopata et al. 1999).

Irradiation processes can be incorporated into a continuous high-speed production (Singh 2001), leading to increased throughput. A 10MeV electron accelerator can produce curing dose to about 900kg/hr as opposed to an autoclave operating at a rate of 200kg/hr (Singh 2001). Other process comparisons in the aerospace study showed increased throughput with e-beam curing, anywhere from ten to 1000 times faster than traditional thermal curing operations (Janke et al. 1998). Continuous processing means no storage space is needed between fabrication and curing as it is in thermal processing, because products are cured in-line immediately after lay-up (Singh 2001; Mehnert 1995). Increased throughput means that fewer e-beam machines are needed to handle the same work load as ovens used for thermal curing. This also contributes to space savings in production facilities.

Fundamentals of Radiation Curing

Radiation curing can be accomplished by a few methods, including electron beam, gamma ray, x-ray and ultraviolet (UV) radiation. The effects of these methods on resins or adhesives are believed to be relatively similar because the high-energy electrons or x-rays or photons all trigger an avalanche of lower energy electrons or photons (Bouchard et al. 2006). Compared to UV radiation, e-beam radiation transfers a higher energy density to the irradiated object with deeper penetration, even into thick or opaque materials (Patacz et al. 2000). X-rays and gamma rays penetrate even deeper than high-energy electrons, but these forms of radiation are more

dangerous and harmful, and more complex technology and higher operating costs make these methods disadvantageous (Patacz et al. 2000). Electron beam radiation generally reaches sufficient depth when irradiating work pieces, and specimens found to be too thick can receive doses from multiple sides to achieve complete exposure. Dose and guidance of electron beam radiation can be administered with very high precision with today's technology and fine-tuned controls.

Curing occurs when high-energy electrons initiate free-radical or cationic polymerization and crosslinking in the irradiated material. When these electrons are absorbed into matter, secondary electrons are produced as a result of the energy degradation process. These enter into a Coulomb interaction with the atoms or molecules of the absorber, resulting in the formation of radicals, ions, and/or excited states of molecules or atoms (Mehnert 1995). Crosslinking and polymerization are then free to occur at these reactive sites. Resins and adhesives that cure by free radical mechanisms have advantages over those that cure by cationic polymerization in that they cure faster, and are not inhibited by nucleophilic materials on fiber surfaces in composites (Goodman et al. 1996).

The degree of cure is related to the dose of ionizing radiation received by the material. Optimum dosage is achieved when values of T_g, the glass transition temperature, reach a maximum, corresponding to maximum conversion of double bonds available in the prepolymer (Cadinot et al. 1994). As the T_g increases above the temperature at which the material is being cured, mobility in the resin is restricted and the rate of cure is then limited by diffusion of the reactive sites (Flory 1953; C. Decker et al. 1997). This means that raising the temperature during curing could lead to a higher degree of cure or to complete cure faster. The cure of the system can then by optimized by some combination of radiation dosage and cure temperature.

The ionizing radiation of polymers often results in degradation of the material in addition to crosslinking and curing (Mehnert 1995). Degradation occurs by scission of the polymer chains. The ratio of crosslinking to scissioning depends on many factors, including total irradiation dose, dose rate, the presence of oxygen, radical scavengers and steric hindrances derived from structural or crystalline forces (Ivanov 1992). In general, crosslinking dominates at lower doses, and scissioning increases at higher doses. Of course, as cure increases and double bonds are saturated by crosslinking, fewer double bonds remain to react and therefore the overall crosslinking rate will decrease. The ratio of crosslinking to chain breaking then may rely heavily on the availability of double bonds, though this is more of a general trend than a rigorous rule.

Acrylic Adhesives

The resins chosen for this study have acrylic and methacrylic functionality, bearing relevant a look at characteristics and qualities of these types of materials in their roles as adhesives. The first acrylic adhesives were brittle, and attempts to make them more flexible resulted in a reduction of shear strength and heat resistance (Cadinot et al. 1994). In the 1970s, a second generation of acrylics was developed which involved graft polymerization between elastomers and acrylic monomers, and displayed much-improved properties including better absorption of fracture energy, prevention of crack propagation, and higher resistance to peel, cleavage and impact forces (Cadinot et al. 1994). Acrylates have also been used in conjunction with epoxies like acrylic-modified bisphenol-A epoxies, which have been used as the basis of structural acrylic adhesives. Crosslinked acrylates form tight networks and exhibit excellent properties such as good solvent resistance, variable mechanical hardness, scratch resistance, variable adhesion and surface tension (Mehnert 1995).

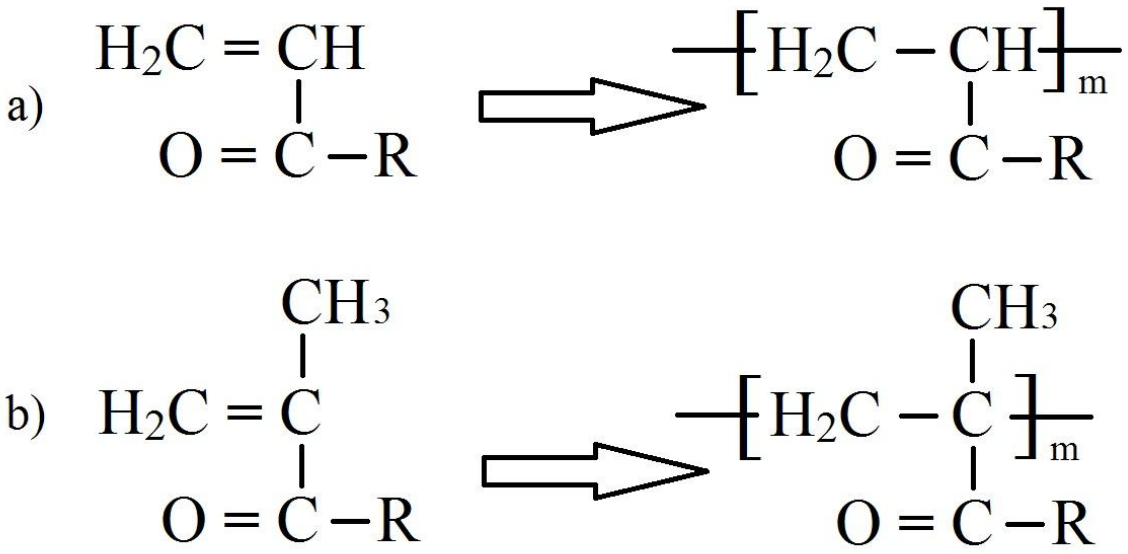

Figure 1: Cure schematic for polymers with a) acrylic or b) methacrylic functionality.

Acrylates, methacrylates and their prepolymers follow typical free radical addition polymerization after initiation by electron radiation (Mehnert 1995), and therefore enjoy the benefits of rapid cure mentioned of free radical polymerization mentioned before. For these types of resin systems, complete cure is generally observed at or around 40kGy, and then molecular rearrangements are observed at higher dosages (Griffith et al. 2006) due to the breaking of chains and side groups as previously discussed. In a study of incremental cure of acrylate compositions, Patacz et al. made an interesting discovery that the degree of cure of acrylates, while directly related to total radiation dose, is not a function of dose rate (Patacz et al. 2000). In other words, they observed the same degree of cure in samples that were irradiated with varied increments of radiation so long as they received the same total dose. Whether this will remain true for acrylates in the context of wood composites remains to be seen, but this could afford some flexibility in the manufacturing process.

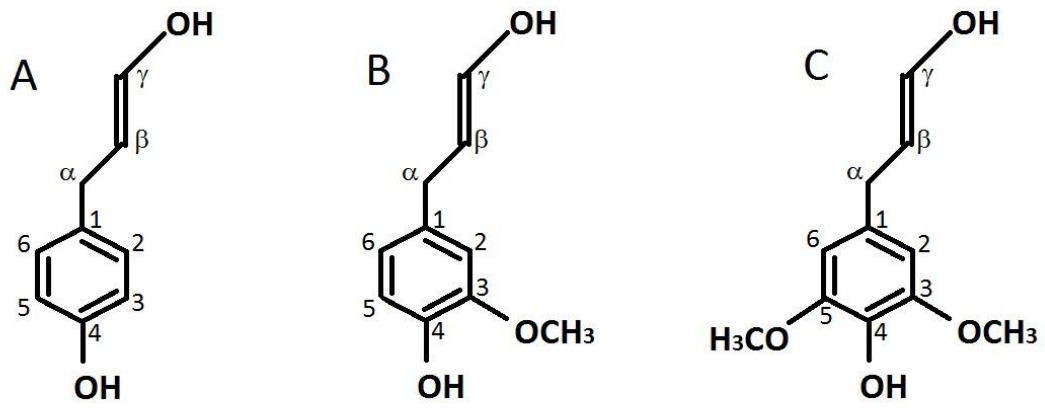

Figure 2: Primary monomeric units that make up lignin.

A) p-hydroxyphenyl, B) guaiacyl, C) syringyl

Radiation of Wood and Wood Components

Wood is made up of three main components - cellulose, hemicellulose and lignin. Cellulose is the main component in the primary cell walls of plants, while hemicellulose and lignin make up the secondary cell walls. Cellulose is generally found in crystalline structures called microfibrils, lignin is a completely amorphous material surrounding them, and hemicellulose forms a network between the two. The composition of wood, by mass, varies from species to species, but can be generalized as 40-50% cellulose, 25-35% hemicelluloses and 18-35% lignin (Pettersen 1984). These naturally occurring polymers are subject to the same effects from radiation that were discussed earlier regarding other types of polymers – at lower doses, crosslinking can be observed and at higher doses degradation by chain scission dominates (Bouchard et al. 2006). Therefore it is important to know what physical effects radiation has on wood, and to make sure that the dose used to cure resin in a composite will not be significantly weakening the wood substrate at the same time.

Much time and study has been given to the degradation of wood suffered as a result of ultraviolet radiation because wood used in exterior structural applications is subject to much radiation from the sun. UV radiation leads to the destruction of mechanical and physical properties caused by the severe structural modification of cellulose, hemicellulose and lignin, though mostly lignin (Hon & Shang-Tzen 1984). As previously discussed, UV radiation experiences limited penetration, even in a porous material like wood, and therefore the effects are mostly concentrated at the surface. Electron beam radiation penetrates the wood more completely, and seems to result in degradation mostly above a dose of 80kGy (Griffith et al. 2006). Lignin forms free radicals upon exposure to ionizing radiation (Fengel & Wegener 1984). As was stated before, lignin is a naturally occurring polymer. It is formed by the combination of three different monomeric units, p-hydroxyphenyl, guaiacyl and syringyl, shown in Figure 2. These units crosslink with each other by coupling either at the β–position, the 4-position or the 5-position (van Parijs et al. 2010). In the case of monomer being crosslinked to an existing oligomer, the β-4 or β-5 linkages are more likely than a β–β bond. Experimental findings revealed that lignin was degraded by UV radiation, breaking down into smaller, low molecular weight compounds containing carbonyl conjugated phenols (Hon & Shang-Tzen 1984). In that study Fourier Transform Infrared (FTIR) spectroscopy was used to detect the generation of carbonyl groups as radiation exposure increased, which was evidence of the degradation of lignin. Likewise, an increase of carboxylic groups signaled the breakdown of cellulose.

Cellulose chains form supramolecular structures made up of crystalline regions and amorphous regions. Within the crystalline regions, chains are arranged in highly ordered three-dimensional lattices which are held together through hydrogen bonding between hydroxyl groups and Van der Waals interactions between hydrogen atoms (Stepanik et al. 1998). The amorphous regions exhibit little or no order among the chains at all, making it weaker and significantly more susceptible to scission. In fact, high-dose radiation of purified cellulose revealed changes in physical response to moisture and thermal stability, but no change in the degree of crystallinity

(Griffith et al. 2006) meaning that all or almost all changes to the cellulose chain happened to the amorphous region.

A study conducted by Bouchard et al. on the effects of electron beam radiation of paper revealed some interesting results. The United States Postal Service employs electron beam accelerators to irradiate mail at a dose of about 50kGy, which is sufficient to kill the anthrax virus, but this lead to concerns regarding the integrity of the envelopes and papers after irradiation (Bouchard et al. 2006). The papers used in their investigation were either cellulose-only or cellulose-hemicellulose blends. They found that the radiation treatment weakened the paper by direct photolytic scission of the cellulose chains, presumably in the amorphous regions. In their study they found that dose rate does affect the rate of chain scission (CSN). They reported that radiation applied by an electron accelerator with a power of 4.5 MeV had a chain scission rate of 0.093 CSN/kGy, while an electron accelerator with a power of 10 MeV broke chains at a rate of 0.048 CSN/kGy (Bouchard et al. 2006). Their recommendation, then, was to use a higher powered e-beam to provide a sufficient dose at twice the rate while degrading the paper at half the rate. This behavior may not be observed when cellulose is in a different environment, like a resin matrix, but it may prove to be helpful by allowing a composite to be sufficiently cured without bringing too much damage to the wood substrate.

Wood/Resin Interactions

Wood fibers have been an attractive option for reinforcing thermoplastics because of their strength, toughness and aspect ratio (Rials et al. 2001). However, the qualities of individual components are not the only factors in determining the final properties of a composite material, nor are they the most important. The strength of wood composites, as with any material that depends on adhesion for its performance, is largely dependent on the strength of interface between its components, in this case resins and wood or wood fibers (Chowdhury & MP Wolcott 2007). If there is no reactivity between the components or if they are otherwise incompatible,

the resulting composite will exhibit weak interfacial properties (Kazayawoko et al. 1997; Felix & Gatenholm 1991). On the contrary, strong interactions (Griffith et al. 2006) or chemical bonding (Sheikh & Afshar Taromi 1993) between the polymer and cell walls of the wood could result in better bond strength, and therefore a better overall product. To that end, the lignocellulosic fibers of wood should be good candidates due to their hydroxyl-rich nature (Rials et al. 2001).

In the past, chemical pretreatments of wood or wood fibers have been used to stimulate or improve reactions between polymers and the natural fibers. Hydrogen peroxide has been used to initiate graft polymerization of styrene onto woody substances (Taneda et al. 1971), and nitric acid has been used to oxidize wood, resulting in the formation of carboxylic acid groups on the surface of the wood (Subramanian & Hofmann 1983). Both of these treatments lead to better interfacial bonding. As was previously stated, ionizing radiation produces carbonyls and carboxylic groups on lignin and cellulose, and should therefore produce similar improvements as the chemical pretreatments. Electron beam radiation treatments create reactive centers in the form of long living free radicals or thermally activated peroxy groups on the surface of cellulose and lignin (Czvikovszky 1996). This was shown to achieve chemical bonds between the wood fiber and resin matrix through grafted side chains and crosslinking. Han and Cho used e-beam treatments of about 10kGy to modify the surface of henequen fiber, a fiber from the leaves of a plant of the same name, resulting in improved interfacial adhesion between the fiber and resin matrix (Han et al. 2006).

Resins with acrylic functionality have been successful in bonding to wood substrates. Acrylates and methacrylates have been used as coupling agents in wood-plastic composites because they improve the fiber-resin bond, improving strength and toughness in the overall product (Kim et al. 2009). In a study of the application of radiation induced vinyl monomers in wood-polymer composites, Sheikh and Taromi showed that a portion of an acrylic/styrene polymer was grafted onto cellulose (Sheikh & Afshar Taromi 1993). In their study they noted that swelling occurred

during impregnation of wood with acrylic monomer, which is evidence of interactions at a molecular level. Some resin-wood systems are held together by physical interaction alone – the monomer fills in cracks and voids in the wood surface and then hardens when it is cured, rendering it immobile (M. J. Smith et al. 2002). Composites in which there are molecular interactions and/or chemical bonding between matrix and filler show much better adhesion and therefore better mechanical performance (Gardner 2006; Gindl et al. 2004; Dixit et al. 2006). Resins with acrylic functionality seem to be capable of such adhesion.

References

Beziers, D., Capdepuy, B. & Chataignier, E., 1990. Electron beam curing of composites. In *Developments in the science and technology of composite materials: Fourth European Conference on Composite Materials, September 25-28, 1990, Stuttgart, FRG*. Kluwer Academic Pub, p. 73.

Bouchard, J., Methot, M. & Jordan, B., 2006. The effects of ionizing radiation on the cellulose of woodfree paper. *Cellulose*, 13(5), 601-610.

Cadinot, N. et al., 1994. Electron-beam curable structural adhesives. Part 1: Study of acrylic resins for structural adhesive applications. *International Journal of Adhesion and Adhesives*, 14(4), 237-241.

Chowdhury, M. & Wolcott, M., 2007. Compatibilizer selection to improve mechanical and moisture properties of extruded wood-HDPE composites. *Forest products journal*, 57(9), 46-53.

Czvikovszky, T., 1996. Electron-beam processing of wood fiber reinforced polypropylene. *Radiation Physics and Chemistry*, 47(3), 425-430.

Decker, C., Decker, D. & Morel, F., 1997. Light intensity and temperature effect in photoinitiated polymerization. In *ACS Symposium Series*. ACS Publications, pp. 63-81.

Dixit, N. et al., 2006. Effect of Interactions between Interface Modifiers and Viscosity Modifiers on the Performance and Processibility of the Rice Hulls-HDPE Composites. *Journal of Reinforced Plastics and Composites*, 25(16), 1691.

Felix, J.M. & Gatenholm, P., 1991. The nature of adhesion in composites of modified cellulose fibers and polypropylene. *Journal of Applied Polymer Science*, 42(3), 609-620.

Fengel, D. & Wegener, G., 1984. Wood: chemistry, ultrastructure, reactions. *Berlin, New York*.

Flory, P.J., 1953. Principles of polymer chemistry. *Cornell University*, 428–429.

Gardner, D., 2006. Surface treatments of wood-plastic composites (WPCs) to improve adhesion. *Journal of Adhesion Science and Technology*, 20(16), 1873-1887.

Gindl, W., Schöberl, T. & Jeronimidis, G., 2004. The interphase in phenol-formaldehyde and polymeric methylene di-phenyl-di-isocyanate glue lines in wood. *International Journal of Adhesion and Adhesives*, 24(4), 279-286.

Goodman, D.L. et al., 1996. Composite curing with high energy electron beams. *Materials and Process Challenges: Aging Systems, Affordability, Alternative Applications.*, 41, 207-219.

Goodman, D.L. & Palmese, G.R., 2001. Curing and Bonding of Composites using Electron Beam Processing. *The Handbook of Polymer Blends and Composites*.

Griffith, W.L. et al., 2006. Electron-Beam Cured Resin Systems for Wood Composites. *ANTEC*.

Han, S.O. et al., 2006. Henequen/poly (butylene succinate) biocomposites: electron beam irradiation effects on henequen fiber and the interfacial properties of biocomposites. *Composite Interfaces*, *13*, 2(3), 231-247.

Harper, D.P. et al., Electron-Beam Curable Additives for Wood-Plastic Composites.

Hon, D.N.S. & Shang-Tzen, C., 1984. Surface degradation of wood by ultraviolet light. *Journal of polymer science. Polymer chemistry edition*, 22(9), 2227-2241.

Ivanov, V.S., 1992. *Radiation chemistry of polymers*, Vsp.

Janke, C.J., Wheeler, D. & Saunders, C., 1998. *Electron beam curing of polymer matrix composites*, Oak Ridge Y-12 Plant, TN (United States).

Kazayawoko, M. et al., 1997. Effects of wood fiber surface chemistry on the mechanical properties of wood fiber-polypropylene composites. *International Journal of Polymeric Materials*, 37(3), 237-261.

Kim, J.Y. et al., 2009. Effect of a Novel Polymeric Coupling Agent on the Water Uptake Property and Warp Stability of Poly (vinyl chloride)/Bamboo Flour Composite. *Composite Interfaces, 16*, 7(9), 837-846.

Lopata, V.J. et al., 1999. Electron-beam-curable epoxy resins for the manufacture of high-performance composites. *Radiation Physics and Chemistry*, 56(4), 405-415.

Mehnert, R., 1995. Electron beams in research and technology. *Nuclear Instruments and Methods in Physics Research Section B: Beam Interactions with Materials and Atoms*, 105(1-4), 348-358.

van Parijs, F.R.D. et al., 2010. Modeling Lignin Polymerization. I. Simulation Model of Dehydrogenation Polymers. *Plant Physiol.*, 153(3), 1332-1344.

Patacz, C., Defoort, B. & Coqueret, X., 2000. Electron-beam initiated polymerization of acrylate compositions 1: FTIR monitoring of incremental irradiation. *Radiation Physics and Chemistry*, 59(3), 329-337.

Pettersen, R.C., 1984. The chemical composition of wood. *Adv. Chem. Ser*, 207, 57-126.

Rials, T.G., Wolcott, M.P. & Nassar, J.M., 2001. Interfacial contributions in lignocellulosic fiber-reinforced polyurethane composites. *Journal of Applied Polymer Science*, 80(4), 546-555.

Scharf, W.H., 1989. Particle accelerators: applications in technology and research.

Sheikh, N. & Afshar Taromi, F., 1993. Radiation induced polymerization of vinyl monomers and their application for preparation of wood-polymer composites. *Radiation Physics and Chemistry*, 42(1-3), 179-182.

Singh, A., 2001. Radiation processing of carbon fibre-reinforced advanced composites. *Nuclear Instruments and Methods in Physics Research Section B: Beam Interactions with Materials and Atoms*, 185(1-4), 50-54.

Singh, A. & Silverman, J., 1992. *Radiation processing of polymers*,

Smith, M.J., Dai, H. & Ramani, K., 2002. Wood-thermoplastic adhesive interface--method of characterization and results. *International Journal of Adhesion and Adhesives*, 22(3), 197-204.

Stepanik, T.M. et al., 1998. Electron-processing technology: a promising application for the viscose industry. *Radiation Physics and Chemistry*, 52(1-6), 505-509.

Stern, M., 2000. Electron-Beam Processing of Plastics: An Alternative to Chemical Additives (15). In *Tecchnical Papers of the Annual Technical Conference-Society of Plastics Engineers Incorporated*. pp. 1772-1776.

Subramanian, R.V. & Hofmann, R., 1983. Study of the kinetics of in situ polymerization in wood by dynamic mechanical measurements. *Journal of Polymer Science: Polymer Letters Edition*, 21(2), 105-109.

Taneda, K., Hasegawa, I. & Kawakami, H., 1971. Dependence of the Mechanical Properties of Wood-Plastic Composites on the Mixture Rule. *Mokuzai Gakkaishi*, 17(5).

White, J.T., 1995. Wood adhesives and binders: what's the outlook? *Forest products journal (USA)*.

Wilson, E.J.N. & Wilson, E.J.N., 2001. *An introduction to particle accelerators*, Oxford University Press, USA.

CHAPTER 2: E-BEAM RADIATION EFFECT ON WOOD

CHAPTER 2: E-BEAM RADIATION EFFECT ON WOOD

Abstract

Radiation curing via electron beam (e-beam) is being considered as an alternative to thermal curing which is currently practiced in the wood composite industry, and which is very costly, time consuming and energy dependent. E-beam has already replaced thermal curing in other industries such as automotive and aerospace, where it has already proved itself to be an effective, economical and energy efficient replacement. Thermal curing also often causes defects in the wood substrates because of the sustained high temperatures and pressures required to cure the resins. If e-beam technology is to replace thermal curing, it will be important to understand how such radiation affects wood, and to make sure that it does not compromise its structural integrity. To this end, maple beams and veneers were irradiated with a variety of e-beam dosages (0 – 180 kGy) and examined to determine the effect of the radiation. The beams were used in three-point bend testing and were investigated with NIR spectroscopy. The veneers were used in dynamic mechanical analysis (DMA) and were investigated with FTIR spectroscopy. The three-point bend tests revealed that the wood became more brittle as a result of irradiation, especially at the highest dose where the beams experienced catastrophic failure. The MOR from the bending tests revealed a significant decline in the wood's resistance to failure after a dose of 80 kGy. DMA results showed evidence of crosslinking of the amorphous content of the wood at low doses, followed by chain scission and degradation at higher dosages. The turning point between the two mechanisms appeared to be at or around 80 kGy. Infrared spectroscopy revealed that the components of wood that were most impacted were the aromatic structures of lignin and cellulose hydroxyls, with the greatest effects being seen after 80 kGy and especially after 180 kGy. Therefore, it was concluded that a dose greater than 80 kGy not be used to cure wood composites.

Introduction

Wood is a remarkable material – it is widely considered beautiful, versatile, useful, and a renewable resource. In structural applications, it can be more useful and versatile when used as a substrate for composite materials. Wood composites, such as plywood, oriented strand board (OSB) and medium density fiberboard (MDF), can be produced in sizes and dimensions that are unavailable from raw lumber. They can be manufactured to be stronger, more durable and resistant to the ill-effects of weathering, insects and fungal attack (Cleland et al. 2009). However, despite the many advantages of wood composites, there are significant disadvantages associated with their manufacturing. The temperatures required for thermal curing can be harmful to the wood components. If the moisture content is not carefully monitored, internal stresses can result from the pressure generated by moisture at such high temperatures. During the cool-down phase after curing is complete, thermal shrinkage of the resin can cause delamination at the wood/resin interface due to differences in their thermal expansion coefficients (Singh 2001). Other issues include volatile emissions, time requirements for curing, and size limitations. Probably the biggest concern regarding thermal curing of wood composites is the immense energy requirements, and therefore processing costs.

Radiation curable adhesives present solutions to most, if not all, of these problems. Electron beam radiation, specifically, has been studied extensively as a means of curing composites made from such resins. It answers the problem of time requirements by allowing much higher product throughput, it reduces volatile emissions significantly, it allows for the curing of much larger, thicker pieces, and most importantly, it drastically reduces energy requirements (Singh 2001). For example, it has been estimated that radiation vulcanization is 3-6 times more energy efficient than thermal vulcanization (Ivanov 1992).

With so many advantages over current thermal curing practices, radiation curing is definitely an alternative that needs to be pursued. However, just like thermal curing, radiation curing has the potential to damage the wood in a composite.

Wood is composed mainly of cellulose (40-50% by mass), hemicellulose (25-35%) and lignin (18-35%), three naturally produced polymers (Pettersen 1984). Lignin has a highly variable structure, which lends itself to very randomized amorphous configurations. Cellulose, on the other hand, is a highly ordered and is mostly found in tightly packed crystalline conformations, though some semi-crystalline and amorphous regions do exist as well. Research regarding the effect of ionizing radiation on wood has found that lignin is the primary target of the radiation, breaking it down into smaller molecular weight units (Hon & Shang-Tzen 1984). When cellulose is affected, it is primarily in the amorphous regions where the chains are not so tightly packed (Mitsui et al. 2008; Tsuchikawa & Siesler 2003). In a study of the effect of e-beam radiation on natural kenaf fibers, Han et al. determined that the molecular weight of the cellulose chains was being lowered due to breakage of the glucosidic linkages, which decreased the amount of alpha-cellulose (DP>90) and increased the amount of beta-cellulose (DP=15-90) (Han et al. 2007). Despite this, their infrared studies indicated no notable change in the spectra of the treated and untreated fibers.

The effect of radiation on wood components is not all destructive, however. Many studies have indicated that crosslinking occurs at lower dose levels, and chain scission occurs at high dose levels (Pruzinec et al. 1981) (Bouchard)(Han 2007). The Han study of kenaf fibers mentioned previously was conducted with e-beam dosages of 100, 200 and 500kGy. On the other hand, a study of the usage of e-beam for fiber preparation for composite reinforcement concluded that a dose of 10 kGy would be useful in contributing to the strength of the interface between the fibers and the resin (Han et al. 2006). In addition to total dosage, dose rate is an important factor in the effect of e-beam radiation on wood. One study reported that chain scissions (CSN) occurred at a

rate of 0.093 CSN/kGy when using an electron accelerator rated at 4.5 MeV, while a 10 MeV accelerator had a scission rate of only 0.048 CSN/kGy (Bouchard et al. 2006).

Therefore, it is important to determine where in the spectrum of e-beam radiation dosages the non-destructive/beneficial behavior ends and where the destructive reactions begin.

Materials and Methods

This research was based on two studies involving maple wood irradiated with a variety of e-beam dosages. Maple beams were used in three-point bending tests and were examined with near infrared spectroscopy. Maple veneers were used in dynamic mechanical analysis and were examined with Fourier-transform infrared (mid-IR) spectroscopy.

Sample Preparation

Eighty maple beams were prepared measuring 25 mm by 25 mm in cross section and 45 cm long. Maple veneer measuring 0.5 mm thick was cut into 48 strips measuring 9.64 +/- 0.04 mm in the longitudinal direction and 50 +/- 2 mm in the radial direction.

The samples were sent to an electron beam facility at Sterigenics in San Diego, CA, where they received one of the following doses of radiation: 0, 5, 10, 20, 40, 80, 120, or 180kGy. The electron accelerator used at Sterigenics was rated at 12 MeV and 8 kW, with a 6 ms pulse at a pulse rate of 180 Hz. The radiation dosage was applied uniformly to the samples, half applied to one side, then the samples were flipped and the remaining dosage applied to the other side. The

final result of sample preparation yielded ten replicates of each dosage for the beams, and six replicates of each radiation dosage for the veneers.

Three Point Bend Tests

The three-point bend testing was conducted on an Instron 5567 universal testing machine (Instron, Norwood, MA) according to ASTM Method D143 to provide a look at the physical effect of radiation that is manifested in the Modulus of Elasticity (MOE) and the Modulus of Rupture (MOR).

NIR Spectroscopy

Near infrared (NIR) spectra were collected after irradiation with a Labspec Pro fiber optic probe made by Analytical Spectral Devices, Inc. (Boulder, CO) over the 350 – 2500 nm range of wavelengths. Four spectra were collected from each sample, one from each long side of the beam, with each spectrum being composed of the average of 30 sample scans.

Dynamic Mechanical Analysis

Dynamic mechanical analysis was performed in a Perkin Elmer Diamond DMA (Perkin Elmer Inc., Waltham, MA) using dual cantilever bending mode, employing sinusoidal oscillation at frequencies of 1, 2, 4, 10 and 20 Hz. Temperature scans were conducted from room temperature up to about 170ºC at a scanning rate of 5ºC/min. Because of the presence of residual stresses in the composites, each sample was run through that temperature range twice, the first time to relieve those stresses, and the second for data collection.

FTIR Spectroscopy

Infrared spectra were collected from the samples using a Perkin Elmer Spectrum One instrument with an attenuated total reflectance (ATR) accessory (Perkin Elmer Golden Gate Diamond 45º).

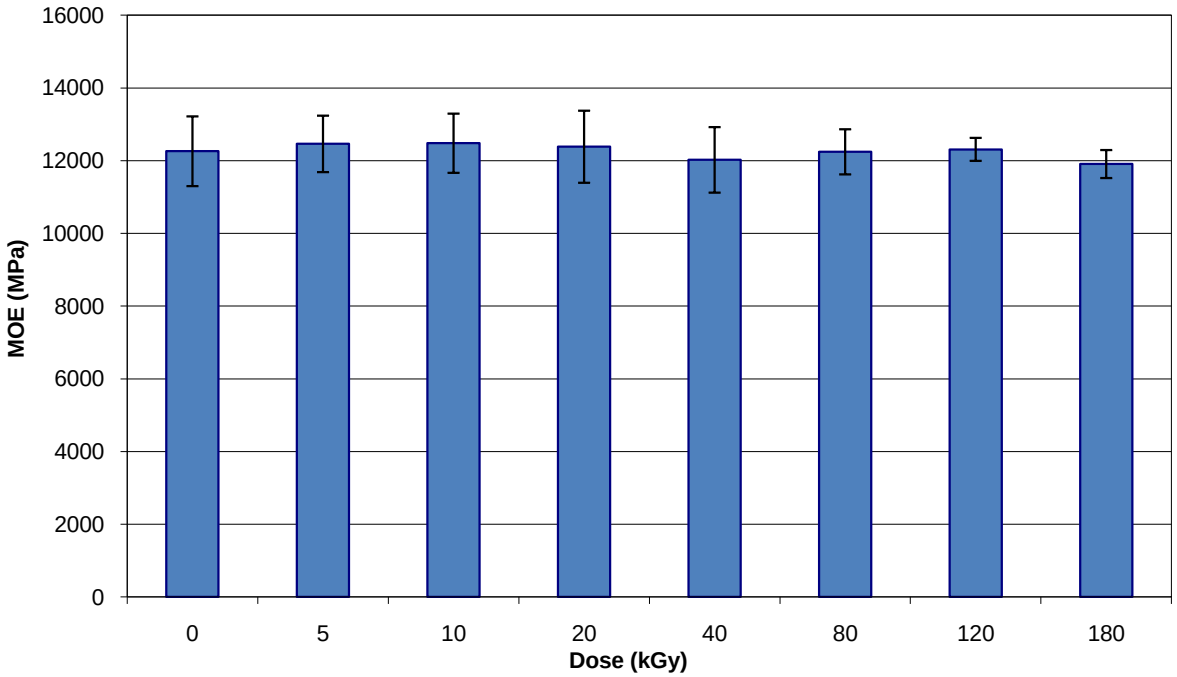

Figure 3: Modulus of Elasticity results from bending tests with irradiated maple beams.

Sixteen scans at a resolution of 8 cm^{-1} were taken and averaged from each sample before and after radiation. To minimize the effects the variations of wood may have on the spectra, a simple jig was created to make sure that the samples were scanned on the exact same spot both times.

Results and Discussion

Three Point Bend Tests

Bending tests were performed on the maple beams to determine the effect e-beam radiation would have on the bulk properties of the wood as described by the modulus of elasticity, MOE, and the modulus of rupture, MOR. The MOE results in Figure 3 show that the elastic modulus is relatively invariable across the full range of radiation dosages. The MOR of the maple beams, however, did not go unchanged. Between the two main components in wood, cellulose

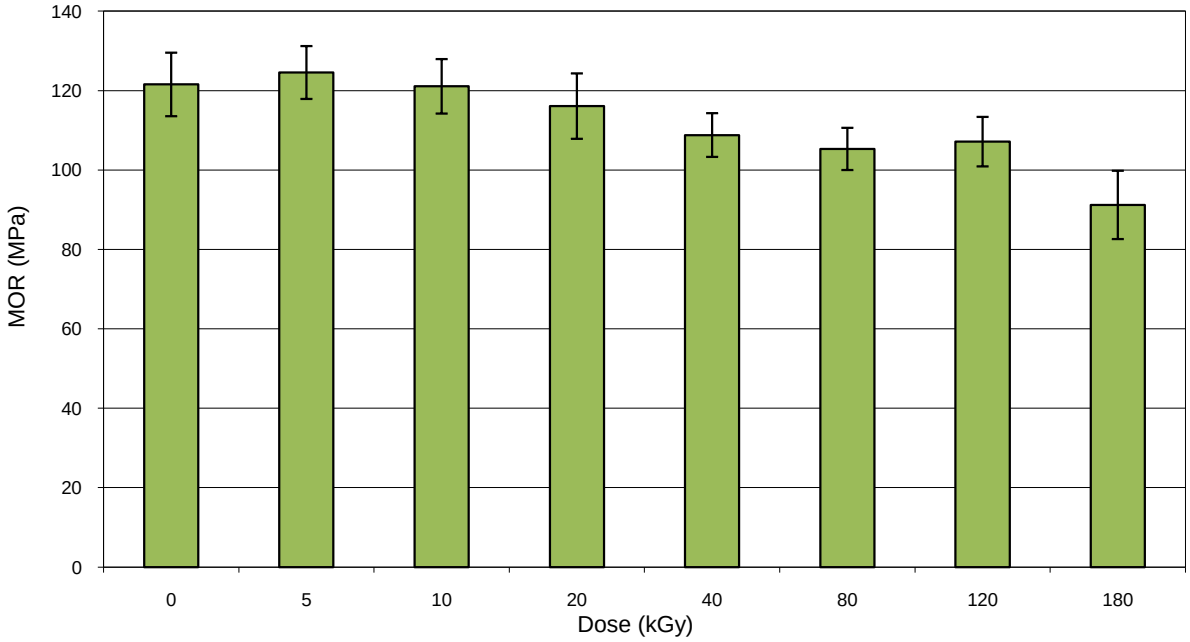

Figure 4: Modulus of Rupture results from bending tests with irradiated maple beams.

represents the elastic portion of the material (especially crystalline cellulose) while lignin represents the viscous portion. The lack of change in the elastic modulus suggests that the cellulose is mostly unaffected by the radiation, but the sharp decreases in the MOR, the maximum load-bearing limit, of the wood indicates that something is being affected.

Figure 4 shows that the wood's resistance to fracture decreases with increased radiation dose, with notably sharp reductions in strength between 5 and 40kGy, and again between 120 and 180kGy. This trend was also apparent during the execution of the bending tests as the style of failure of the maple beams gradually changed from hairline fractures at low dosages to brash failures at high dosages, with the 180kGy specimens having particularly catastrophic failures.

The implication of the bending study is that almost any exposure to e-beam radiation will result in some amount of loss of strength. Only very low doses (< 10kGy) would not show any

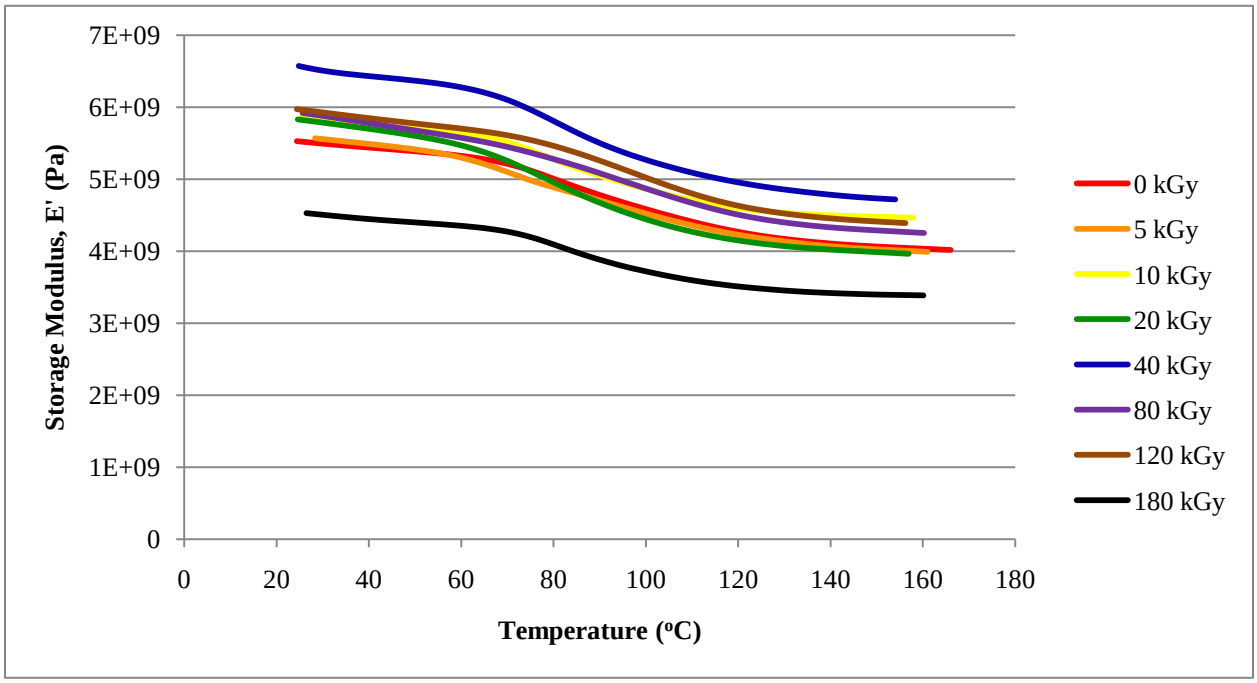

Figure 5: Averaged storage modulus plots for irradiated maple veneers.

appreciable difference in strength, but no resin suitable for wood composites could be fully cured with such a low dose. As the radiation dose is increased beyond 5 kGy, there is a steady decrease in MOR until a plateau is reached at 40kGy. This plateau is a promising result because most e-beam curable resins need at least 40kGy to reach complete cure, but if a higher dose is required to obtain better properties in the composite, or if a higher dose is needed because of the electron-scavenging by the wood, that higher dose can be used without sacrificing any more strength in the wood. Of course, the use of any radiation dose approaching or beyond 120kGy seems ill-advised because of the further loss of strength.

Dynamic Mechanical Analysis

Dynamic mechanical analysis of the maple veneers yielded many results. Results for individual samples, including the storage modulus (E'), the loss modulus (E") and the tan δ curves can be found in Appendix A. First, Figure 5 shows averaged plots of the storage modulus (E') of the irradiated wood samples as they were heated from room temperature to about 170ºC. The

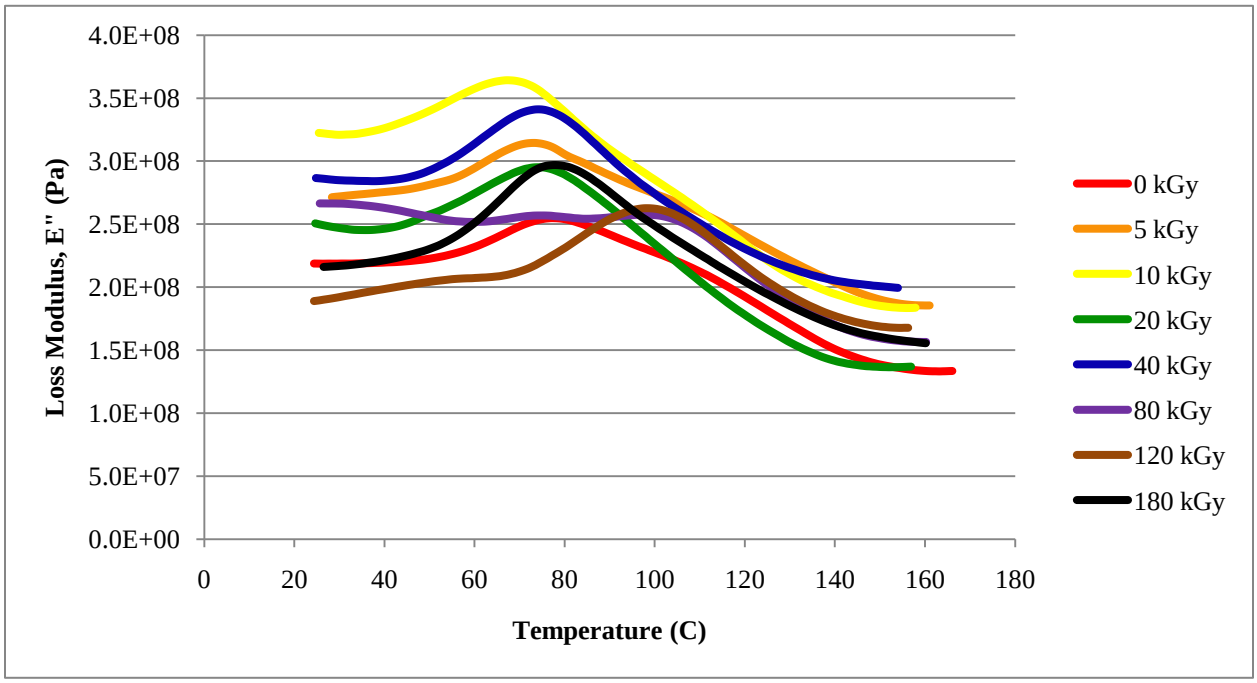

Figure 6: Averaged loss modulus plots for irradiated maple veneers.

storage modulus curves are created by measuring the amplitude of the sample's response to the strain imposed during testing. The storage modulus represents the elastic response of the sample, which stores the energy input as the stress is applied and then uses it to drive the return to the sample's original shape. As the samples are heated, they experience a relaxation as, on the molecular level, the polymer chains are allowed to move more freely at higher temperatures. This relaxation is called the glass transition, below which the polymer behaves in a stiffer, more glassy manner, and above which it behaves in a more flexible, rubbery manner. The glass transition temperature, T_g, is sometimes defined as the midpoint of the relaxation on an E' plot, sometimes as the onset of that relaxation, sometimes as the peak of the loss modulus (E") curve (shown later in Figure 6), but most commonly it is defined as the peak of the tan δ curve (shown later in Figure 8), which is the case in this study. In wood, this transition is especially gradual and broad because of the variety of components involved, and the non-uniformity of those components. Cellulose does not experience a glass transition until much higher temperatures; lignin and hemicellulose are both composed of a variety of monomeric units, lending them to

greater variation of composition and molecular weight, and therefore very broad, gradual transitions (Georget et al. 2002).

No single trend in Figure 5 stands out to describe the changes in the storage modulus of the samples as dose increases. For the most part, the E' curves for all doses are grouped closely together, meaning that they exhibit approximately the same stiffness behavior over the tested temperature range. Two curves, however, stand out from the group. The 40 kGy curve is noticeably above the rest, indicating that it exhibits overall higher stiffness than the other samples, and the 180 kGy curve is well below the rest implying a lack of stiffness. Since electron beam radiation has the ability to both crosslink and cleave polymer chains, and since it has been established that in wood crosslinking occurs at lower doses and chain scission at higher doses (Bouchard et al. 2006), it is possible that crosslinking is going on among the available unsaturated bonds lignin up to 40kGy, after which at higher doses cleavage of existing bonds dominates the reaction to the radiation. This would explain a slight increase in modulus from 0-40 kGy, followed by a downward trend in modulus, especially at the 180 kGy dose. Again, it seems that no single trend is responsible for the changes in the physical properties of the wood as the radiation dose increases, and that there are multiple competing events occurring in the chemistry of the wood.

Figure 6 shows the averaged loss modulus curves, E", of the maple veneer samples through their glass transition. The loss modulus is the viscous portion of the sample's response to testing. It describes the energy lost to internal molecular motions when energy from the applied stress is not stored, but is rather consumed by chain slippage. The glass transition occurs around the maximum of the peak that each curve exhibits. That peak itself is actually a distribution of transitions occurring near the same temperature. The breadth of these peaks again indicates the non-uniformity of amorphous content of the samples. Materials composed of uniform, homogeneous polymers with little or no variance in molecular weight, crosslink density, side

groups, etc. will exhibit very sharp, narrow peaks as all of the chains go through the transition at approximately the same temperature. Such is not the case for wood where lignin, the primary component responsible for viscous behavior, has such a random structure that no specific chemical structure has ever been agreed upon as the repeating unit of that naturally occurring polymer. Some of the chains, being less hindered by size, crosslinking or entanglement, begin their transition well below the average temperature and some, requiring more energy to overcome their entanglements, don't go through the transition until a much higher than average temperature. A greater amount of energy is consumed during the glass transition as the molecules are rearranged into freer conformations, hence the peak in the loss modulus curve. Above the T_g, the molecules experience more free volume than below the T_g where they are packed closer together and are subject to more entanglements and secondary attractions that hinder movement. This explains why the E" values are lower in the rubbery region than in the glassy region. This also explains why there is greater variance in E" among all of the samples before the transition than after – whatever factors permitted or prohibited movement before the T_g are less of a factor afterwards when there is greater free volume. As in the analysis of the storage modulus curves, the loss modulus curves do not indicate any single trend that correlates changes in the properties of the wood to the increased dosages.

Tan δ curves for each dosage are shown in Figure 8. The value, δ, is found during DMA by measuring the phase lag between the applied sinusoidal stress and the resulting oscillating response of the material. Purely crystalline materials will be completely in phase with the applied oscillation while purely viscous materials will be 90^o out of phase. Viscoelastic materials fall somewhere in between based on composition. δ is sometimes called the phase angle because of the equation of the complex modulus:

$$E^* = E' + iE''$$

which can be shown as

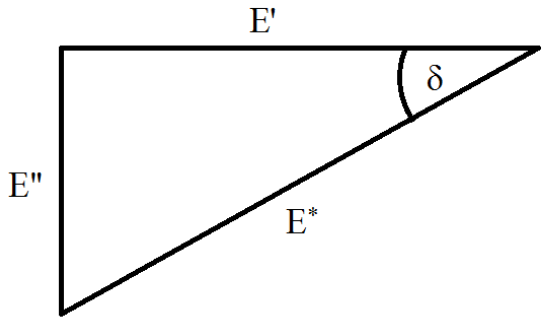

Figure 7: The relationship between storage modulus (E'), loss modulus (E"), complex modulus (E*) and the phase angle, δ.

Therefore, tan δ is the ratio of the loss modulus to the storage modulus, E"/E'. Tan δ is a measurement of damping, which is the dissipation of energy in a material during cyclical loading. Thus, it is mathematically, conceptually and visually similar to and related to the loss modulus. As was stated before, the glass transition temperature is most commonly defined as the peak of the tan δ curve. It should also be noted that a testing frequency of 1 Hz is traditionally used for such determinations. The T_gs of the irradiated maple veneer samples are shown in Figure 9, along with error bars that represent the highs and lows of the averaged replicates. From 0 to 40 kGy, the T_g values vary somewhat, but generally go unchanged. Then the 80 and 120 kGy samples report much higher T_gs, followed by a dramatic decrease at 180 kGy. This indicates that notable stiffening occurred between 40 and 80 kGy, and then equally notable weakening occurred between 120 and 180 kGy. Once again, the idea of crosslinking at lower doses and chain scission at higher doses seems to be supported by these trends.

In addition to the 1 Hz tan δ plots, which were used to calculate the T_gs, DMA was also performed at 2, 4, 10 and 20 Hz, which reveals a time effect in the glass transition. When the testing is done at higher frequencies, and the stress is being applied faster, the polymer chains

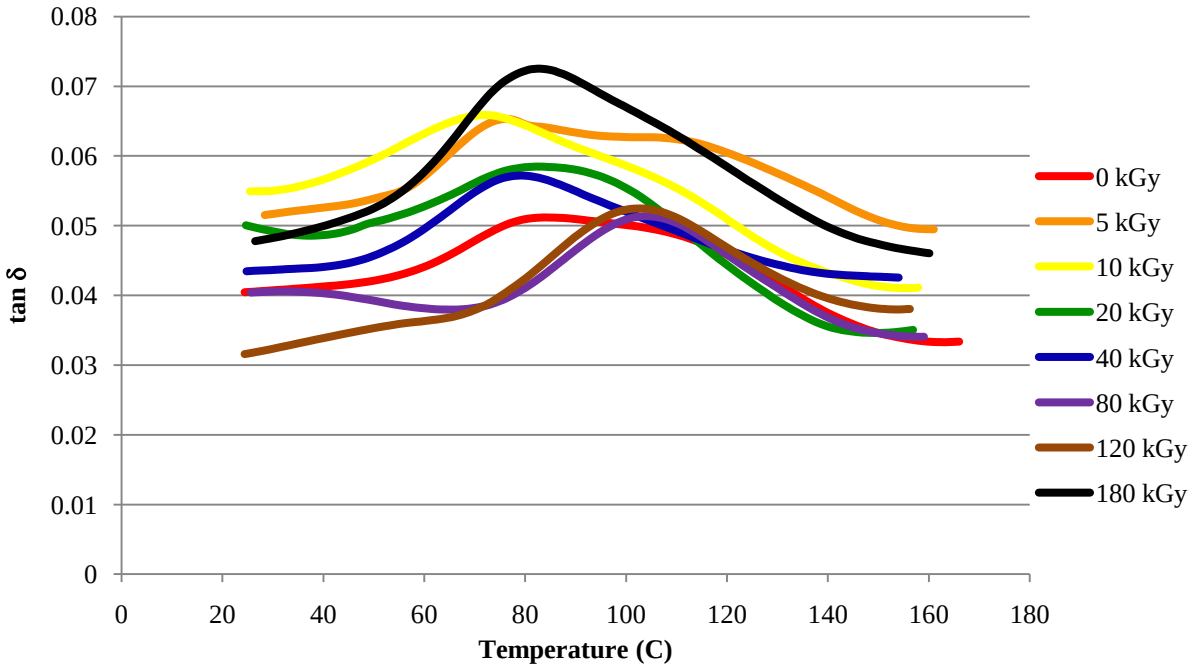

Figure 8: Averaged tan δ plots for irradiated maple veneers.

don't have as much time to move in response, so the material appears to be less flexible. This results in a shift in the tan δ curve and thus, the T_g. Five different frequencies with five different T_gs gives five pairs of data points that can be used to determine the activation energy required to overcome the glass transition, making use of the Arrhenius equation:

$$\lambda = \lambda_o e^{\frac{-Ea}{RT}}$$

where λ is the frequency, λ_o is the pre-exponential factor, T is the temperature at the peak of the tan δ curve, and R is the constant 8.314 J/mol·K. Plotting 1/RT versus log (λ) for every temperature/ frequency pair from a given sample gives a line whose slope is equal to the activation energy, E_a. The E_as were calculated and averaged among replicates of each radiation dose, and are shown in Figure 10. Similar to the T_g plot, the activation energy doesn't vary much between 0 and 40 kGy, then spikes sharply at 80 kGy before descending through 120 to 180 kGy. The glass transition involves an expansion of the free volume between polymer chains that allows for more freedom of movement, and the activation energies shown here represent the

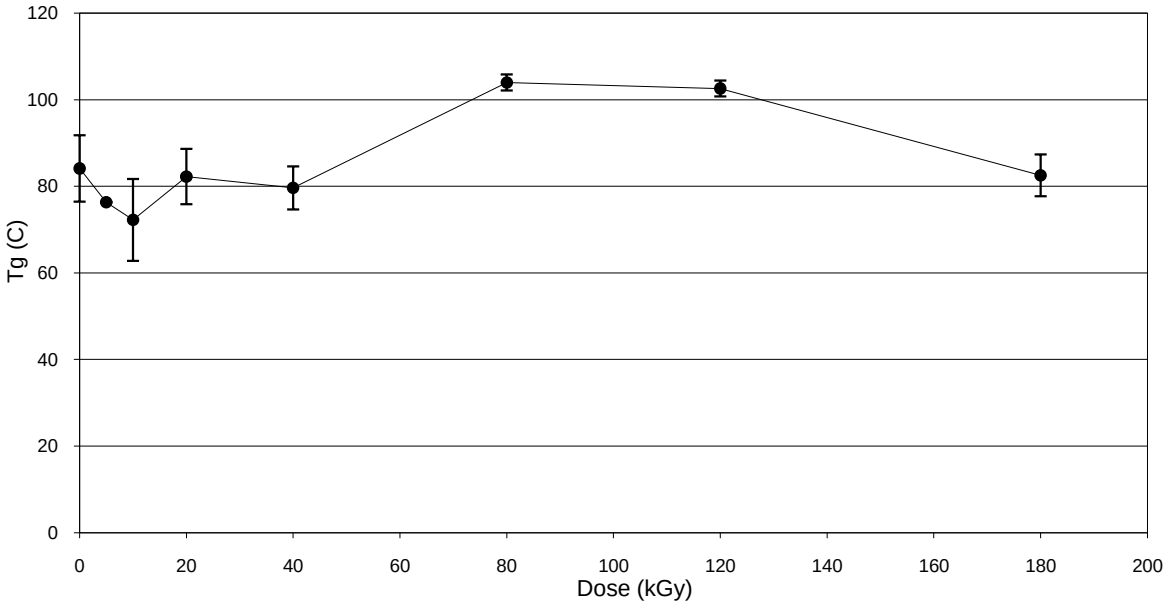

Figure 9: Glass transition temperatures for irradiated maple veneers.

amount of energy required to allow those movements. Materials with higher degrees of structure – like more crosslinking, for example – require more energy to get through that transition. Therefore, Figure 10 indicates that the samples are being crosslinked in the early stages of radiation, peaking at 80 kGy, and then at higher doses the bonds that have been restricting the transition are disappearing.

Infrared Spectroscopy

The maple samples were also investigated using infrared spectroscopy – both near (NIR) and Fourier-Transform (mid-IR). The three-point bending tests of the maple beams showed bulk mechanical properties of the wood, and changes in it as radiation increased. Then, dynamic mechanical analysis of the maple veneers provided a smaller scale study of the physical properties of irradiated wood. Now, on a smaller scale yet, IR spectroscopy was used to look into the chemical changes of the wood.

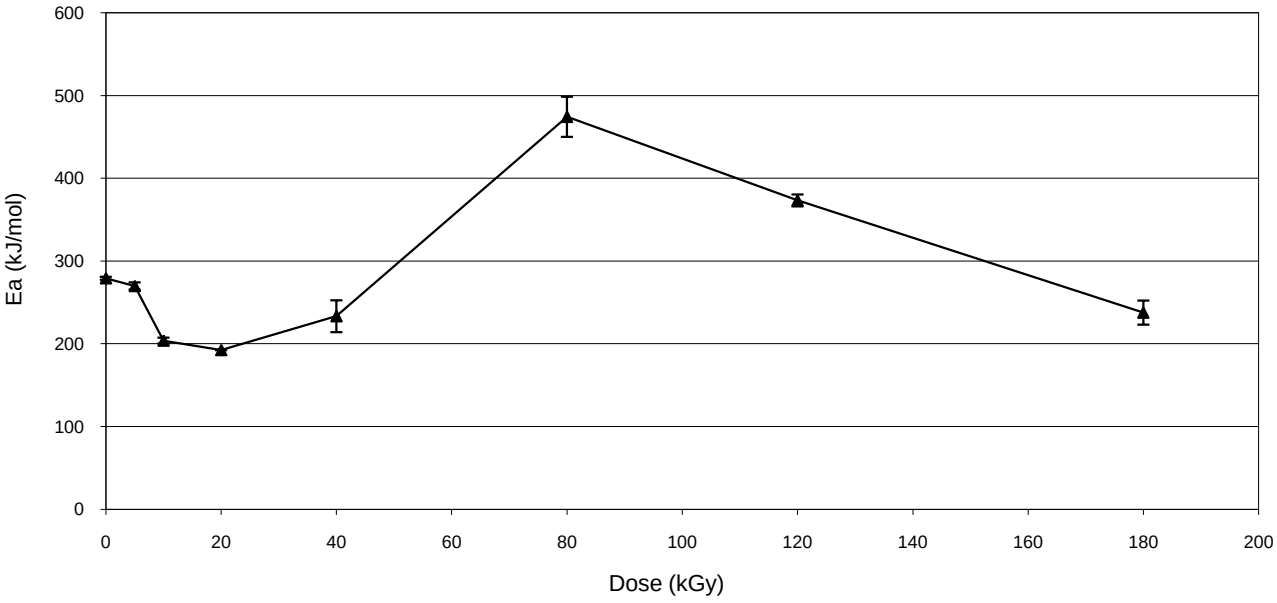

Figure 10: Activation energies for irradiated maple veneers.

Near IR

NIR spectra were collected from the maple beams after irradiation. Figure 11 shows representative spectra for some of the dosages. It is obvious that visual inspection alone would not be enough to identify differences between the dosages since the curves are so similar. Therefore, Principle Component Analysis (PCA) was used to analyze the spectral data. PCA is a mathematical tool that identifies which linear combination of variables out of a multivariate data set are most responsible for the difference between samples, and groups them into principal components (PCs). Each PC explains as much of the difference between the samples as possible, with each one explaining a higher percentage of the sample variance than the next PC, placing highest importance on the first. Every variable has a loading value in each principal component, which indicates whether or not it was a significant factor in that PC, and whether it was positively or negatively significant. Values close to zero indicate insignificance of a variable in a given PC. Stronger values, either positive or negative, indicate that a variable has more

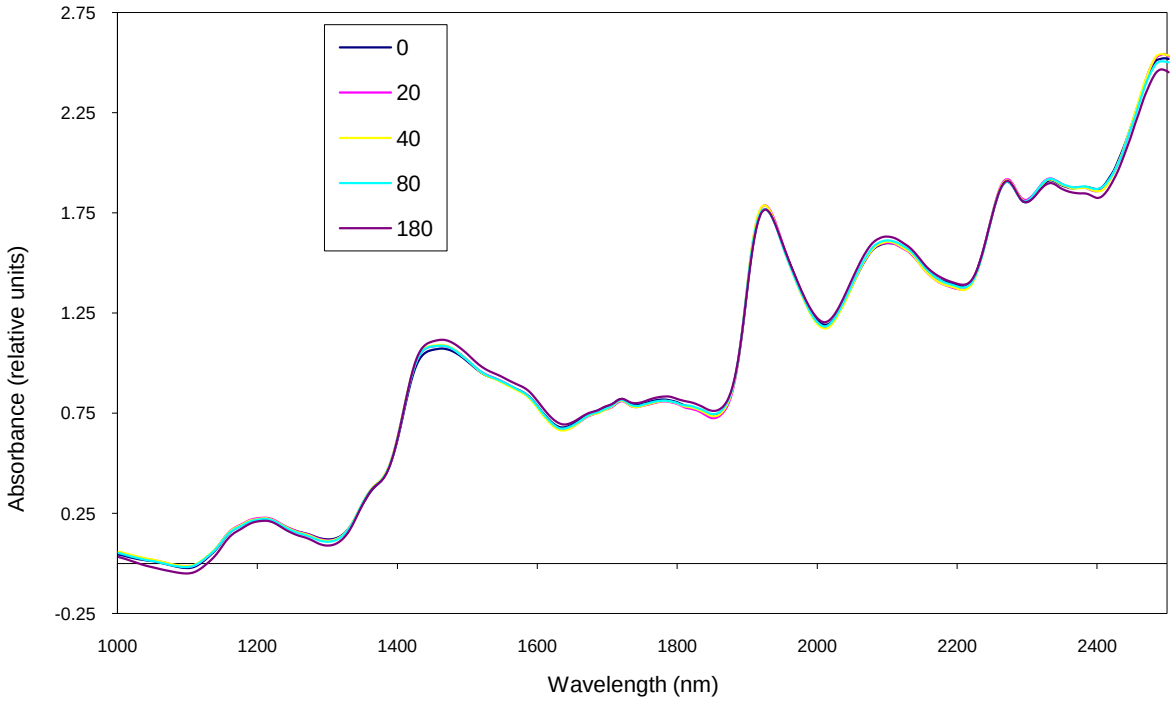

Figure 11: A few select representative NIR spectra of irradiated maple beams.

importance in the definition of the PC. The meaning of the sign of a loadings value is determined in combination with the sample scores. Each sample is assigned a score on each principal component, which is used to show similarity and dissimilarity between samples. Samples with the same or similar scores on a PC are defined the same way by the variables that have been determined to be significant in that PC. Samples with scores that are greatly different on a PC are dissimilar with regards to those significant variables. A two-dimensional plot allows the scores for two PCs to be displayed and analyzed simultaneously. This scores plot in conjunction with the loadings plots for each PC defines differences among samples, and what variables are responsible for those differences.

Based on MOR values (shown in Figure 4), the sample doses were divided into three groups of similar MOR: High MOR (0-20 kGy), Mid MOR (40-120 kGY), and Low MOR (180 kGy). PCA performed on the NIR collected from the maple beams shows distinct separations of these

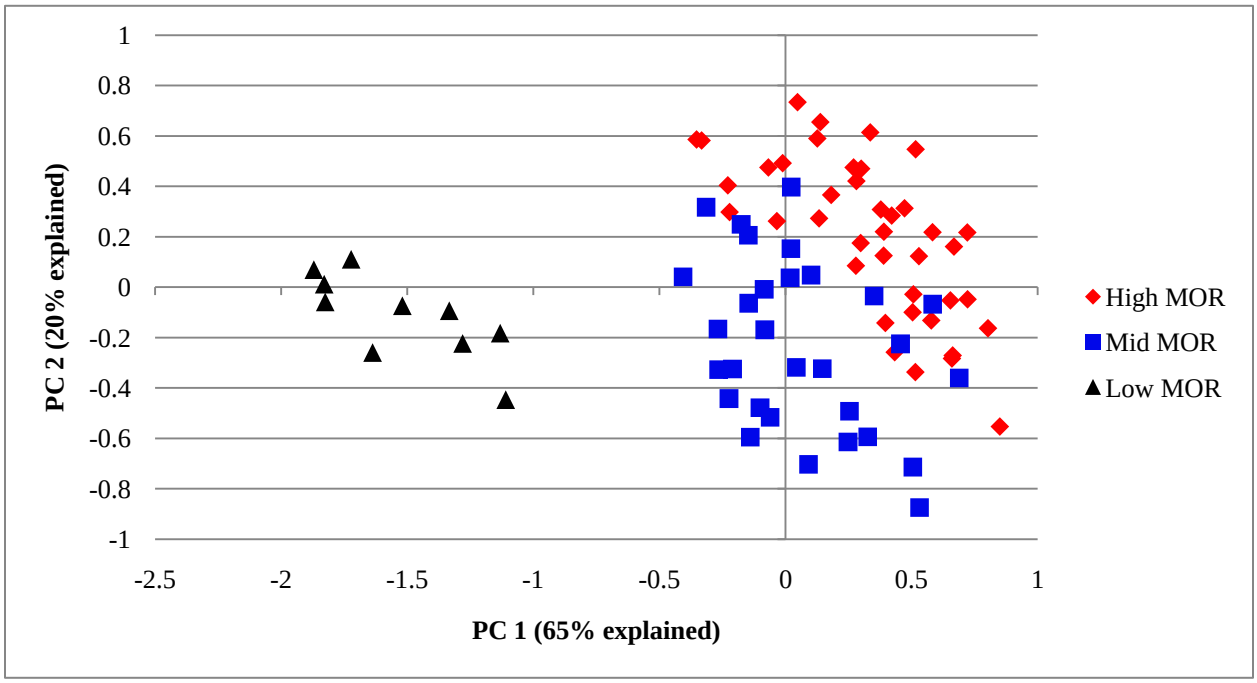

Figure 12: Scores plot for PCs 1 and 2 from PCA of irradiated maple beams NIR spectra.

three groups, which can be seen in the scores plot in Figure 12. Primarily, the 180 kGy samples (Low MOR) are separated from the rest of the samples along PC1, which offers explanation of 65% of the variance among all samples represented. Within the rest of the group, the High and Mid MOR groups are clearly divided along a combination of PCs 1 and 2 (note the diagonal line of separation between the two groups). Based on the PC1 loadings plot in Figure 13, the primary contributor to PC 1 is a strong positive band around 1924nm, which is associated with cellulose hydroxyls (Mitsui et al. 2008). Since the High and Mid-MOR groups are positive on PC1 and the Low MOR group is negative on PC1, this means that this peak is decreasing with increasing dose. In other words, the cellulose hydroxyls are being negatively impacted by increasing radiation. Two notable, but not as strong, negative peaks are apparent in the PC1 loadings: 1632 and 1780nm, which represent C-H first overtones in lignin and both lignin and cellulose, respectively (Tsuchikawa & Siesler 2003). Their negative loading values indicate that these peaks increase with increasing dosage.

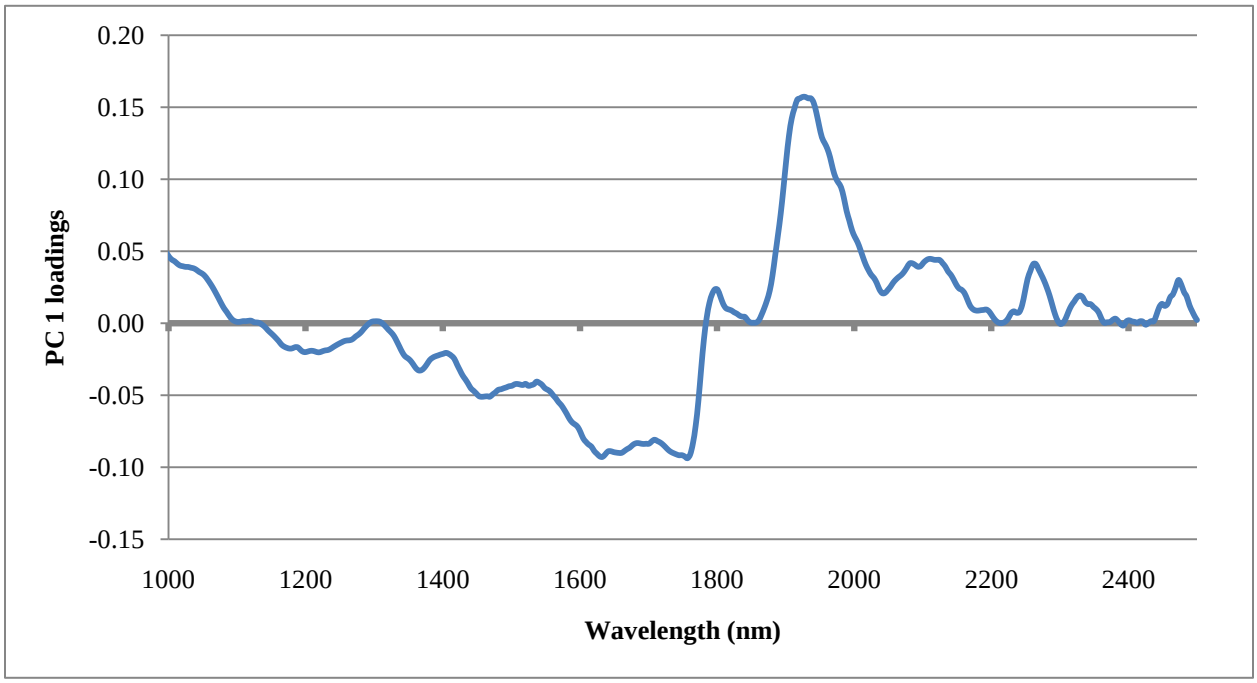

Figure 13: PC1 loadings plot for NIR of irradiated maple beams.

FTIR spectroscopy

In addition to NIR spectroscopy, Fourier-Transform spectroscopy was also taken in the Mid IR range (~4000-650 cm^{-1}). Of particular interest is the fingerprint region, roughly from 1800 to 800 cm^{-1}, in which the absorption pattern is not just a collection of absorption bands based on the types of bonds present, but rather is the result of interacting vibration patterns generated by the combination of bonds and their arrangements. In this region, two different molecules that have the same types of bonds can be distinguished because their difference in structure creates differences in their absorption profile. Each type of molecule has a unique absorption pattern in the fingerprint region. This uniqueness and sensitivity to variation may lead to a degree of uncertainty when it comes to lignin that does not have an established uniform structure. FTIR spectra of irradiated maple beams in the fingerprint region are shown in Figure 14. Much like the NIR spectra visual evaluation of the FTIR spectra is not enough to detect changes and trends in the samples as a function of radiation dosage, so once again PCA was used to analyze the data.

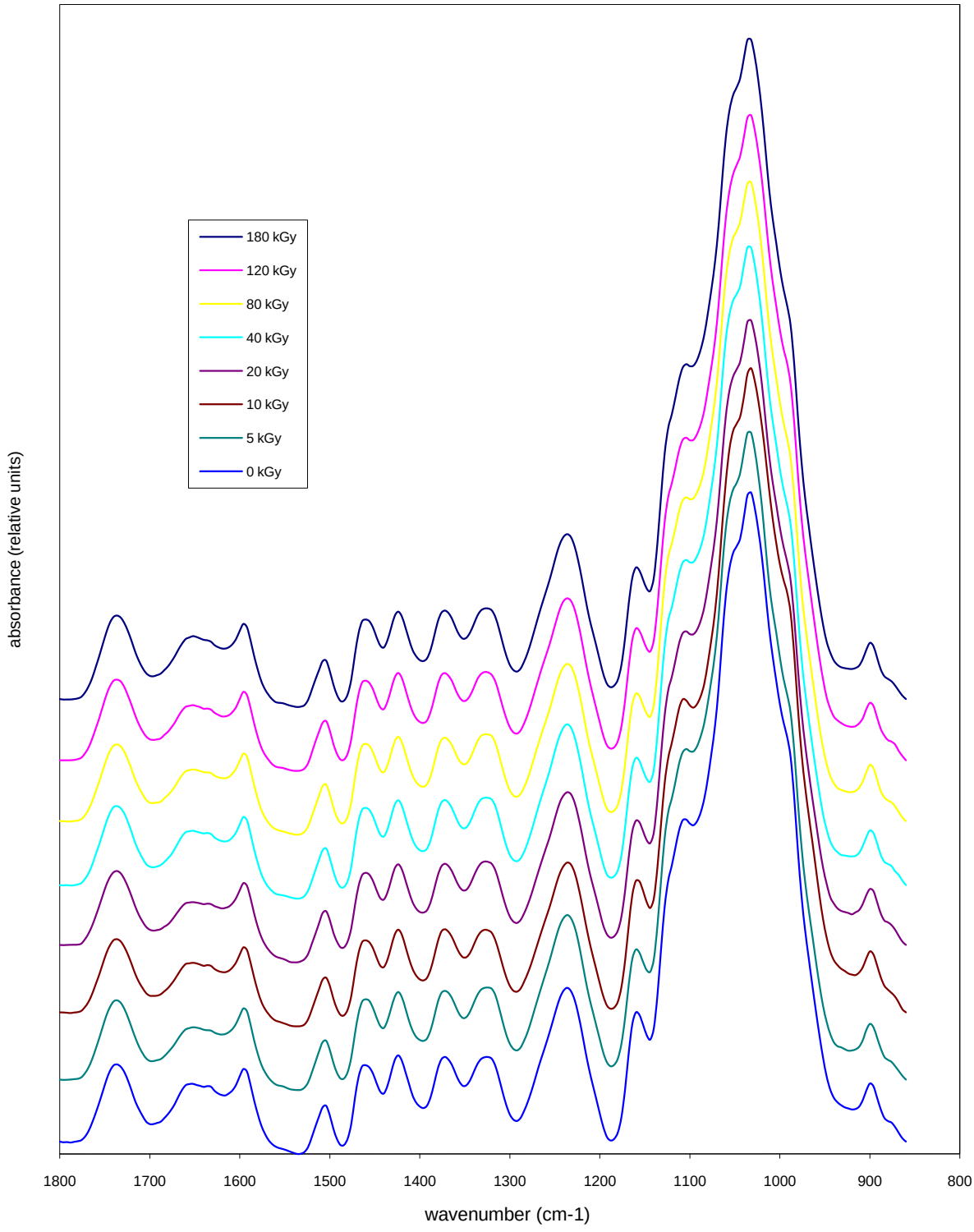

Figure 14: FTIR spectra in the fingerprint region of irradiated maple veneers.

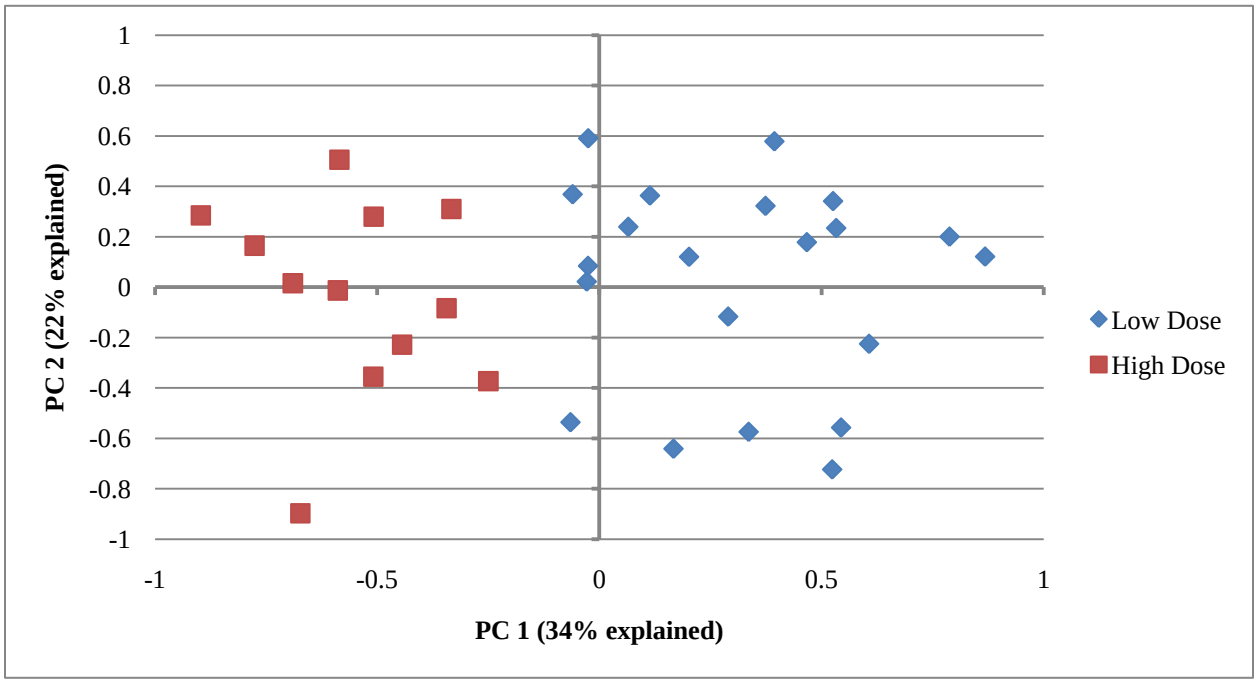

Figure 15: PCA scores plot for FTIR of irradiated maple veneers, with 5 kGy samples withheld from analysis.

Data pretreatments were applied to the spectra before analysis. First, multiplicative scatter correction (MSC) was used to remove scatter effects that were produced more by physical characteristics on the surface of the wood than chemical information. Then, each spectrum was normalized by its mean, which causes all spectra to have the same area under the curve, which increases the quantitative significance of each peak. Finally, the variables were averaged by 4 to reduce the noise, and to lighten the computational load.

Initially, the PCA results were obscured by a few unruly variables that dominated the 5kGy sample set (see Appendix B), so those samples were removed. With the undesired influence of the 5 kGy samples gone, there is a very distinct line of demarkation between the low dose and high dose samples along PC1, which is a better result. According to the loadings plot in Figure 16, the key components of PC1 are the peaks at 1592 cm^{-1}, 1033 cm^{-1}, and 1059 cm^{-1} – all with positive loading values, and the peak at 1720 cm^{-1} which has a negative loading value. The peak

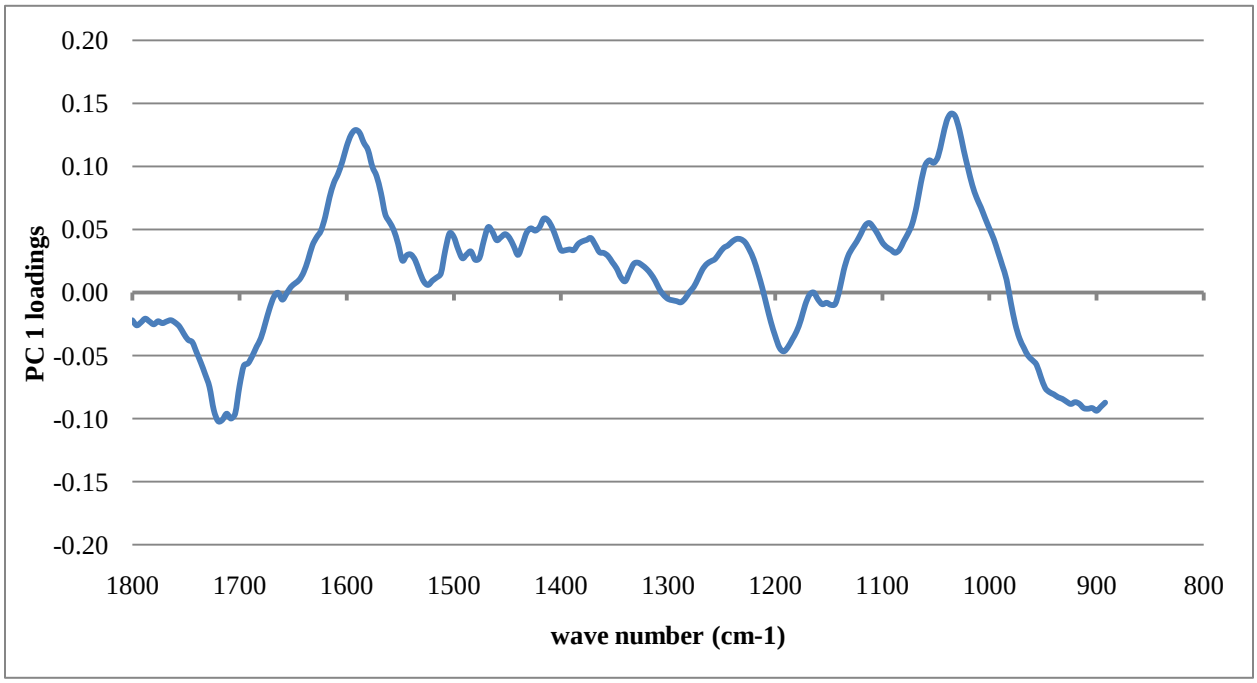

Figure 16: PC1 loadings plot for PCA of irradiated maple veneers, with 5 kGy samples withheld from analysis.

at 1592 cm^{-1} is due to aromatic skeletal vibrations in lignin (Azadfallah et al. 2008), and the peaks at 1033 and 1059 cm^{-1} are from vibrations of the ring structures in cellulose (Kauráková et al. 2000). These three, according to PCA, are decreasing with increasing radiaition dosage. The peak at 1720 cm^{-1} is assigned to C=O stretching (Colom et al. 2003).

The NIR study showed that the primary change in the wood as it was irradiated was a decrease in hydroxyls, especially at 180 kGy. According to the FTIR analysis, carbonyls were on the rise, and the aromatics in lignin and the ring structures in cellulose were negatively impacted as radiation dosages increased.

Conclusion:

Bending tests showed almost no change in MOE, but significant drops in load-bearing limit (MOR). From MOR tests alone, it is recommended that radiation dosages for curing of composites be restricted to the plateau between 40 – 120 kGy where increased dosage showed no further decrease in physical performance. From the DMA experiments, the storage modulus plots (E') suggest that the 40 kGy dosage caused a rise in overall stiffness as compared to the other dosages, and the 180 kGy samples were noticeably less stiff. This along with the T_gs, which peaked at 80 and 120 kGy, and the E_as which peaked at 80 kGy seemed to indicate early cross linking at lower doses and chain scission at higher doses.

PCA of NIR spectra showed excellent grouping when samples were grouped by MOR level. The 180 kGy samples stood out significantly from the rest of the samples, and the High and Mid MOR were samples were also distinguishable. The defining trends were decreasing hydroxyls and increasing C-H first overtones (from both cellulose and lignin) as dose increased. There was no evidence of two separate trends at lower and higher doses. This could be due to the typically exponential response to radiation not being well described by linear approximations in PCA.

PCA of FTIR displayed grouping once the 5 kGy samples were removed and when comparing low dose (0-40 kGy) and high dose (80-180 kGy) sample classification. The defining trends here were decreasing aromatic skeletal vibrations in lignin, decreasing ring structure vibration in cellulose, and increasing C=O vibrations in lignin with increasing dose.

Elimination of hydroxyls in cellulose (evident from NIR study) and changes in ring structures (evident in FTIR study) would negatively impact the strength by reducing hydrogen bonding, which is especially important in crystalline regions. Any actual chain scissions, which would

most likely occur in the amorphous regions of cellulose and in lignin would also be main contributors to the loss of strength observed in bending tests.

Analysis of the storage modulus, T_g, E_a, and infrared studies all seem to point to 80 kGy as the point at which the most destructive effects start to take place. Therefore, a dose higher than 80 kGy should probably not be used to cure composites.

References

Azadfallah, M. et al., 2008. Analysis of photodegraded lignin on cellulose matrix by means of FTIR spectroscopy and high pressure size exclusion chromatography. *Iranian Polymer Journal*, 17(1), 73.

Bouchard, J., Methot, M. & Jordan, B., 2006. The effects of ionizing radiation on the cellulose of woodfree paper. *Cellulose*, 13(5), 601-610.

Cleland, M.R. et al., 2009. X-ray initiated polymerization of wood impregnants. *Radiation Physics and Chemistry*, 78(7-8), 535-538.

Colom, X. et al., 2003. Structural analysis of photodegraded wood by means of FTIR spectroscopy. *Polymer Degradation and Stability*, 80(3), 543-549.

Georget, D.M.R., Smith, A.C. & Waldron, K.W., 2002. Dynamic mechanical thermal analysis of cell wall polysaccharides extracted from lyophilised carrot Daucus carota. *Carbohydrate Polymers*, 48(3), 277-286.

Han, S.O. et al., 2006. Henequen/poly (butylene succinate) biocomposites: electron beam irradiation effects on henequen fiber and the interfacial properties of biocomposites. *Composite Interfaces*, *13*, 2(3), 231-247.

Hon, D.N.S. & Shang-Tzen, C., 1984. Surface degradation of wood by ultraviolet light. *Journal of polymer science. Polymer chemistry edition*, 22(9), 2227-2241.

Ivanov, V.S., 1992. *Radiation chemistry of polymers*, Vsp.

Kauráková, M. et al., 2000. FT-IR study of plant cell wall model compounds: pectic polysaccharides and hemicelluloses. *Carbohydrate polymers*, 43(2), 195-203.

Mitsui, K., Inagaki, T. & Tsuchikawa, S., 2008. Monitoring of hydroxyl groups in wood during heat treatment using NIR spectroscopy. *Biomacromolecules*, 9(1), 286-288.

Pettersen, R.C., 1984. The chemical composition of wood. *Adv. Chem. Ser*, 207, 57-126.

Pruzinec, J. et al., 1981. Study of the effects of high-energy radiation on cellulose. *Name: Radiochem. Radioanal. Lett*.

Singh, A., 2001. Radiation processing of carbon fibre-reinforced advanced composites. *Nuclear Instruments and Methods in Physics Research Section B: Beam Interactions with Materials and Atoms*, 185(1-4), 50-54.

Tsuchikawa, S. & Siesler, H.W., 2003. Near-infrared spectroscopic monitoring of the diffusion process of deuterium-labeled molecules in wood. Part I: softwood. *Applied spectroscopy*, 57(6), 667-674.

Appendix A: DMA Outputs for Maple Veneers

Data outputs from dynamic mechanical analysis are shown in the following section for each sample tested. Sample nomenclature is as follows: NR indicates "no resin", these samples are raw wood only; the number indicates the received e-beam dosage (0 – 180 kGy); the final letter identifies individual replicates (A-F). Storage modulus (E') plots are shown in green, loss modulus (E") in red, and the tan δ curves are shown in blue. The T_gs are marked as the peak of the tan d curve, and the onset and offset of the glass transition are marked on the E' curves.

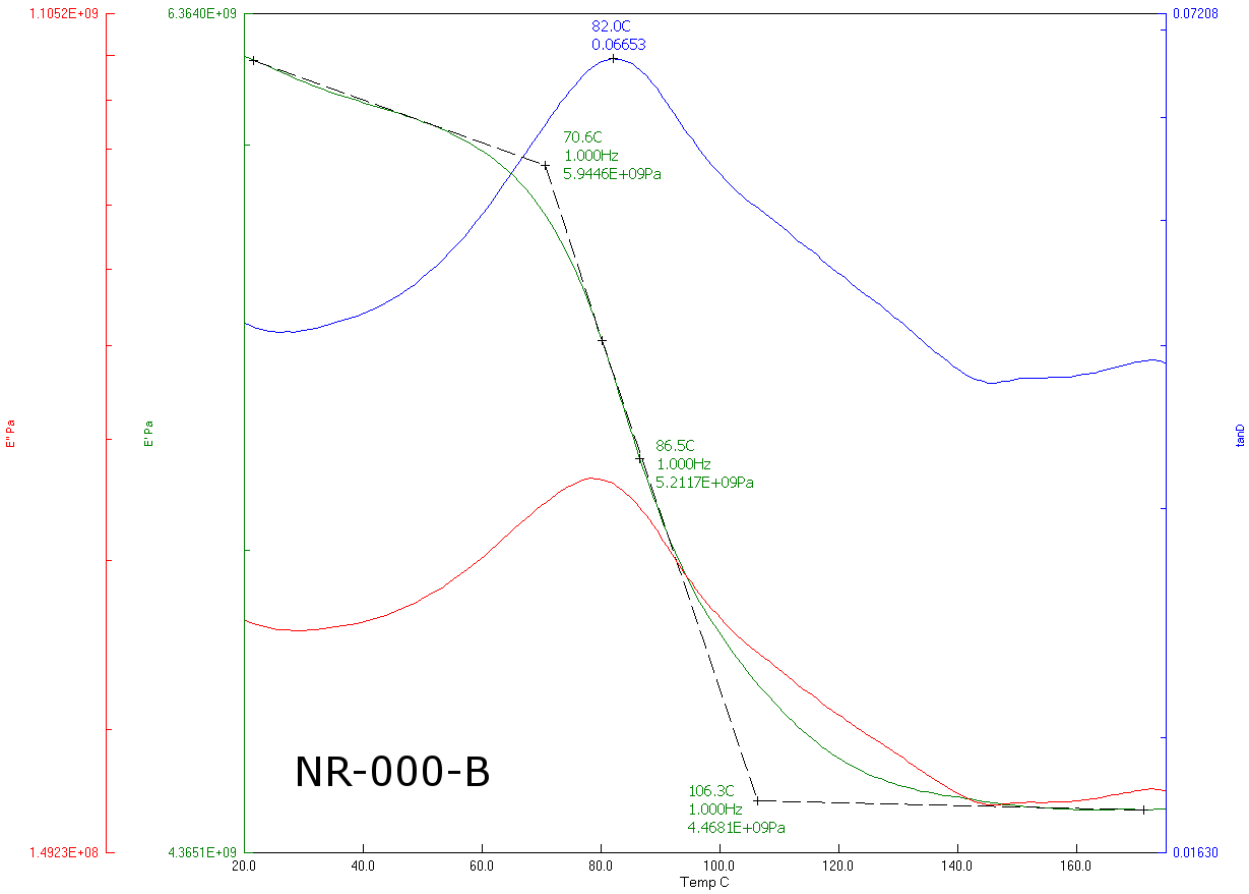

Figure 17: DMA output for NR-000-B

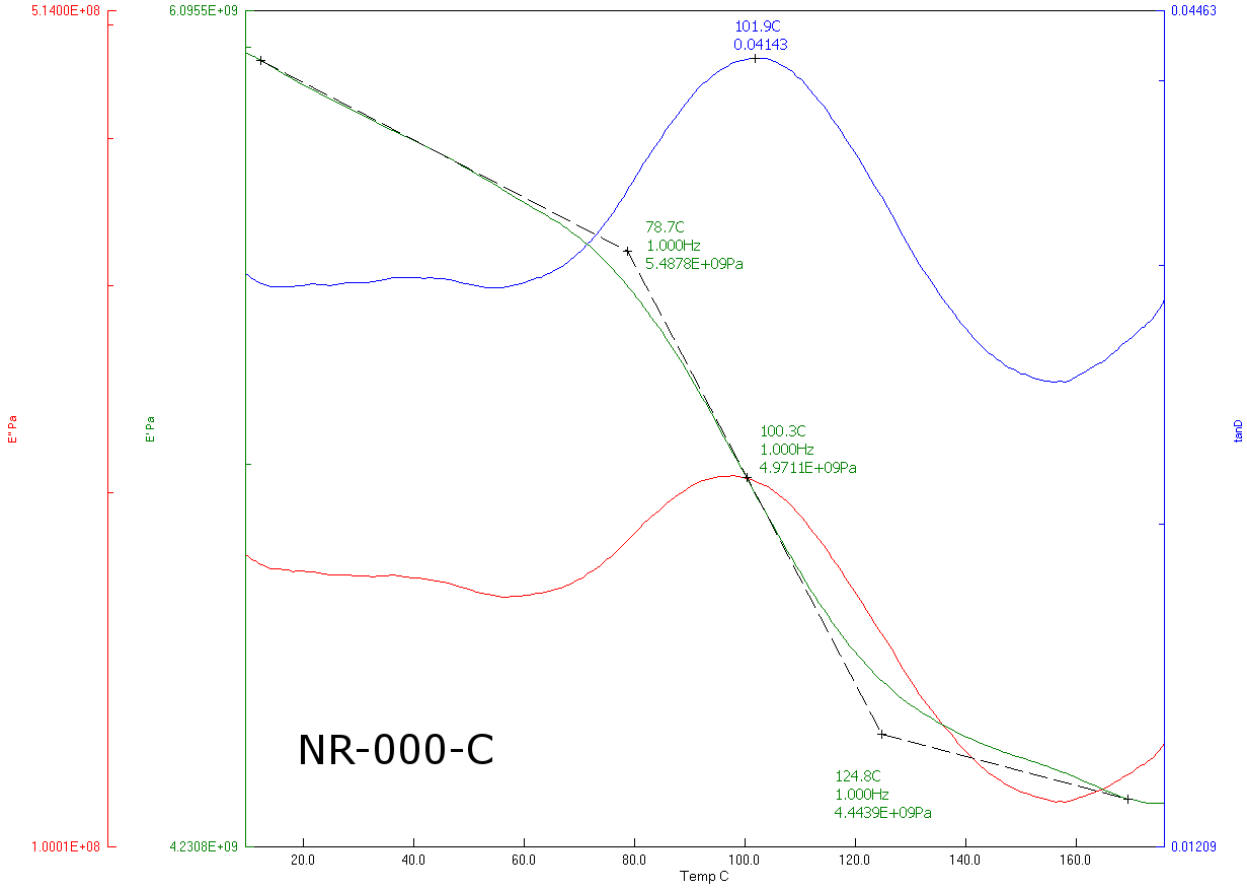

Figure 18: DMA output for NR-000-C

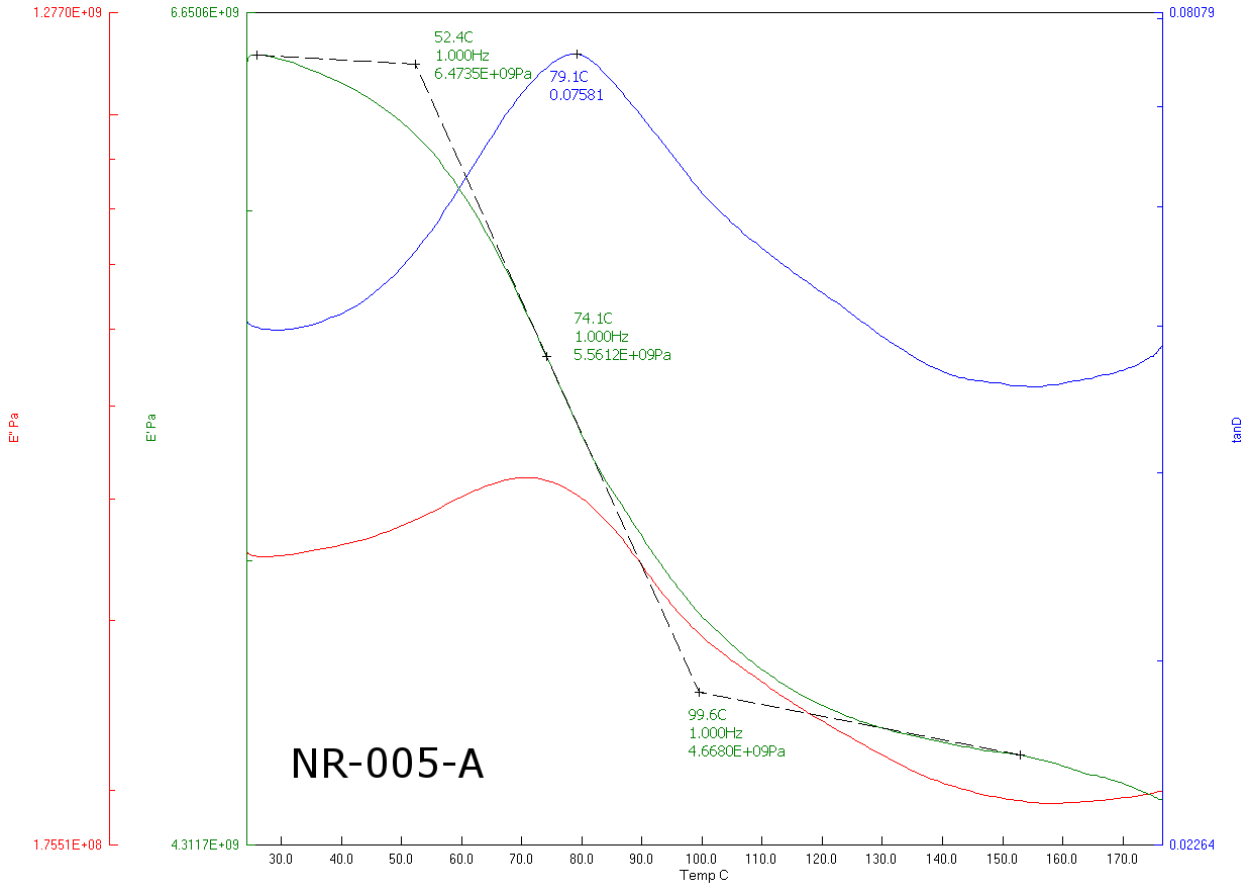

Figure 19: DMA output for NR-005-A

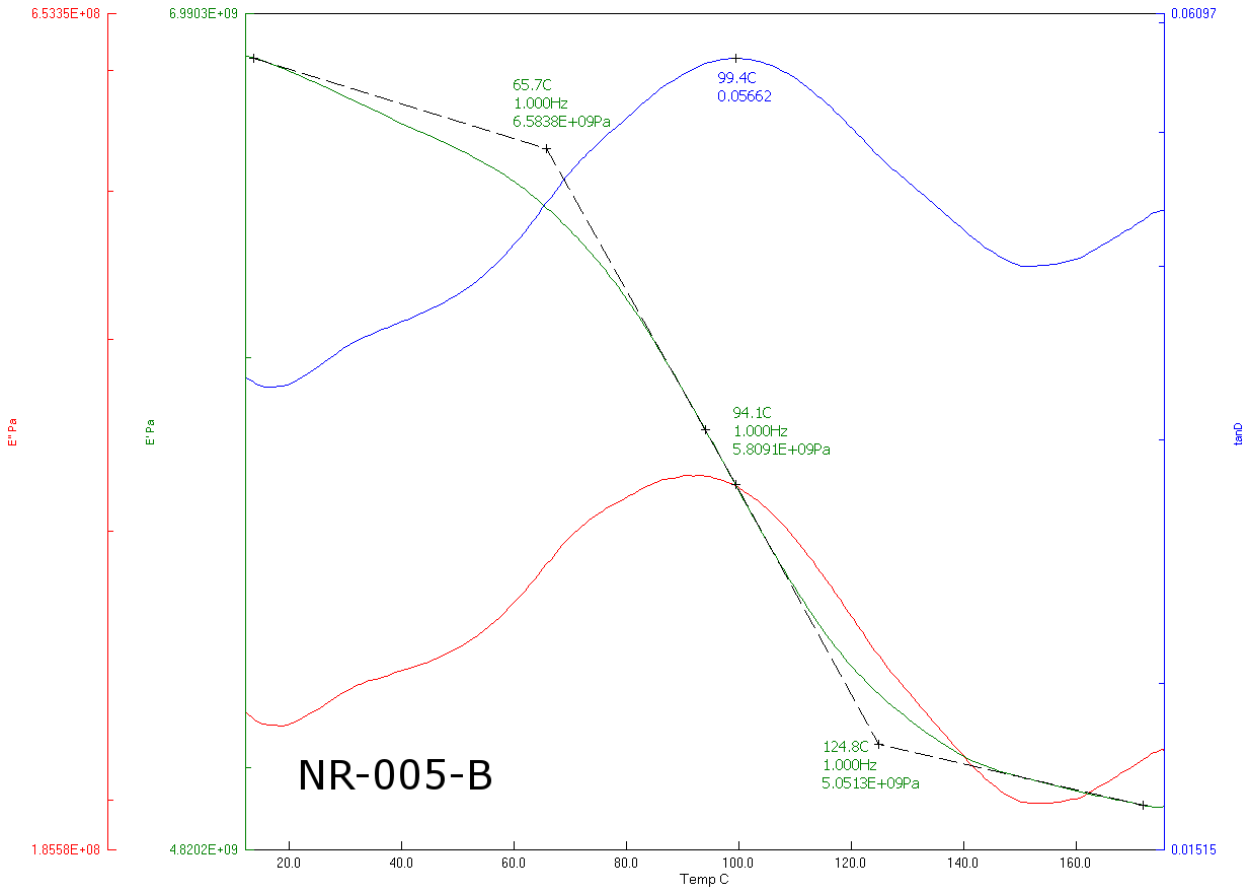

Figure 20: DMA output for NR-005-B

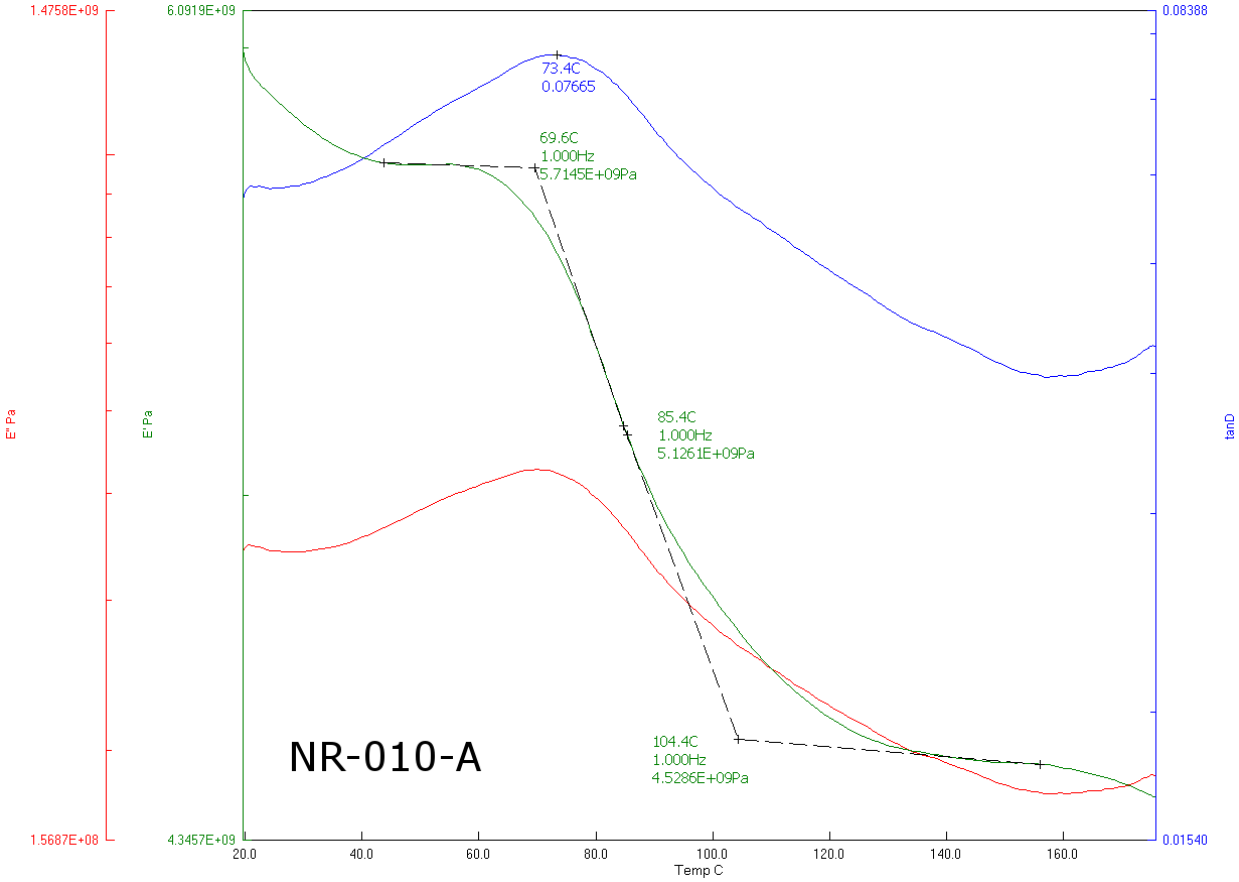

Figure 21: DMA output for NR-010-A

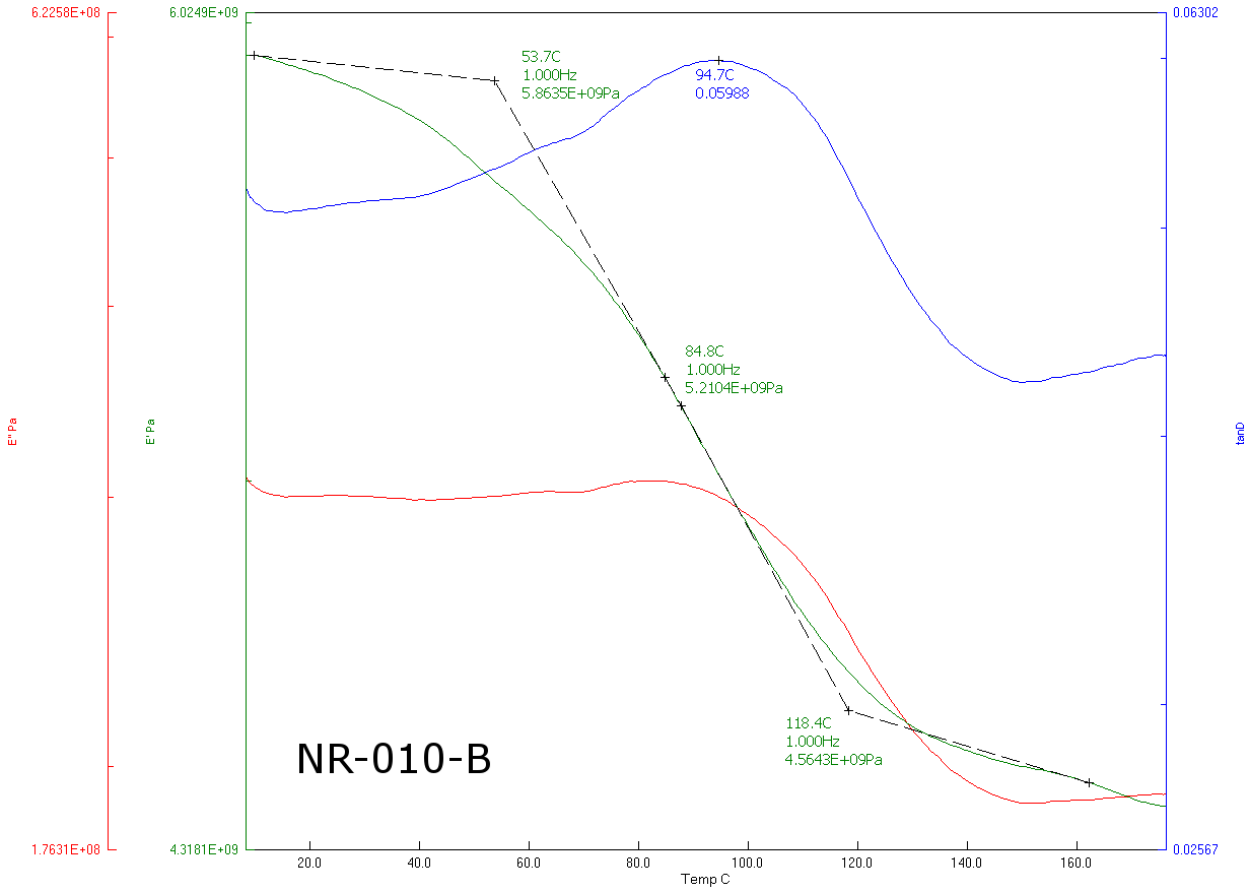

Figure 22: DMA output for NR-010-B

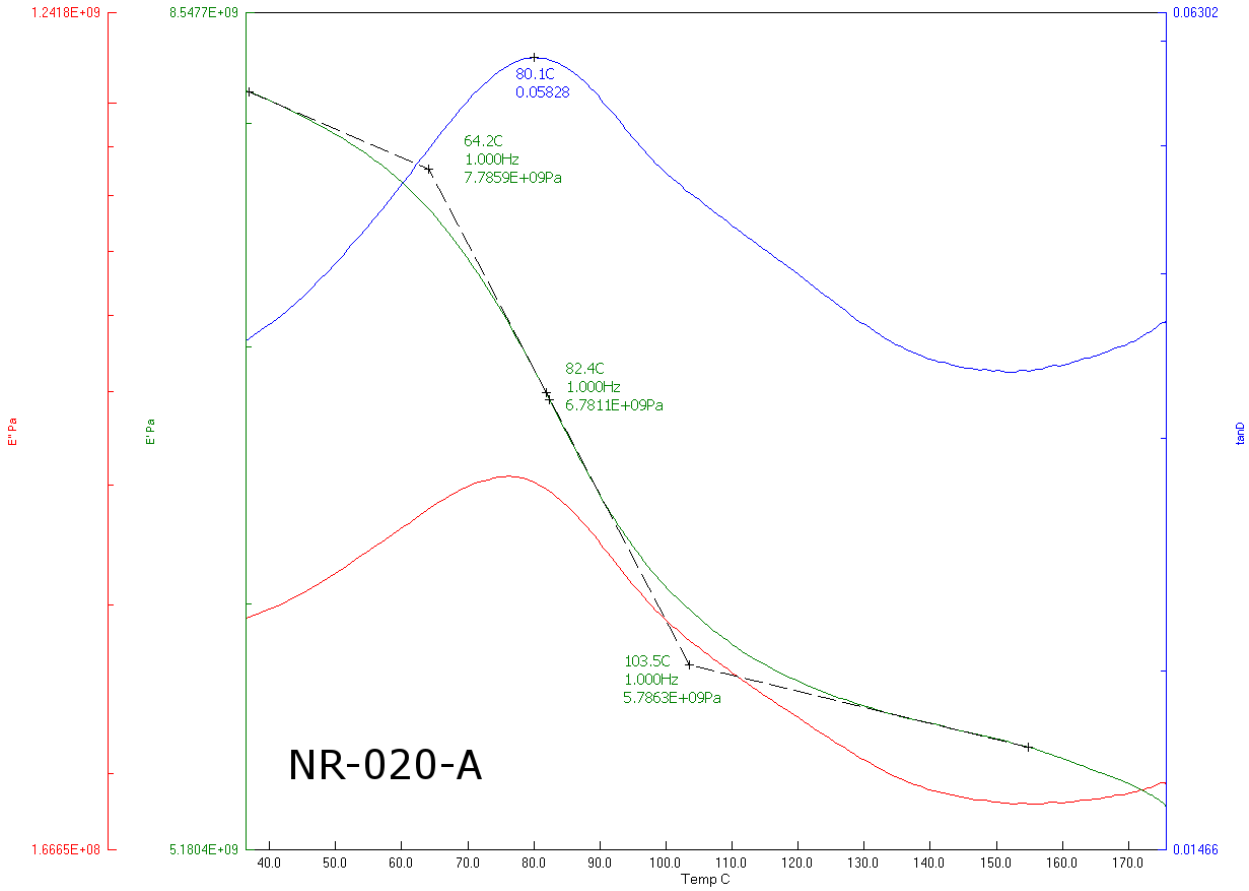

Figure 23: DMA output for NR-020-A

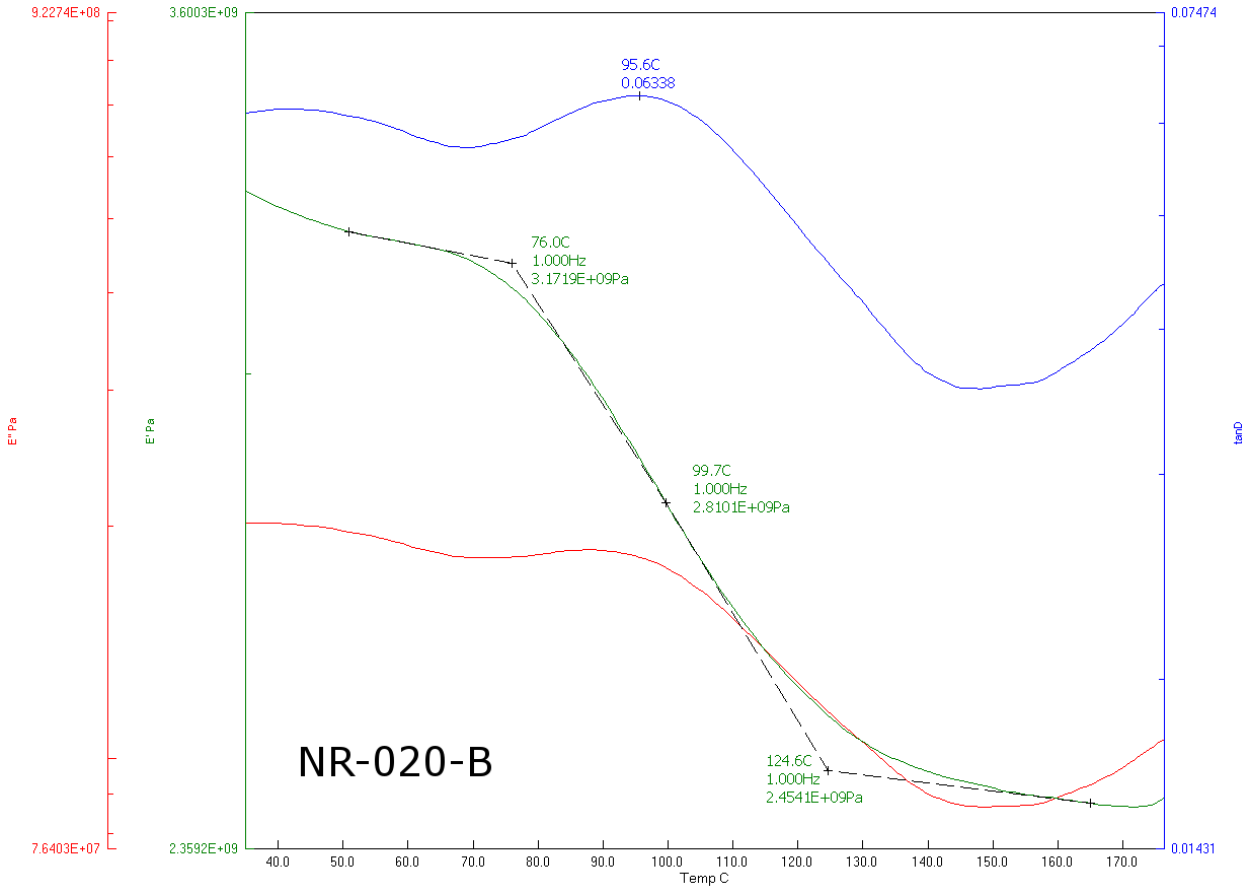

Figure 24: DMA output for NR-020-B

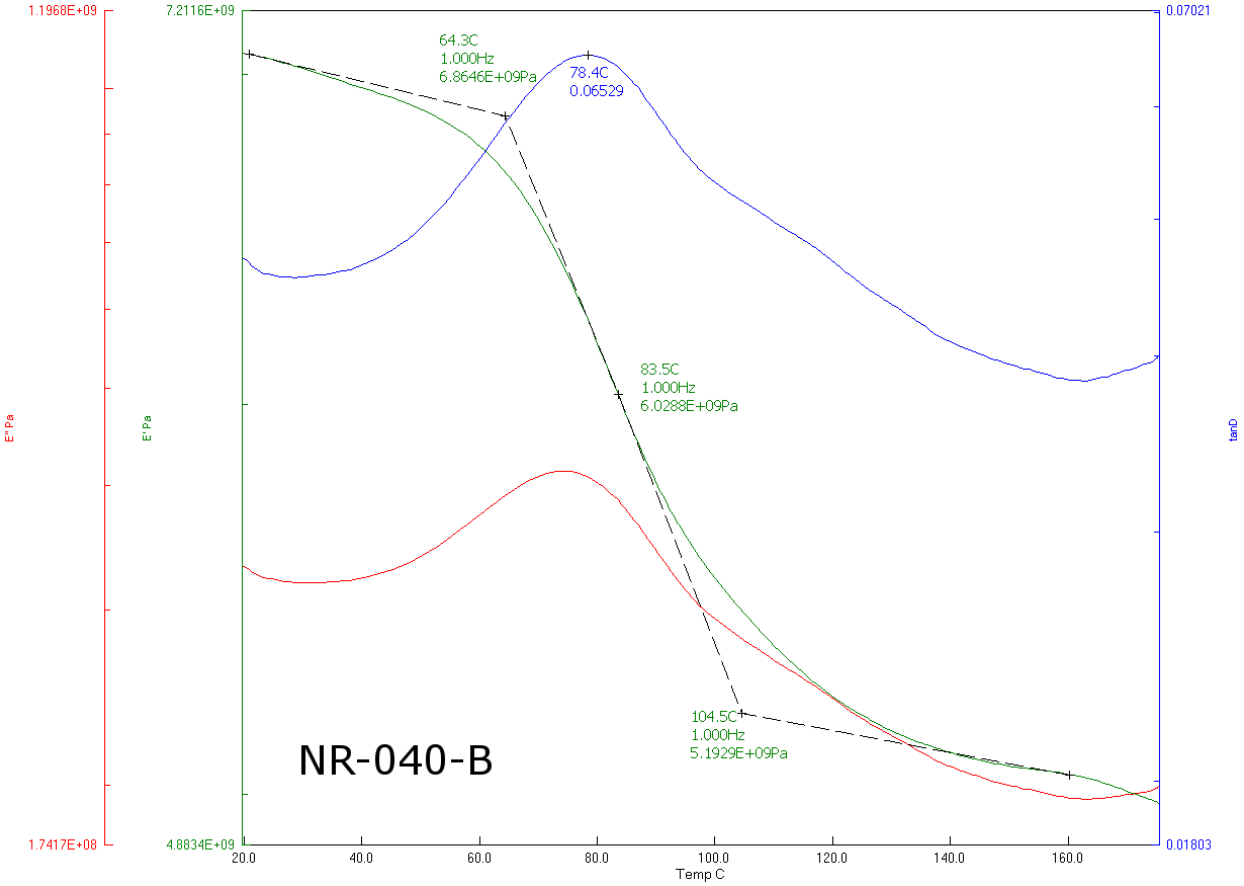

Figure 25: DMA output for NR-040-B

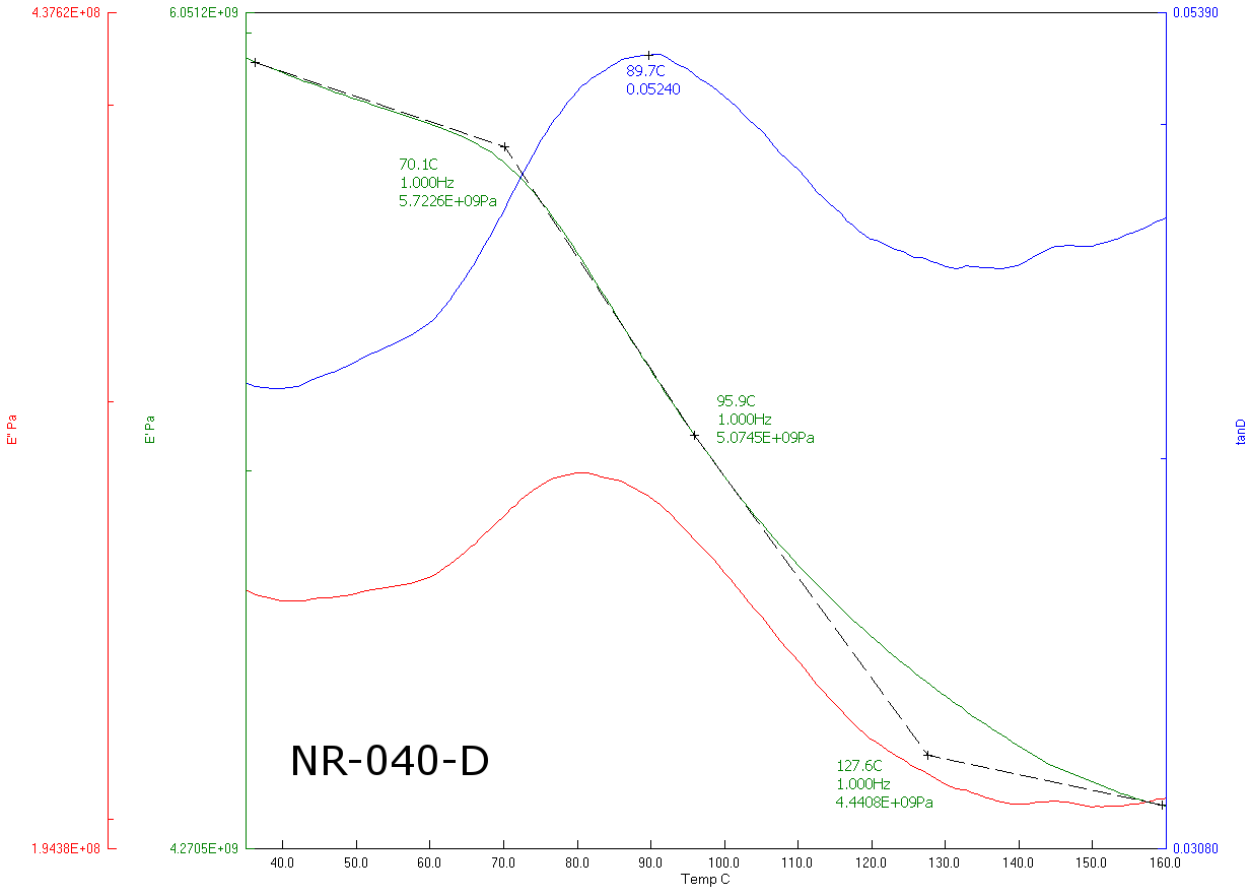

Figure 26: DMA output for NR-040-D

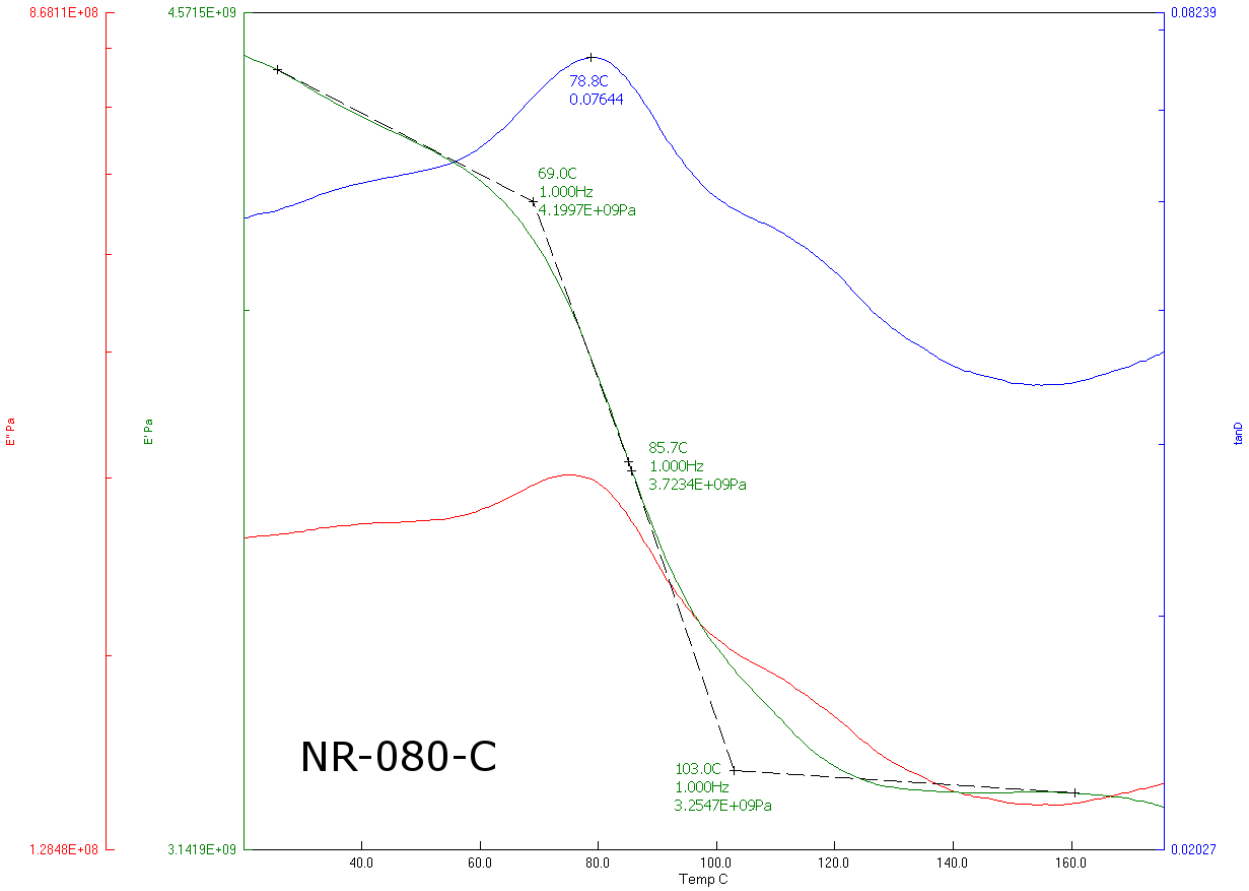

Figure 27: DMA output for NR-080-C

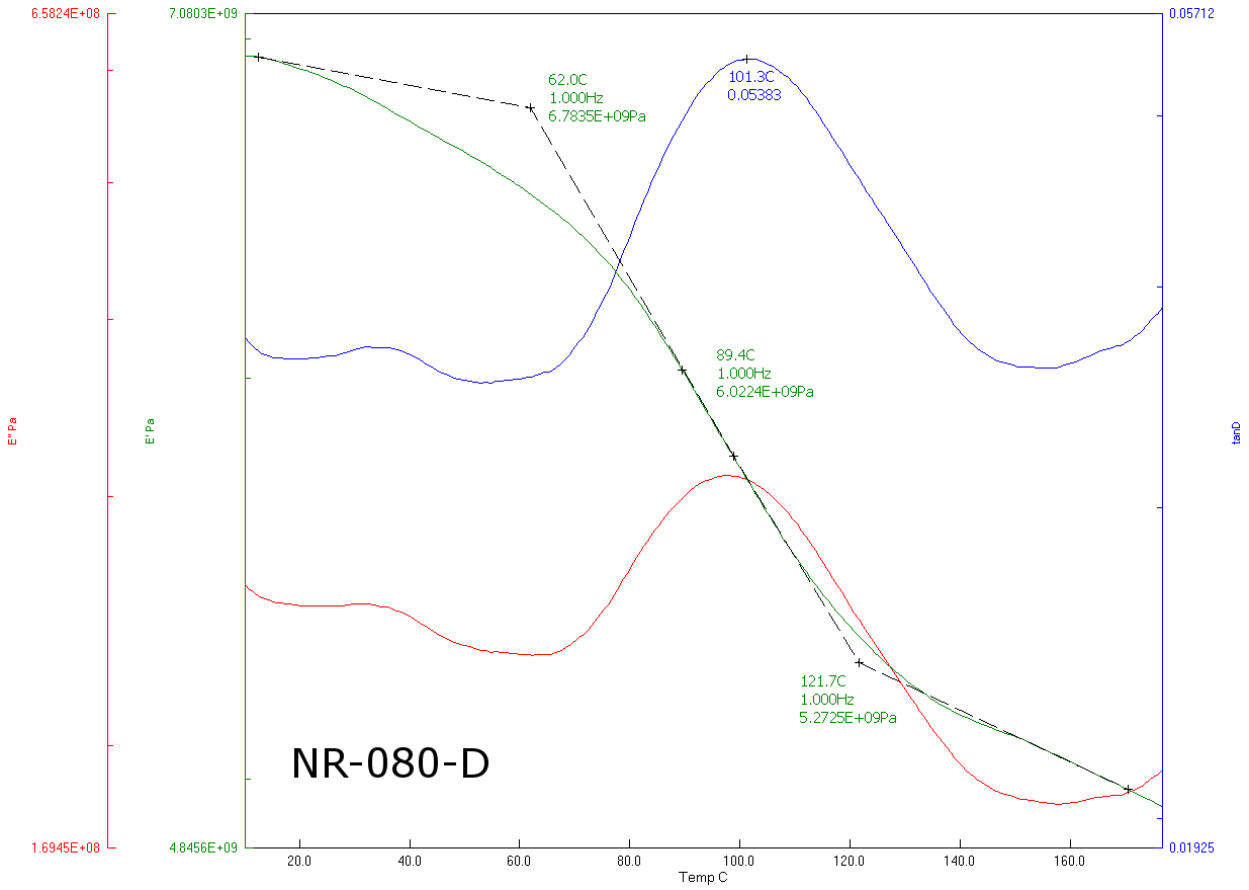

Figure 28: DMA output for NR-080-D

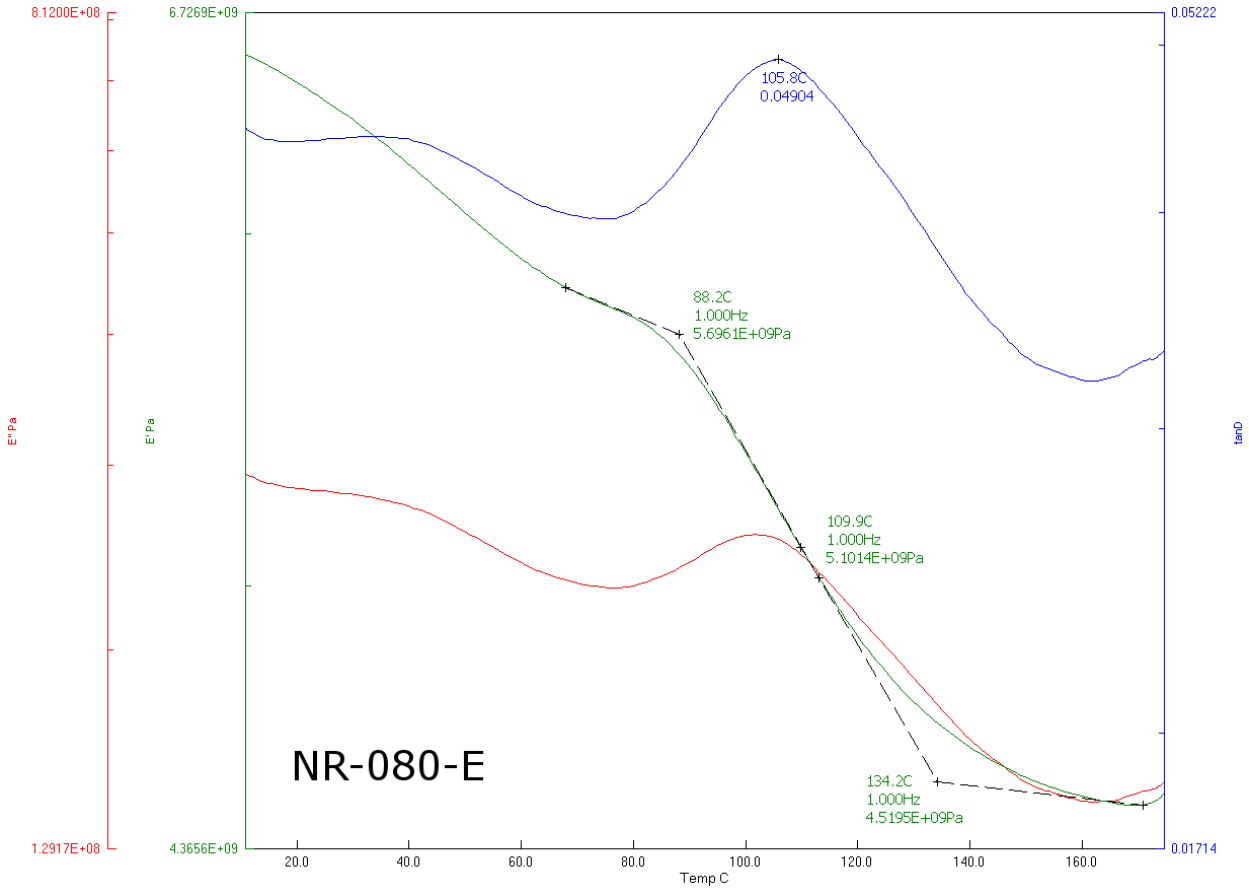

Figure 29: DMA output for NR-080-E

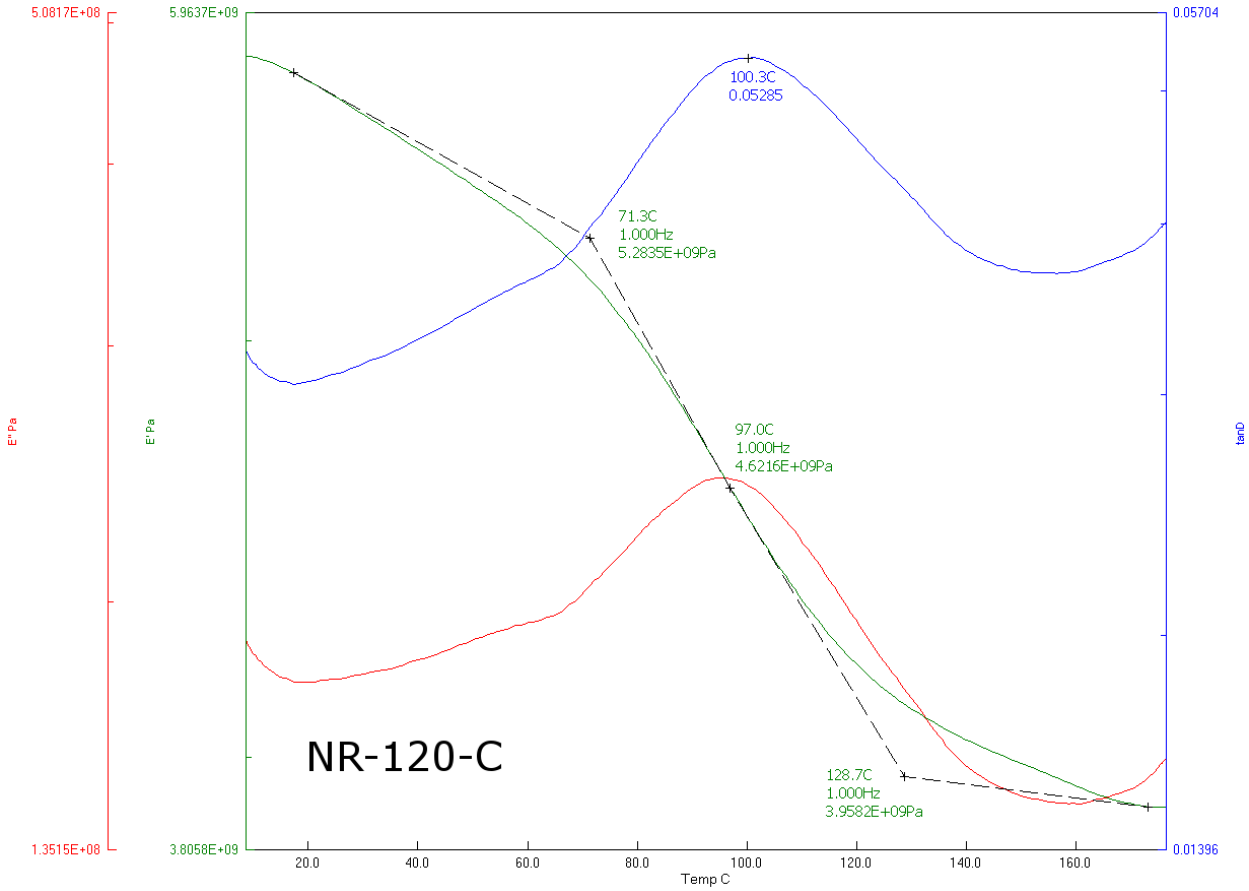

Figure 30: DMA output for NR-120-C

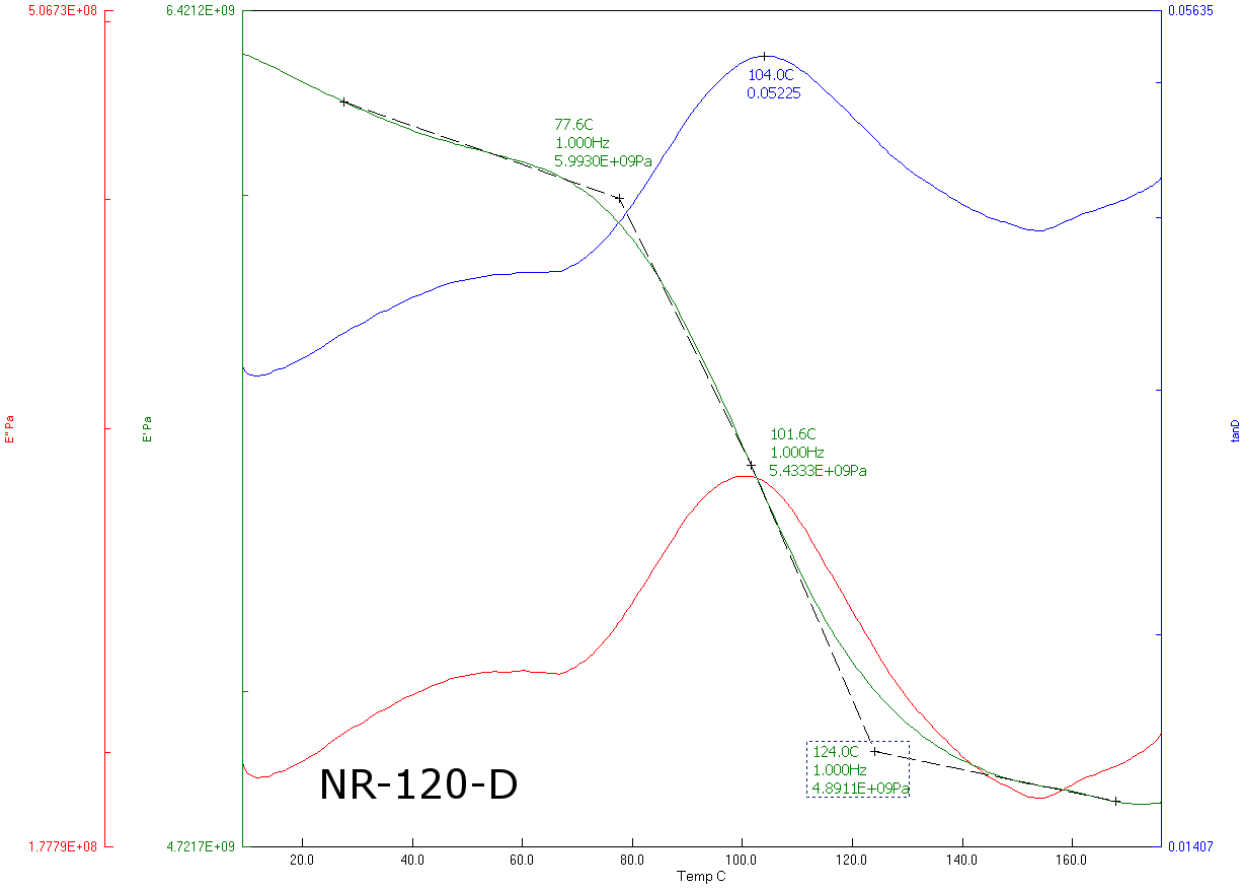

Figure 31: DMA output for NR-120-D

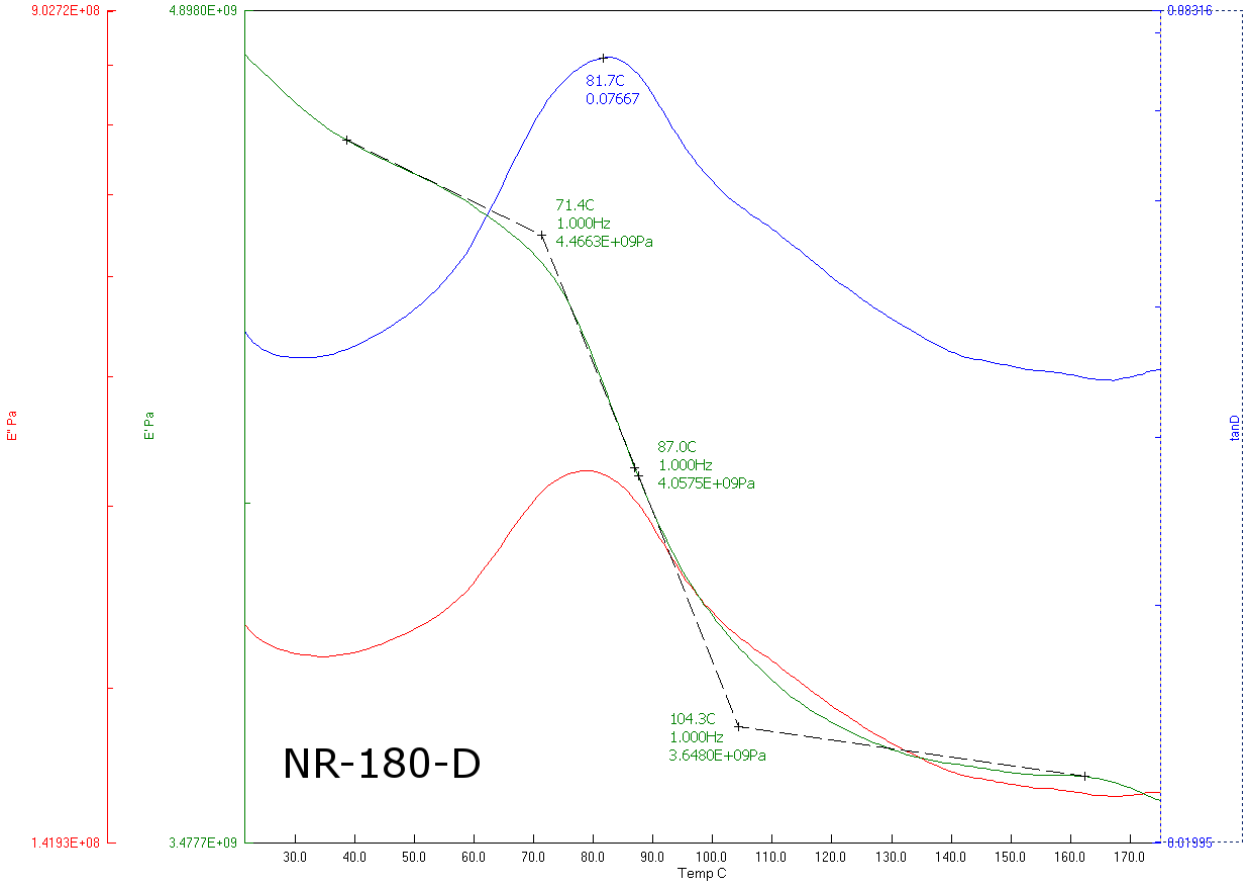

Figure 32: DMA output for NR-180-D

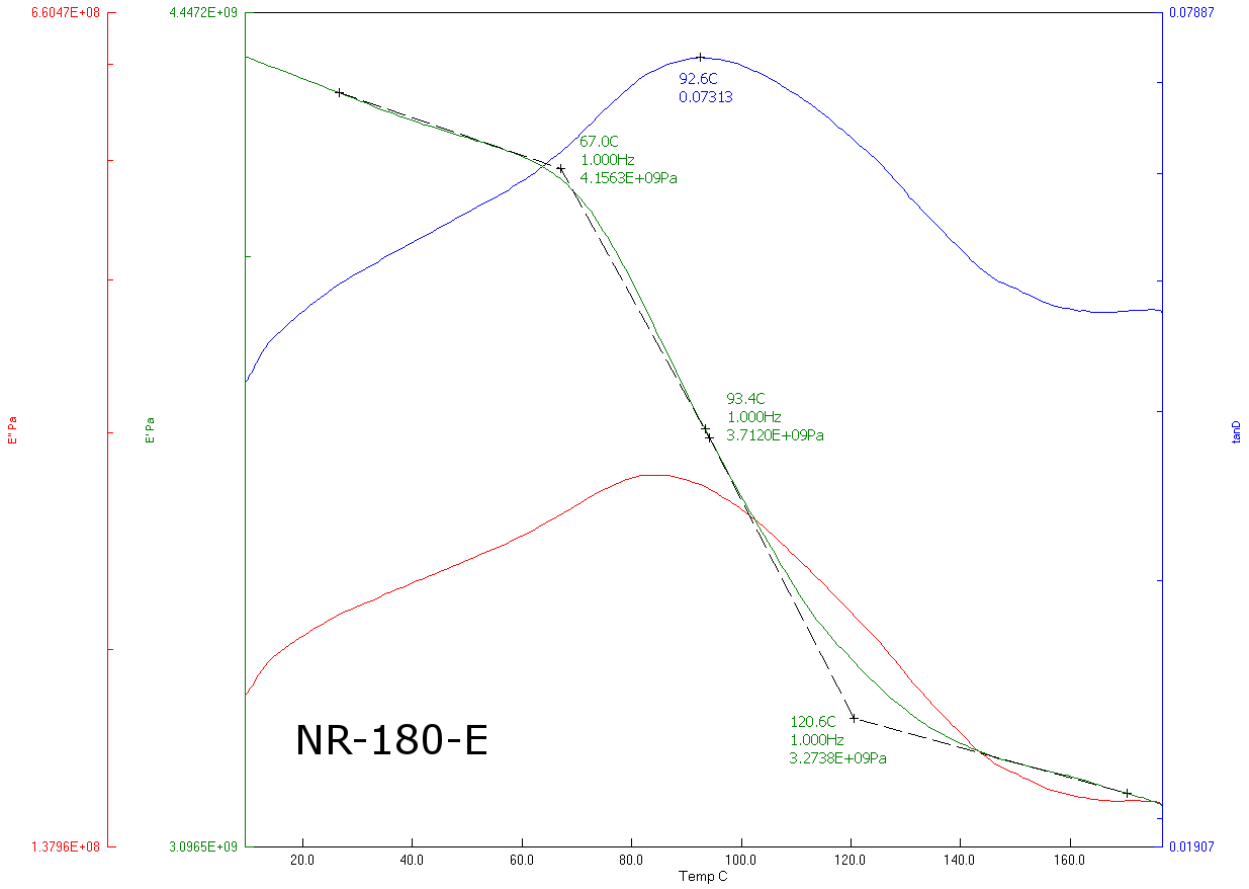

Figure 33: DMA output for NR-180-E

Appendix B: Exclusion of 5 kGy wood samples from principal component analysis of FTIR study

Figure 34 shows the scores plot for PCs 1 and 2 when all dosages are analyzed simultaneously. Each dosage is assigned it's own symbol, but all low dose samples (0-40 kGy) are colored red while all high dose samples (80-120 kGy) are in black. Notice first of all how the greatest distinction is the separation of the 5 kGy sample set from all other dosages along PC1, and that the 5 kGy samples are not exactly grouped well on that axis. All six 5 kGy samples have very similar scores on PC2, but they vary significantly on PC1. According to Figure 35, the variables with the highest loadings on PC1 are the peak around 1654 cm^{-1} and the trough centered around 1550 cm^{-1}. The peak at 1654 cm^{-1} is associated with attached H_2O molecules (Azadfallah et al. 2008), and since moisture content control was not attempted during experimentation, this

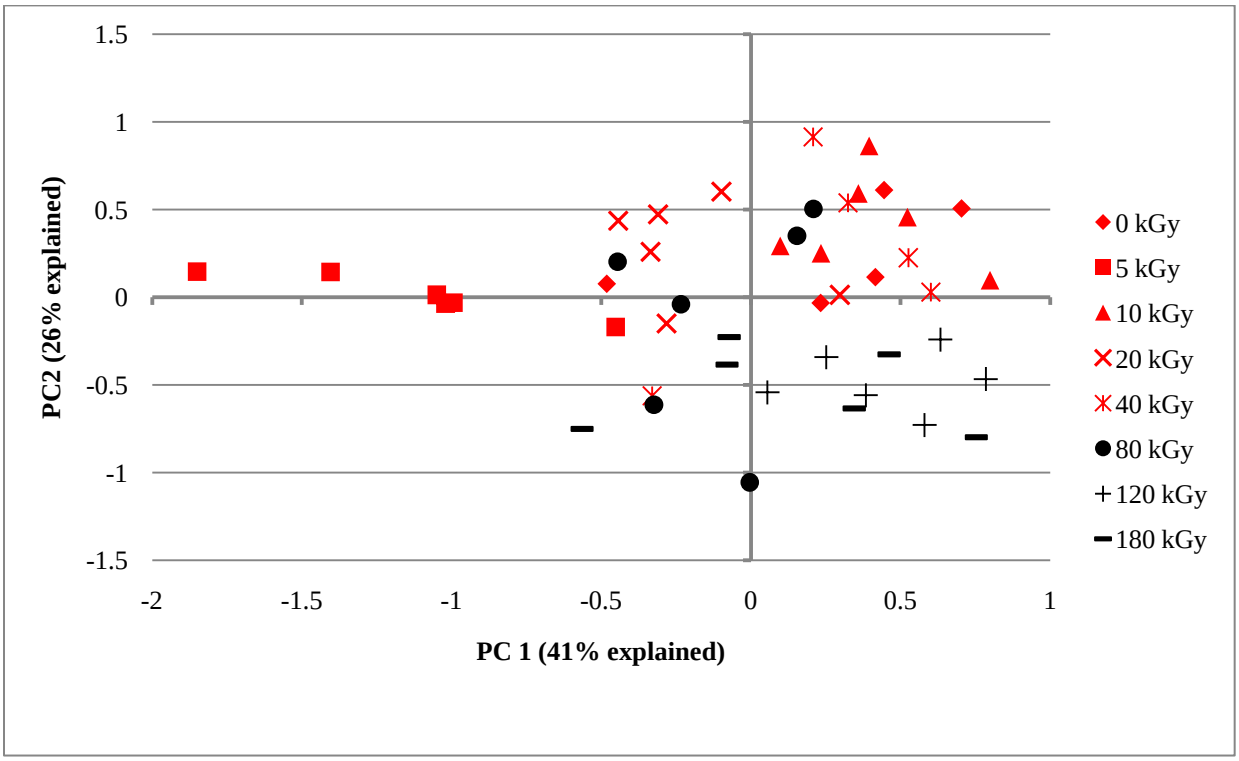

Figure 34: PCA scores for irradiated maple veneers.

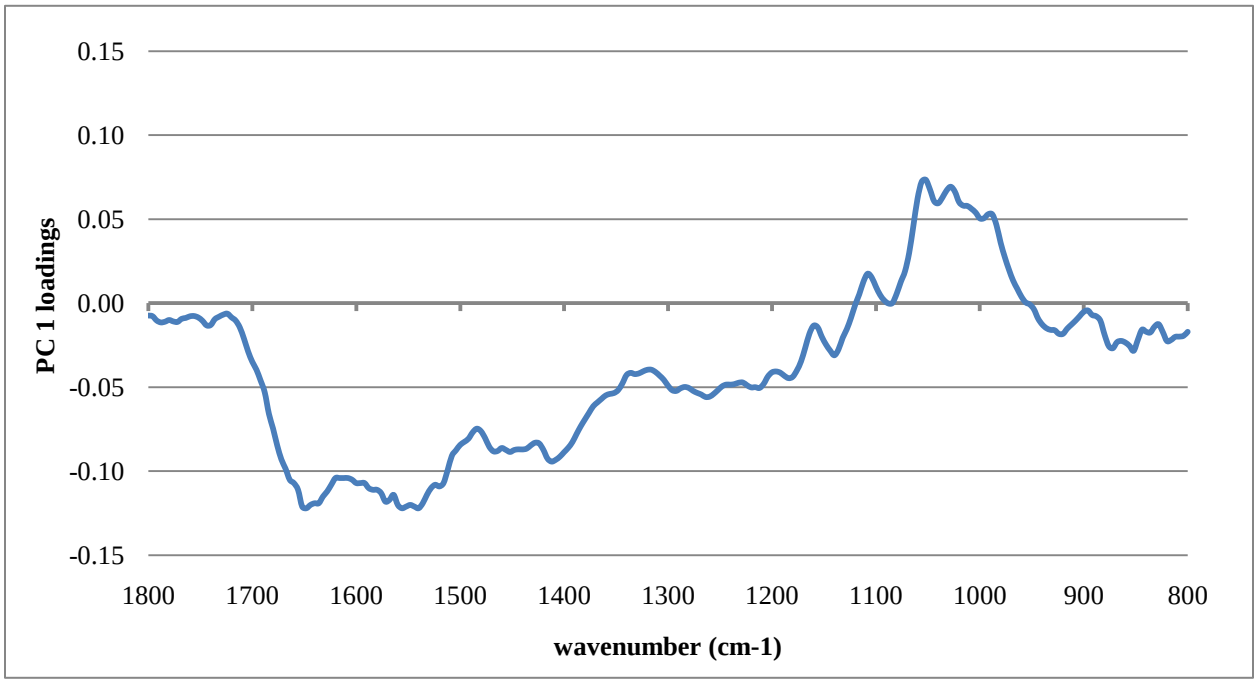

Figure 35: PC 1 loadings plot for irradiated maple veneers.

becomes highly variable and highly unreliable as a point of comparison. In fact, while here it is most obvious for the 5 kGy samples, this peak has unhelpful variability among replicates of all dosages. As for the trough around 1550 cm^{-1}, it lies between two peaks associated with aromatic skeletal vibrations in lignin (Colom et al. 2003), but does not itself have any particular molecular assignment. Because PCA including all dosages is so heavily influenced by these two unhelpful variables, and because they seem to be mostly from the distinction of the 5 kGy samples, the 5 kGy sample set was removed and PCA was run again without them. The resulting PCA scores plot and loadings plot can be seen in Figures 15 and 16 in Chapter 2.

CHAPTER 3: RADIATION CURING OF WOOD COMPOSITES

CHAPTER 3: RADIATION CURING OF WOOD COMPOSITES

Abstract

Current thermal curing practices in the wood composite industry have many downsides, including high energy consumption and cost, time requirements, and internal defects in the wood caused by the elevated temperatures and high pressures. Electron beam (e-beam) radiation curing is a potential alternative to the thermal curing of wood composites, and has already replaced thermal curing in other industries with excellent results as regards energy, cost and time. Preliminary studies have already projected that these same benefits can be brought to the wood composite industry. Some research has already been done to identify radiation curable resins that would work well with wood, and their cure has been characterized. However, wood is made up of components known to be electron scavengers, which means that in a composite system the presence of wood could hinder the cure of the resin. The goal of this study was two-fold: first, to determine whether or not there was good interaction between the resins and the wood, and second, to determine whether or not the cure of the resin was impeded by the presence of the wood. To this end, maple veneers were impregnated with one of two resins and were irradiated with a variety of e-beam dosages (0 – 180 kGy), and then were investigated by means of dynamic mechanical analysis (DMA) and FTIR spectroscopy. The resins used were both di-functional monomers, one with acrylic (R67) and the other with methacrylic (R46) functionality. Also, swelling tests were conducted on maple tiles with the resins to detect interaction between the two. The swelling tests revealed that both resins were able to penetrate the cell walls in the wood. Further evidence of interaction was seen in the reduced T_g of the uncured composites, and via IR spectroscopy which revealed shifts in spectral bands. DMA testing revealed that the cure of the resins was in fact hindered by the presence of the wood. While both neat resins only required 40 kGy to be fully cured, the R67 composites required 120 kGy and the R46 composites required 180 kGy.

Introduction

Wood composites are widely used in structural applications due to their excellent qualities, improved strength and durability over raw wood, and the ability to tailor them to specific needs such as sizes and shapes not possible with wood alone (Ellis 2000). As useful as they are, however, the current manufacturing practices used in their production have many downsides associated with the high process temperature required for the thermal curing of the resins that bind them. The energy usage and costs are high, and the high temperatures can be damaging to the wood. If the moisture content of the wood is too high, steam pressure from the elevated temperatures can cause internal blows in the wood, and if the moisture content is too low, cracks can develop from drying stresses. Internal stresses are created during the cooling cycle after the resin is cured because of the difference in thermal expansion coefficients between the components of the composite (Singh 2001). There are also health and environmental issues associated with the thermally curable resins.

Several other industries facing similar problems have turned to an alternative to thermal curing, namely electron beam (e-beam) radiation curing. E-beam has proved to be a fast, effective method that is much more efficient and economical. For example, in the tire industry, e-beam vulcanization of rubber has proven to be 3-6 times more energy efficient than thermal vulcanization (Stern 2000; Ivanov 1992). In other automotive applications, e-beam is used to bond composites to metal without delamination that typically occurs during the cool-down phase after thermal curing due to differences in thermal expansion coefficients (Goodman & Palmese 2001). In the aerospace industry, e-beam has been used to bond large, integrated structures in fewer steps and at lower cost than via autoclave (Goodman & Palmese 2001). Also, a French aerospace company found that the process time for curing rocket motors was reduced from about a week to less than 8 hours (Beziers et al. 1990). An electron accelerator for radiation curing can be worked into a continuous process able to cure 900 kg/hr, as opposed to 200 kg/hr possible with the batch style production of an autoclave (Singh 2001). Several studies have projected that these same benefits can be brought to the wood composite industry. It is expected that the

energy use requirement for e-beam curing would be about a factor of five lower than thermal curing of wood composites (Singh 2001), and the switch to e-beam curing could potentially save about 65 trillion BTU/yr (Griffith et al. 2006).

In choosing resins to use in a wood composite, compatibility between the wood and the resin is an important factor. The overall success of a composite is greatly affected by the interfacial interaction between its components (Chowdhury & MP Wolcott 2007). If there is no interaction between the wood fibers and the resin matrix, the result will be weak interfacial properties (Kazayawoko et al. 1997), but if strong interactions are present, the composite will exhibit better bond strength (Griffith et al. 2006). Acrylic monomers have been used successfully to bond with wood. Acrylates and methacrylates have been used as coupling agents between wood and other resins because they improve the fiber-resin bond (Kim et al. 2009). One study involving composites made of balsa wood and acrylic monomers cited many benefits of this combination including increased dimensional stability and improvements in the absolute mechanical properties – modulus and toughness (Wright & Mathias 1993). They specifically attributed these benefits to good penetration of the monomer into the cell walls in the wood.

A previous work was conducted to screen potential e-beam curable resins for use in wood composites (Song, 2005). Of the resins studied two difunctional monomers were selected, one with acrylic and the other with methacrylic functionality. Their cure was characterized by tracking the glass transition temperature via dynamic mechanical analysis. Both resins reached full cure by 40 kGy (see Figures 42 and 43) (Bowman, 2006). However, wood has been shown to be affected by e-beam radiation, especially in components containing aromatics and hydroxyls, and therefore in a composite, the wood would act as an electron scavenger, taking some of the dose away from the curing of the resin. As a result, a higher dose may be required to completely cure the composites.

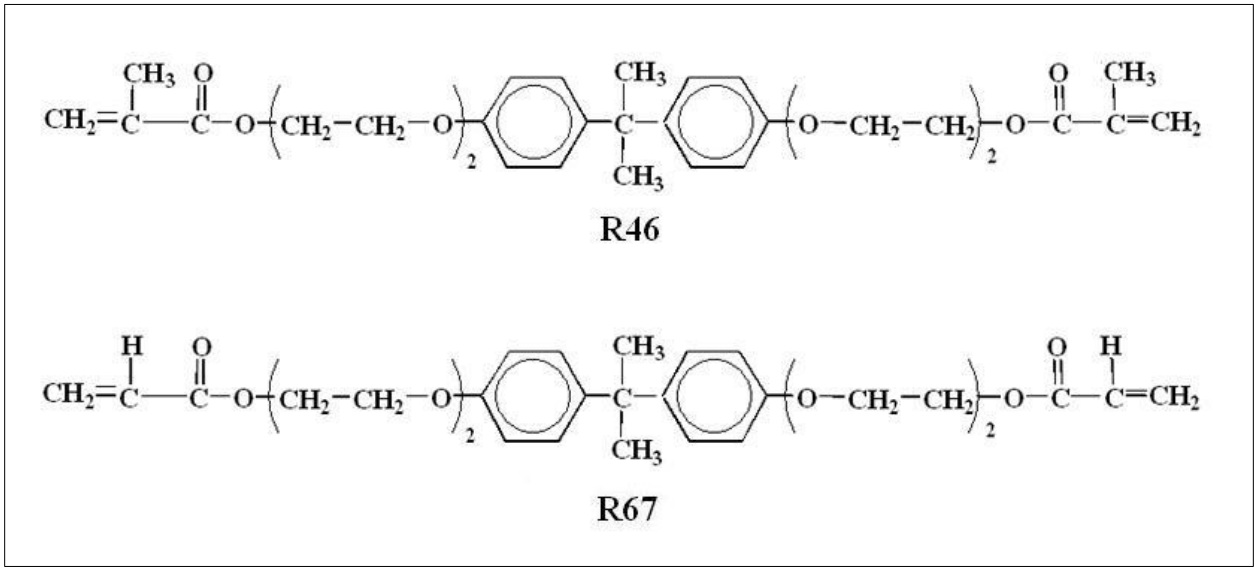

Figure 36: Chemical structures of R46 (methacrylic functionality) and R67 (acrylic functionality). Courtesy of www.sartomer.com.

The goal of this study is to identify whether or not there is good interaction between these resins and the wood, and to determine whether or not the cure of the resins will be hindered by the presence of the wood, and by how much.

Materials and Methods

This study was based on the dynamic mechanical analysis and Fourier-transform infrared spectroscopy of maple veneers loaded with one of two resins, and irradiated with one of eight radiation dosages. Six replicates were created for each combination yielding a total of 96 samples. Also, swelling experiments were conducted with small maple tiles soaked in each resin.

Materials and Sample Preparation:

Maple veneer measuring 0.5 mm thick was cut into strips measuring 9.64 +/- 0.04 mm in the longitudinal direction and 50 +/- 2 mm in the radial direction. Given the heterogeneous nature of the composition of wood, great measures were taken to eliminate as much variation as possible between samples in every stage of sample production. Less emphasis was placed on the length of the samples than the width because the equipment used in the DMA dictated a uniform length, provided that the samples were at least 48 mm long.

The resins used were provided by Sartomer Company, Inc. (Exton, PA). In this study, R46 refers to ethoxylated (4) bisphenol-A dimethacrylate resin (Sartomer trade name SR540), and R67 refers to ethoxylated (4) bisphenol-A methacrylate resin (Sartomer trade name SR601). Figure 36 shows the chemical structures of these resins. The resins were warmed to 50ºC, a temperature high enough to lower the viscosity but not cause degradation. Resin loading was accomplished by submerging the veneers into the preheated resins for several minutes, beyond the point at which bubbles stopped forming on the surface of the wood. In all, 48 veneers were soaked in each resin. After the samples were removed from the resin baths they were handled with only non-absorbent tools and materials so as to not draw out the impregnated resin. Excess resin was wiped off of the veneers and they were placed immediately into individual pre-labeled and pre-weighed bags. The samples were then reweighed and the amount of resin loading calculated. The average weight fraction of resin in the R46 samples was 30.7%, and 29.2% in the R67 samples.

The samples were sent to an electron beam facility at Sterigenics in San Diego, CA, where sample sets from each resin treatment received one of the following doses of radiation: 0, 5, 10, 20, 40, 80, 120, 180kGy. The electron accelerator at this facility is rated at 12 MeV and 8 kW with a six ms pulse at 180 Hz.

Swelling experiments:

Swelling experiments were conducted with ten pieces of maple wood measuring approximately one inch wide (tangential), two inches long (longitudinal), and 1/16" thick (radial). Each dimension of each sample was measured with calipers in two locations and recorded. Then four samples were submerged in resin R46, four in resin R67 and the remaining two in water and left to soak for several hours, after which they were removed and remeasured in the same locations.

Dynamic Mechanical Analysis:

Dynamic mechanical analysis was performed in a (Perkin Elmer Diamond DMA) using dual cantilever bending mode, employing sinusoidal oscillation at frequencies of 1, 2, 4, 10 and 20 Hz. Temperature scans were conducted from room temperature up to about 170ºC at a scanning rate of 5ºC/min. Because of the presence of residual stresses in the composites, each sample was run through that temperature range twice, the first time to relieve those stresses, and the second for data collection.

Infrared Spectroscopy:

Infrared spectra were collected from the samples using a Perkin Elmer Spectrum One instrument with an attenuated total reflectance (ATR) accessory. Sixteen scans at a resolution of $8cm^{-1}$ were taken and averaged from each sample before resin loading and after radiation. To minimize the effects the variations of wood may have on the spectra, a simple jig was created to make sure that the samples were scanned on the exact same spot both times.

The infrared spectra were analyzed using the Unscrambler, a multivariate data analysis program produced by Camo. Data pretreatments were performed on the collected spectra to prepare them for analysis. First, to remove scatter effects from the data, multiplicative scatter correction (MSC) was applied. Scatter effects are the result of physical characteristics, such as particle size and density, rather than chemical characteristics and therefore need to be removed from the spectral data. The non-uniformity of wood from sample to sample is a source of such effects.

Next, the spectra were normalized by mean normalization, which is to say that each variable in each spectrum was divided by the mathematical average of the variables in that spectrum. The result of this transformation is that the areas under the spectra are made equal, which increases the quantitative value of the study. Finally, the variables were averaged by four, which was a significant enough reduction of variables to reduce noise and decrease the data process time, but without compromising the resolution of the spectra.

Results and Discussion:

Swelling Experiments

Swelling experiments were conducted with small tiles of maple wood and each of the experimental resins to determine whether or not those resins would plasticize the wood. An increase in the dimensions of the wood when soaked in resin would be the result of an increase in the free volume among the lignin and cellulose chains, and would be an indication of interaction between the resin and the wood polymers (Sheikh & Afshar Taromi 1993). The results of the swelling experiments can be seen in Table 1.

	R46	**R67**	**Water**
Radial	4.47 (0.78)	3.75 (1.01)	7.38 (1.10)
Tangential	4.73 (0.66)	4.48 (0.69)	7.77 (0.36)
Longitudinal	0.34 (0.15)	0.42 (0.22)	0.24 (0.04)

Table 1: Percent swelling of maple wood in R46, R67 and water. Standard deviation noted in parentheses.

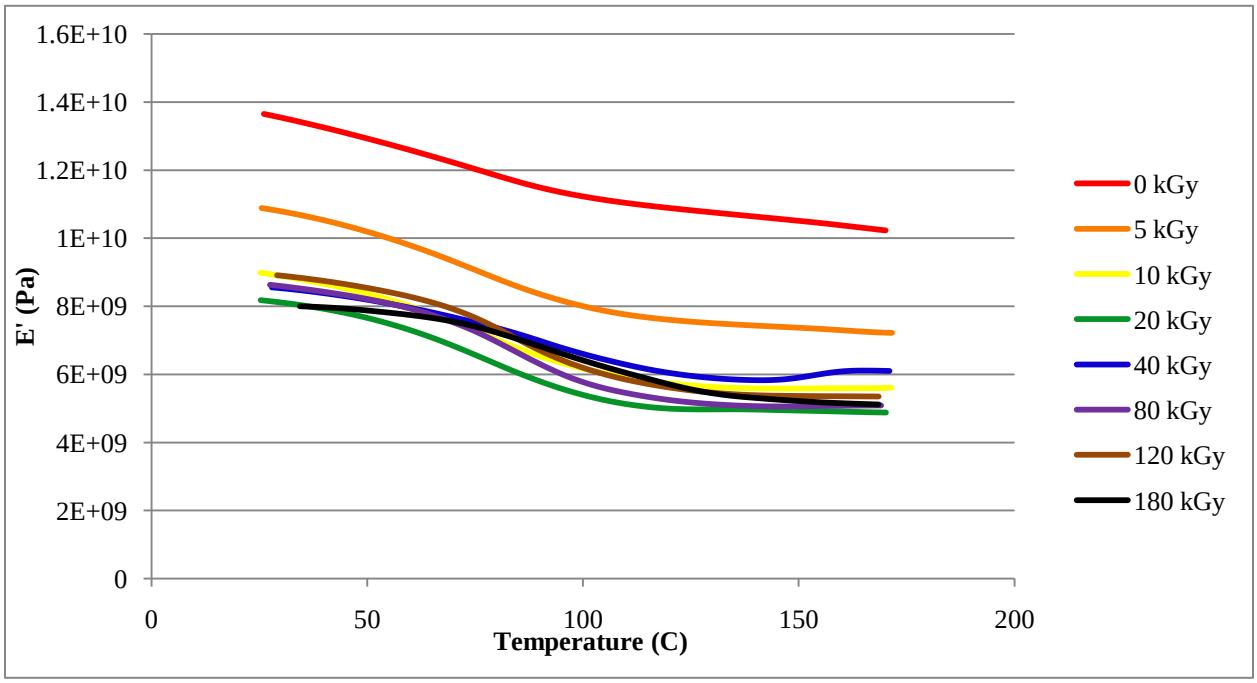

Figure 37: Storage modulus (E') curves for R46 composites at different doses of radiation.

The same experiment was conducted with water, which is already known to swell wood, and those results are also reported in Table 1 for comparison with the two resins. In all cases, almost no swelling occurs in the longitudinal direction, which was expected due to the orientation of the cellulose chains along the wood grain. Also, all results indicate more swelling in the tangential direction than the radial direction, but only fractions of a percent separate the two figures. Both resins caused notable and consistent swelling in the wood, though neither of them as much as the water. R46 caused slightly more swelling in the radial and tangential directions than the R67, which hints at the R46 being able to plasticize the wood a bit more than the R67. Further evidence of plasticization of the wood by the resins will be discussed with the DMA and infrared spectroscopy results.

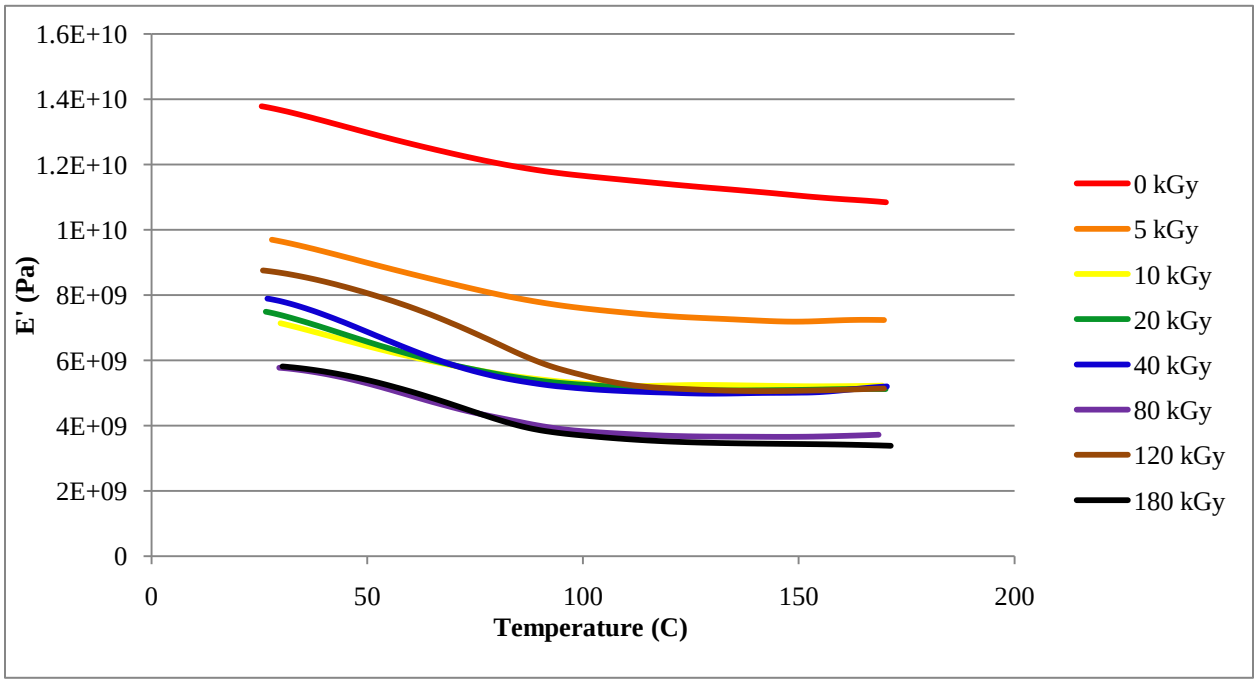

Figure 38: Storage modulus (E') curves for R67 composites at different doses of radiation.

Dynamic Mechanical Analysis

Dynamic mechanical analysis measures the response of the samples to oscillatory flexing over a range of temperatures. A stress is applied to the sample and the resulting strain and response time are measured. This is done repeatedly at a variety of frequencies – in this study 1, 2, 4, 10 and 20 Hz were used. The temperature range used was from room temperature (about 20^{o} C) to 170^{o} C, which was sufficient to cover the glass transitions of the wood (lignin at about 90^{o}C), and the resins (R46 at about 120^{o}C at final cure; R67 at about 80^{o}C at final cure). From these measurements, the DMA outputs the storage modulus (E'), loss modulus (E") and tan δ curves for each sample. These outputs can be seen for each individual sample in Appendix C, and the results of averaged replicates of each output type are shown in Figures 37-38, and 40-43.

The storage modulus represents the relative stiffness of the sample, which is higher before the transition from the glassy region to the rubbery region. Both Figure 37 and Figure 38 show that

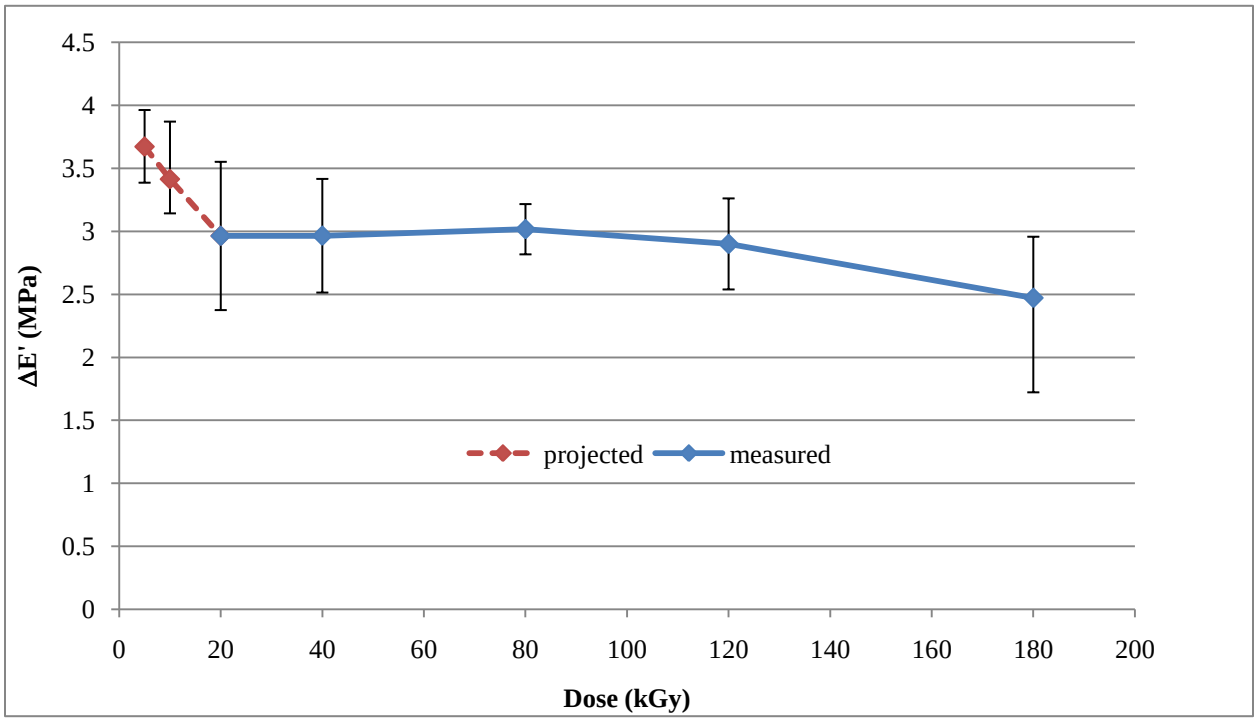

Figure 39: ΔE' for irradiated R46 composites.

for R46 and R67, respectively, the uncured (0kGy) and 5kGy samples exhibited higher storage modulus than the rest of the samples and, in fact, seem to indicate that with increased dosage, decreased stiffness was observed. This is counterintuitive to what is expected for such a system. First of all, given the evidence of plasticization from other tests, the modulus should be lower for uncured, resin-laden wood samples. Furthermore, as the resin in the composite is cured, the samples should be exhibiting more stiffness, not less. In other words, the modulus should be increasing, not decreasing. However, both R46 composites and R67 composites, including two or three replicates of each sample, consistently show this reversed behavior.

Figure 39 shows the ΔE' values calculated for R46 composites, with error bars indicating high and low values from replicates of each dosage. ΔE' is the measure of the decrease in modulus across the glass transition. According to Sepe, "in semi-crystalline and crosslinked systems the reduction in storage modulus is less severe due to the supporting influence of the crystalline or

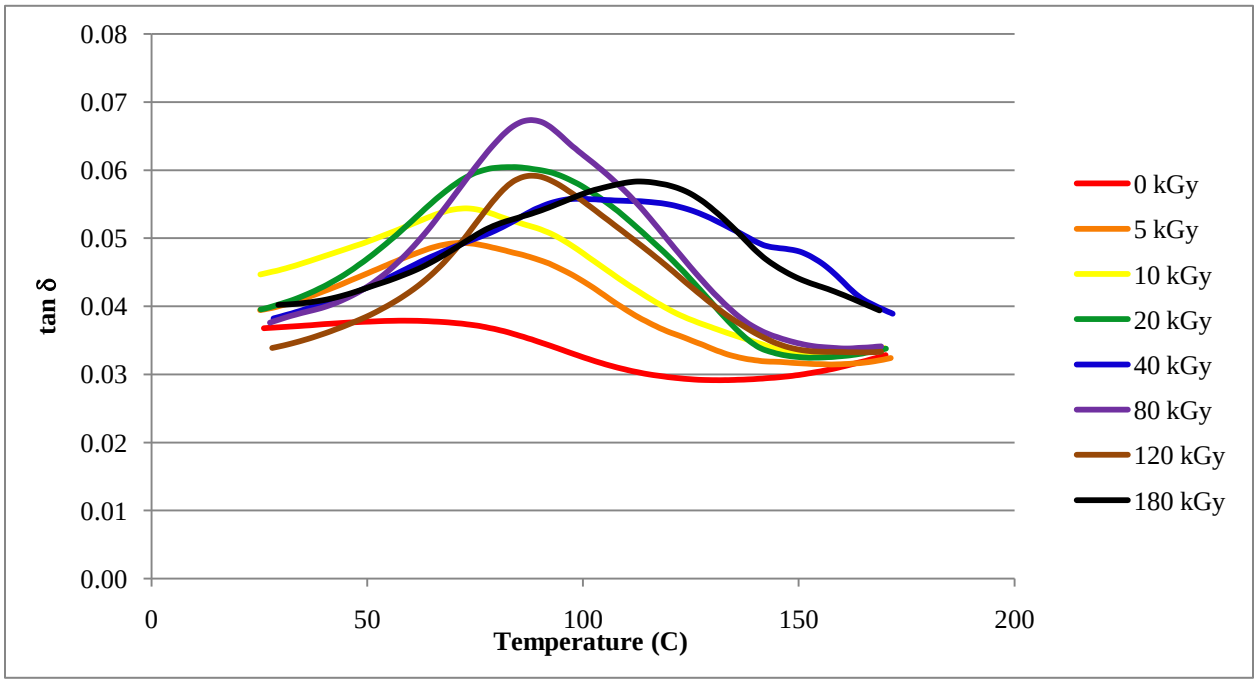

Figure 40: Tan δ curves for irradiated R46 composites.

crosslinked network" (Sepe 1997). It has been shown previously that even at very high doses of radiation, the degree of crystallinity in the cellulose does not change (Griffith et al. 2006), so the only contributing factor could be an increase in crosslinking. Therefore, ΔE' can be used to track curing of a resin system because the change in storage modulus should decrease as crosslinking increases. In calculating ΔE', one problem with the lower doses was that the glassy plateau was not visible within the testing temperature range and therefore the E' values at the onset of the glass transition were unknown. However, for the 5 and 10 kGy doses, enough of the relaxation slope was present that the change in modulus could be approximated simply by taking the highest point available and subtracting the E' value from the rubbery plateau. The glassy plateau would be at least that high, if not higher, so the approximated ΔE' values are at least as big as reported, if not bigger. These are shown in Figure 39 in red. There was not enough data from the uncured samples (0 kGy) to even attempt such an approximation.

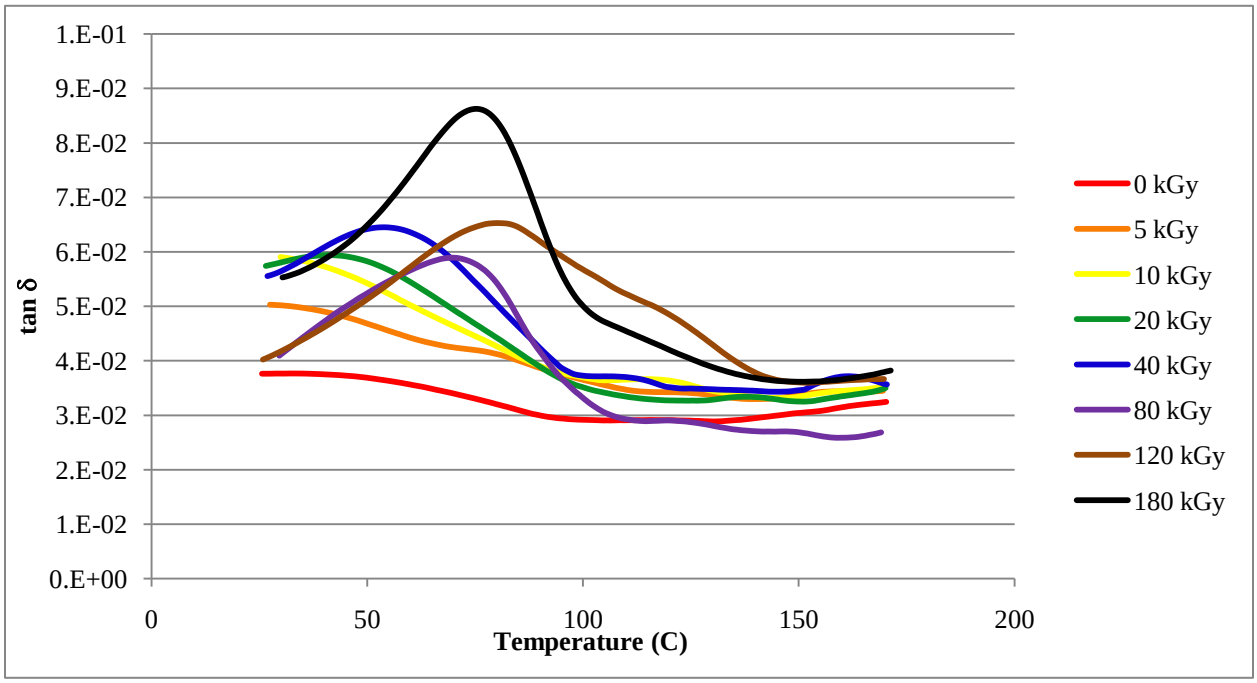

Figure 41: Tan δ curves for irradiated R67 composites.

From Figure 39 we can see that in R46 composites, crosslinking increased through the 20 kGy dosage before stalling until it began to increase again somewhere after 80 kGy. In cure studies of neat R46 resin, 40 kGy was required to reach complete cure (Bowman, 2006) (see Figure 42 for graphical representation). It seems that in the composite system cure was hindered from progressing around 20 kGy, and finally proceeded to completion (or closer to it) at much higher doses. This is not an unexpected result given the hydroxyls and unsaturated components in wood, which are electron scavengers.

R67 does not have the methacrylic functionality that R46 has, and therefore R46 has a higher T_g due to the presence of the CH_3 side group which encumbers chain movement. This, along with the curing hindrance provided by the presence of the wood, results in a lower glass transition for R67, and as can be seen in Figure 38, even less of the glassy plateaus and relaxation slopes of the

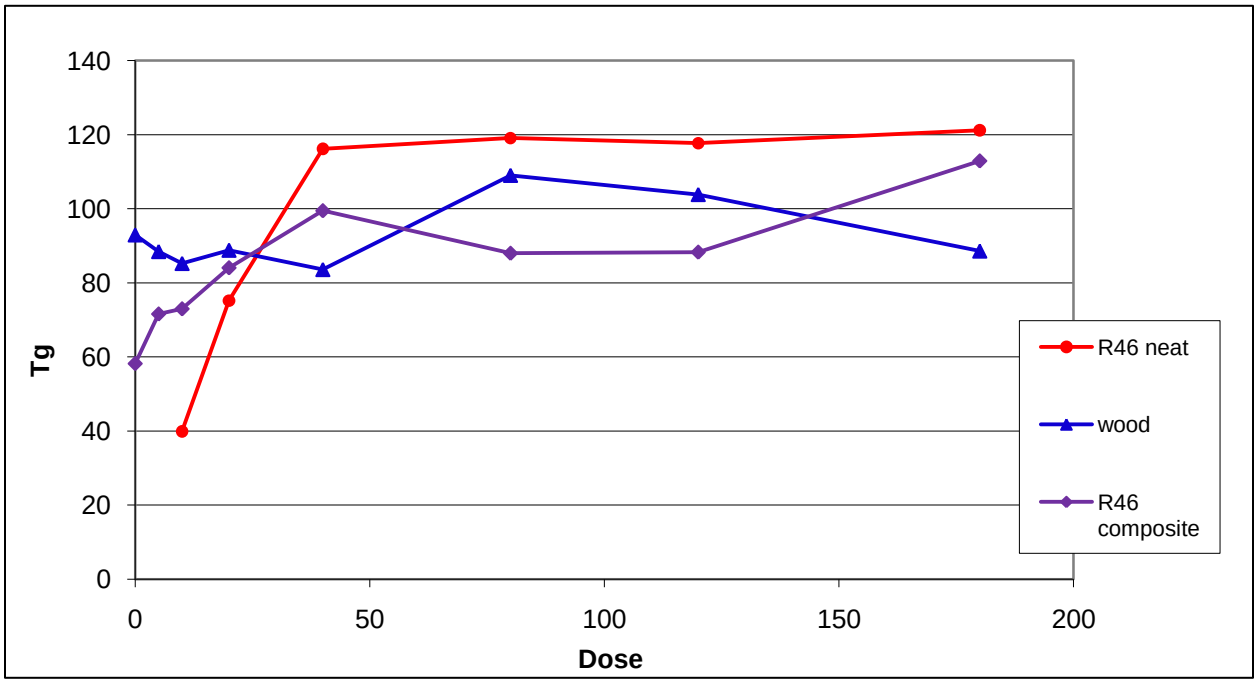

Figure 42: Glass transition temperatures for raw wood, R46 neat resin, and R46 composites. (R46 neat resin data courtesy of Bowman, 2006).

E' curves can be seen because they begin below the temperature range used in testing. As such, ΔE' calculations were not possible.

Figures 40 and 41 show the tan δ curves for R46 and R67 composites, respectively. In both cases the curves start out relatively flat and generally grow in intensity as dose increases, with their peaks shifting to the right. The glass transition temperature is defined here as the peak of the tan δ curve, and those values are shown in Figure 42 for R46 and in Figure 43 for R67. In the case of R67, the 0 and 5 kGy curves do not have a discernable peak within the tested temperature range, so their T_gs cannot be calculated.

The T_gs are also displayed for raw wood and neat R46 resin at the same dosages in Figure 42 for comparison since to some extent the behavior of the composite should mimic a combination of

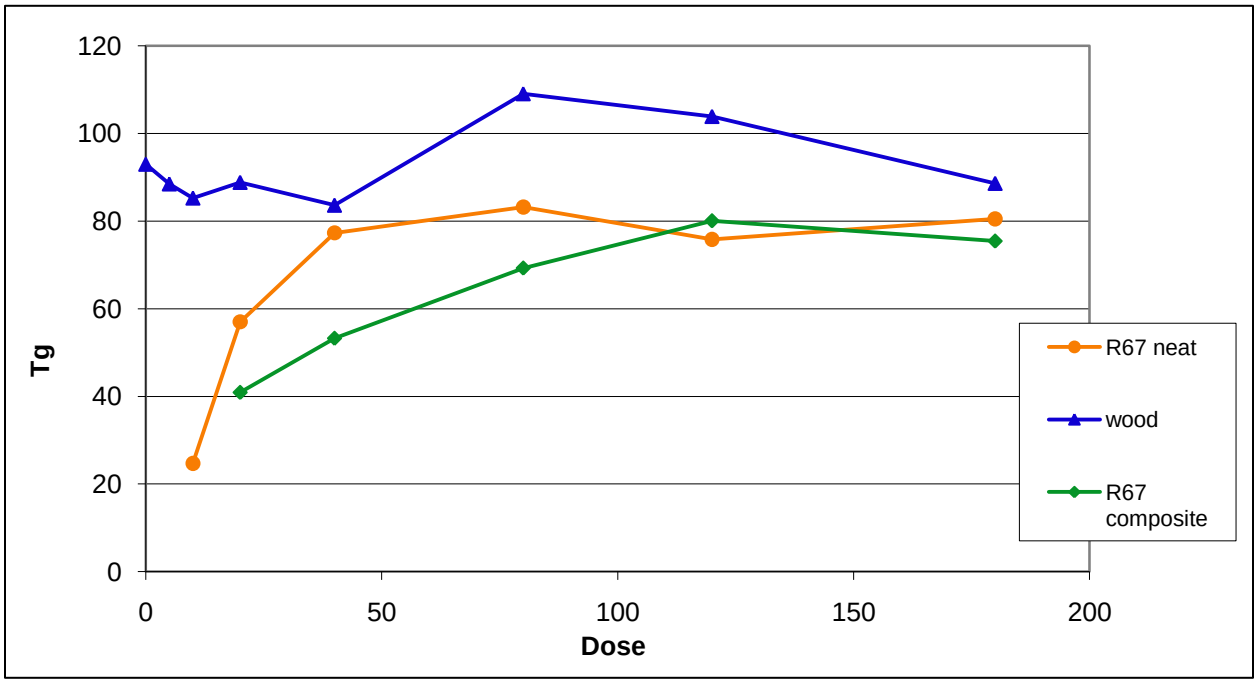

Figure 43: Glass transition temperatures for raw wood, R67 neat resin, and R67 composites. (R67 neat resin data courtesy of Bowman, 2006).

the behaviors of its components. Note that there are no values for neat R46 resin at 0 or 5 kGy since the resin is a liquid in the former state, and not cured enough for testing in the latter. At 0 kGy, there is about a 30 degree difference between the T_g of raw wood and the T_g of the uncured composite. This indicates that the resin plasticizes the wood, as was also seen in the swelling tests. By swelling the wood, the resin increases the free volume between the polymer chains, which allows greater movement and greater ease of movement under deformation, thus lowering the glass transition temperature. A reduction of the T_g, therefore is an indication of interaction between the wood and the resin (Backman & Lindberg 2002).

As the resin cures in the composite, the T_g increases steadily through the 40 kGy dose, and generally looks like an average of the values of the raw components. From 40 to 80 kGy there is a slight regression in the T_g before it rises again and approaches the T_g value of the neat resin. This is somewhat similar to the $\Delta E'$ plot for R46 which showed evidence of increasing

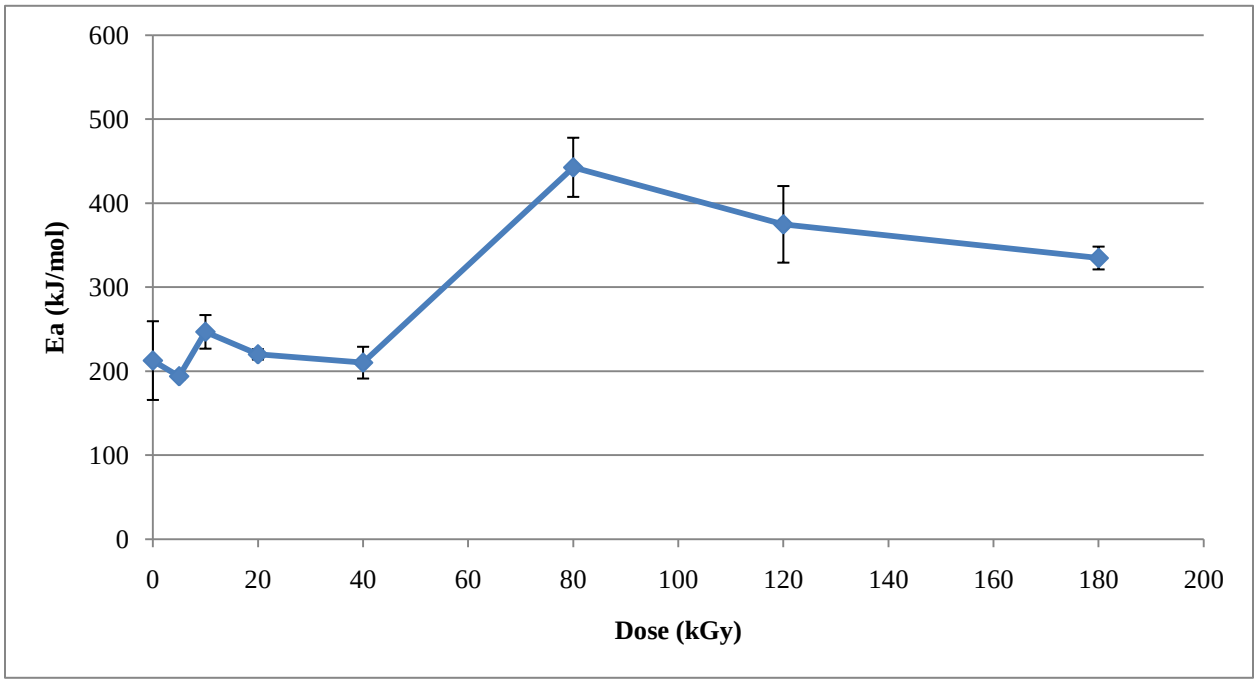

Figure 44: Activation energies for R46 composites as radiation dose increases.

crosslinking through 20 kGy, followed by a plateau through 120 kGy, and then more crosslinking at the 180 kGy dose. In both cases, it seems that the presence of wood is inhibiting complete cure of the resin until higher dosages.

The glass transition temperatures for neat R67 resin, raw wood, and the composite of the two are displayed in Figure 43. Again, there is a significant reduction in the T_g of the uncured composite – in this case it is off the chart due to the limits of the temperature range tested. This indicates interaction between the wood and the resin (Backman & Lindberg 2002). The R67 resin, like the R46, reached a maximum T_g at 40 kGy when cured by itself, though for R67 had a $T_g$max of about 80^{o}C compared to about 120^{o}C for R46. Once again, the initial T_g of the composite begins well below the T_g of raw wood, indicating plasticization by the resin. In this case, the Tg of the uncured composite is well below that of the R46 composite, which may suggest that R67 is capable of greater plasticization of wood. Also similar to the R46 composite, the cure of the R67 composite lags behind the cure of the neat resin until about 120 kGy.

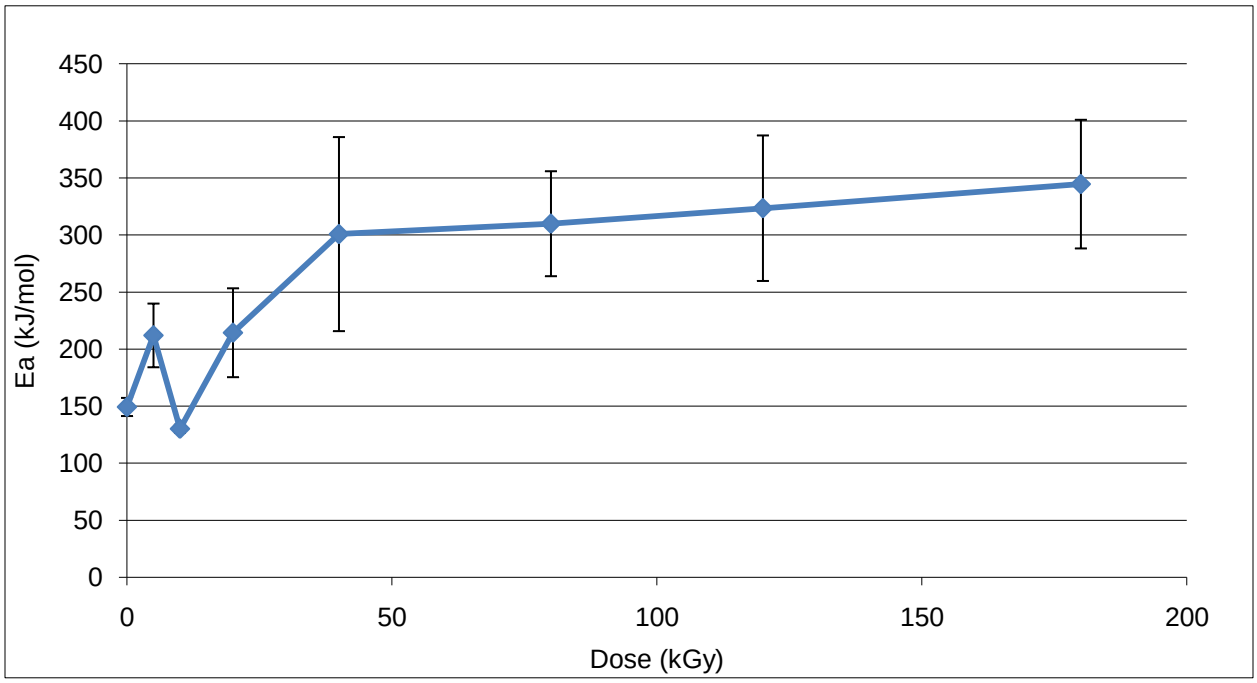

Figure 45: Activation energies for R67 composites as radiation dosage increases.

Since the DMA was operated at multiple frequencies – 1, 2, 4, 10 and 20 Hz – the time-dependent shift factor can be used along with the Arrhenius equation:

$$\lambda = \lambda_o e^{\frac{-Ea}{RT}}$$

where λ is the frequency, λ_o is the pre-exponential factor, T is the temperature at the peak of the tan δ curve, and R is the constant 8.314 J/mol·K. Plotting 1/RT versus log (λ) for every temperature/ frequency pair from a given sample gives a line whose slope is equal to the activation energy, E_a, required to overcome the glass transition at each dose. Figure 44 shows the activation energies for R46 composites at different radiation dosages. A higher activation energy is indicative of a higher cross-linked system, which is inhibiting the transition into greater free volume with its more bound and restricted structure. Therefore, it seems that the greatest amount of crosslinking is achieved at 80 kGy, with most of the change occurring after 40 kGy. The main changes in the activation energy curve seem to lag behind the T_g curve by a step.

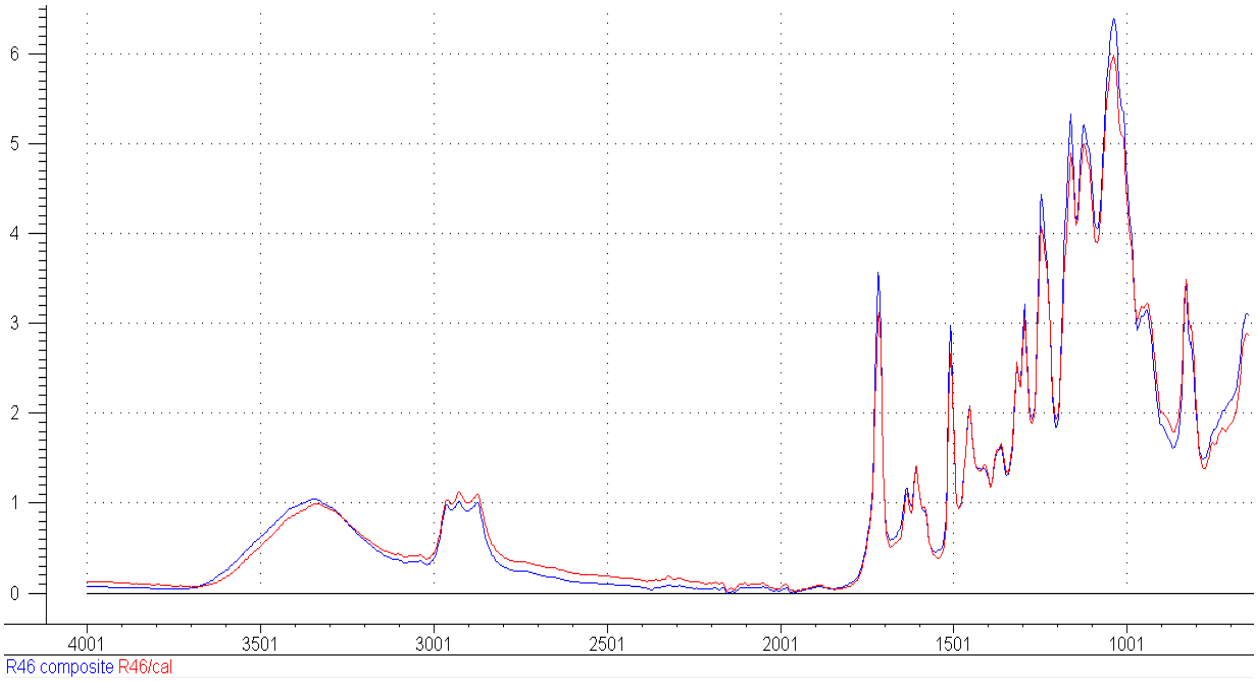

Figure 46: Comparison of the spectra of uncured R46 composite and the calculated theoretical prediction of the same based on spectra of raw wood and neat R46 resin.

In Figure 45, the activation energies for the R67 composites are displayed. After some initial variation at the lower doses, the E_a increases sharply until 40 kGy, whereupon it continues to increase gradually all the way to 180 kGy. This suggests that most of the crosslinking is accomplished by a dose of 40 kGy, but there is still some residual curing going on well beyond that point. This seems consistent with the T_g results which indicated that cure of the resin in the composite was gradual and steady, but not complete until about 120 kGy.

FTIR spectroscopy

Having gained many results from the dynamic mechanical analysis of the composites, the next stage of this study was to look at the cure of the composites at a smaller scale by means of infrared spectroscopy. Fourier-Transform infrared spectra were used to analyze chemical

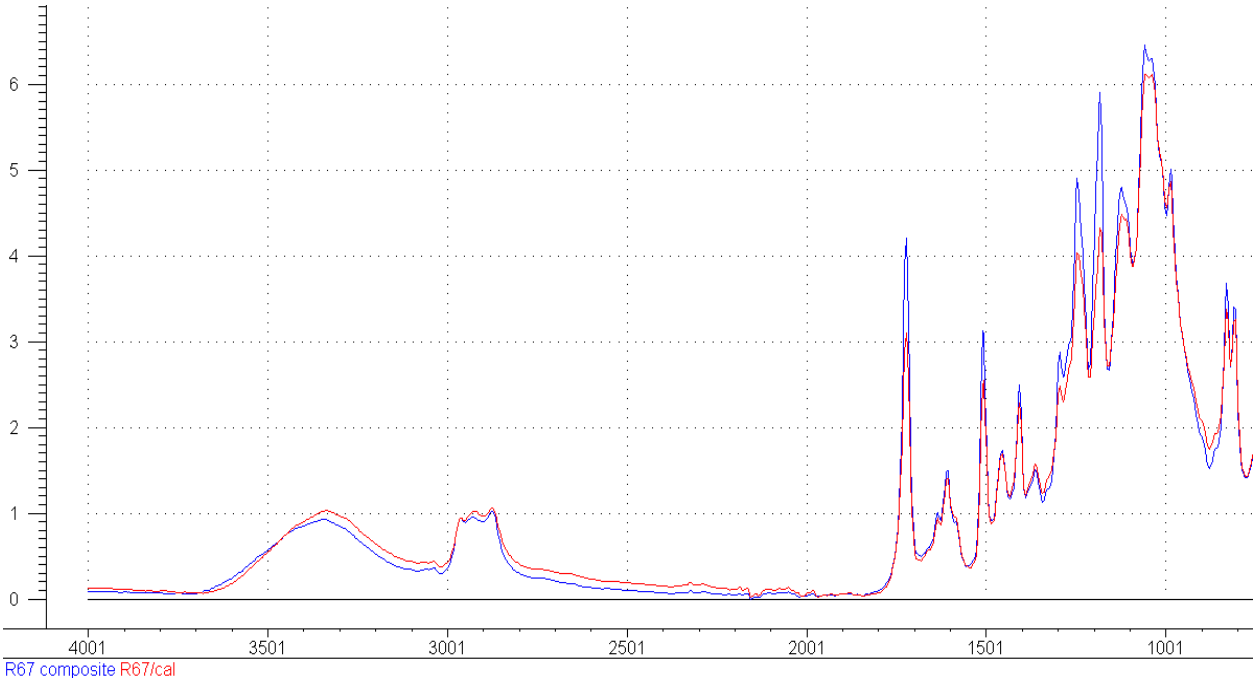

Figure 47: Comparison of the spectra of uncured R67 composite and the calculated theoretical prediction of the same based on spectra of raw wood and neat R67 resin.

changes in the composites as they underwent irradiation. Spectra were also taken of raw wood and neat, uncured resins for comparison. In an attempt to detect interactions between the wood and the resin, spectra of the uncured composites were compared to mathematically derived spectra that represented what was expected in the composites solely based on rule of mixtures. Since the composites were 30% resin by weight, these theoretical spectra were generated by taking the values in the spectra of the wood (multiplied by a 0.7 weight fraction), and adding them to the values in the resin spectra (multiplied by a 0.3 weight fraction). The intent was to see if any unexpected features appeared in the actual composite spectra that weren't present in either the wood or the resin by themselves, or a theoretical combination of the two. The effect of any interactions would not be predictable in the calculated spectra. The results of this experiment are shown in figures 46 and 47 for R46 and R67 composites, respectively.

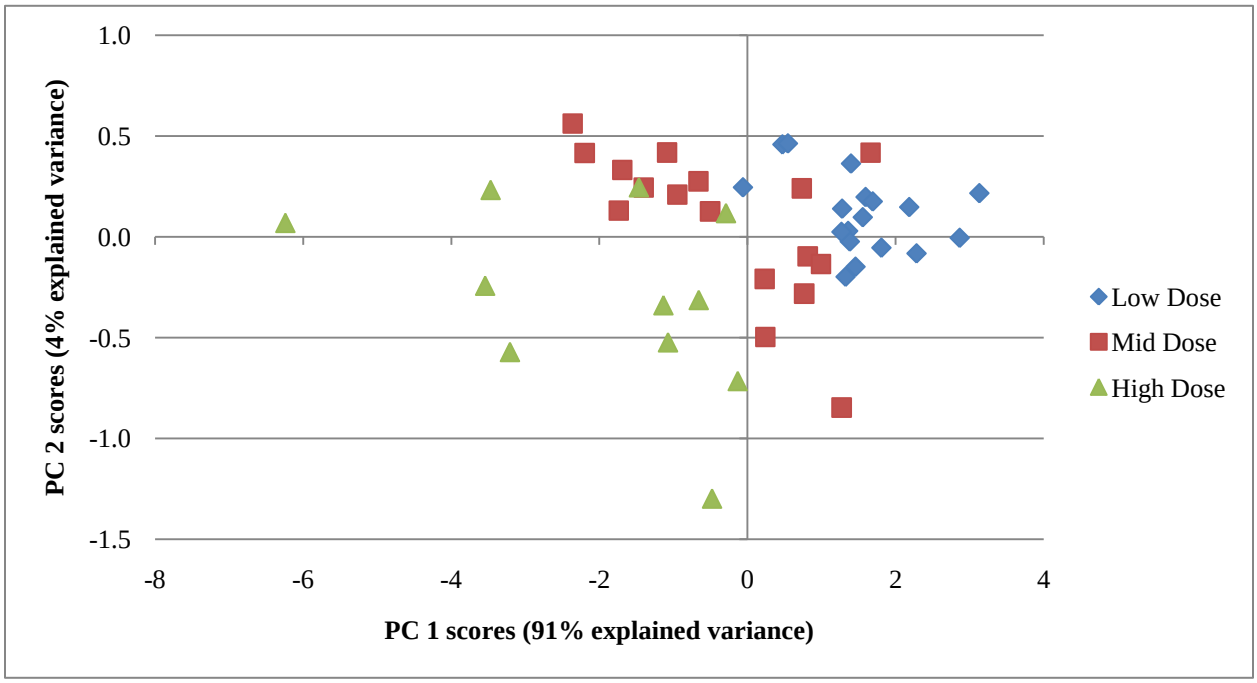

Figure 48: PCA scores plot for irradiated R46 composites.

The accuracy of the theoretical spectra was remarkable, as the curves sit right on top of each other, which makes subtle differences between them more obvious. In both cases, the broad peak centered on ~3300 cm^{-1}, which is assigned to bending of hydroxyl groups (Garidel & Boese 2007), is shifted to the left of the calculated prediction. This hints at the influence of some interaction between the resins and the OH groups in the wood. Also, several peaks in the fingerprint region of each composite are notably higher than expected, especially in the R67 composite, which may again suggest more interaction between the resin and wood for R67 than R46. These changes in the infrared spectra indicate interaction between the wood and the resin (Awal et al. 2009).

Generally, cure of acrylics and methacrylics can be tracked via FTIR spectra by watching certain peaks. The peak at 810 cm^{-1} is an acrylic peak, which should decrease as cure proceeds (Rekha & Asha 2008). The peak at about 1636 cm^{-1} can be used to monitor cure of methacrylates, and

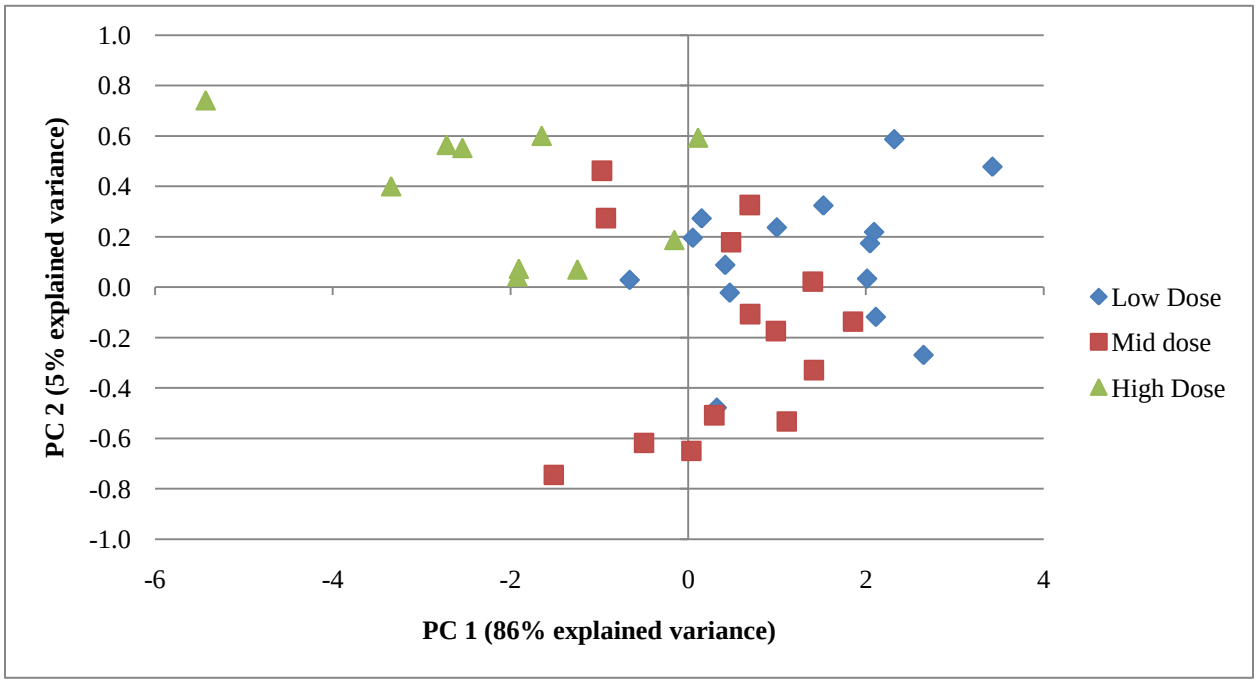

Figure 49: PCA scores plot for irradiated R67 composites.

should also decrease as the resin cures. However, visual inspection does not reveal any notable trend or change in those peaks. Also, the methacrylic peak at 1636 cm^{-1} in the neighborhood of the troublesome 1654 cm^{-1} peak in wood, which was unpredictably varied due to unchecked moisture content (see Appendix B). This obscures the reading of the methacrylic peak.

Principle component analysis was used to analyze the spectra of each composite and identify the effect of the radiation. This analysis was focused on the fingerprint region that contains most of the identifying spectral data. Figure 48 shows the PCA scores for the R46 composites. The samples were identified by dose level – low dose (0-10 kGy), mid dose (20-80 kGy) and high does (120-180 kGy). Note that these groupings are well defined along PC1, and that PC1 explains 91% of the variance between samples. The high dose samples seem to separate out along PC 2, but PC2 is only responsible for explaining 4% of sample variance, and the scale on PC 2 is much smaller than that of PC 1, so this is of little significance.

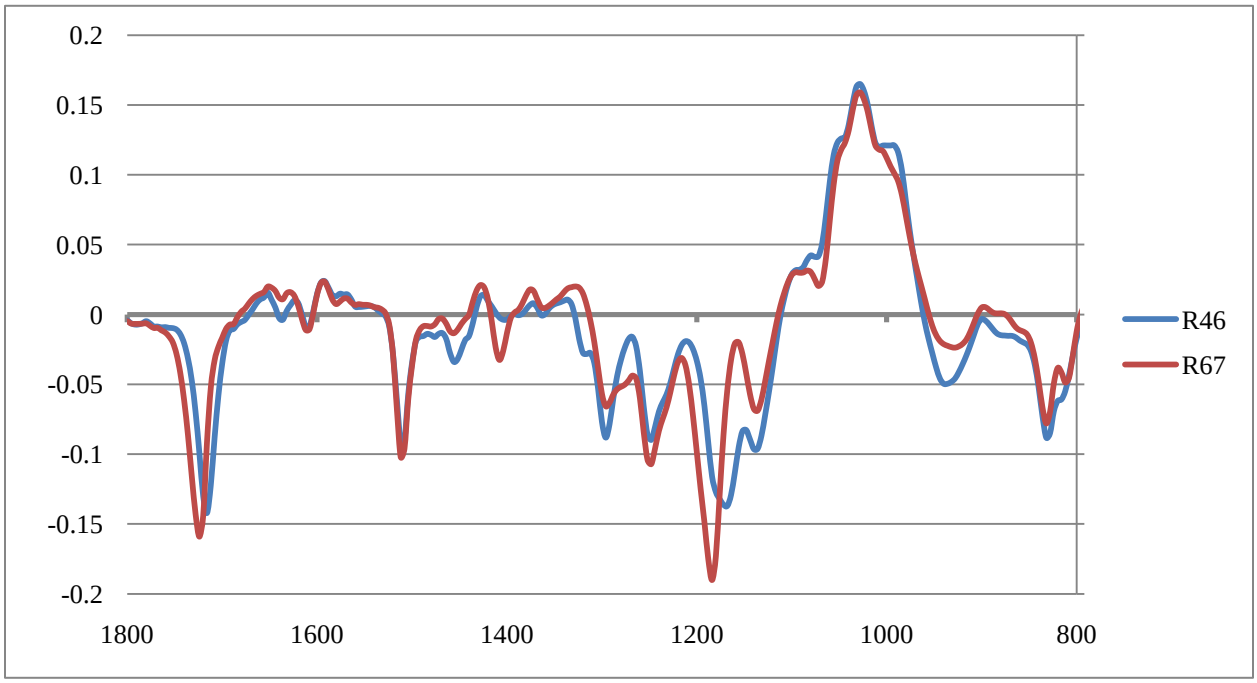

Figure 50: PC 1 loadings plots for both R46 and R67 composites.

Similarly, Figure 49 shows the PCA scores plot for R67 composites. The samples are grouped by the same dosage divisions, and are also distinct along PC 1. PC 1 explains 86% of the variance among the samples, and PC 2 explains a much smaller portion (only 5%) and the scores on PC 2 are on a much smaller scale than PC 1.

The loadings plots for both types of composite are shown in Figure 50 simultaneously for easy comparison. Given the positioning of the sample groupings along PC 1 – low doses on the positive side and high doses on the negative side – negative values on the loadings plot indicate peaks that are increasing with increasing dosage, and positive values indicate peaks that are decreasing with increasing dosage. For the most part, the variables of significance are the same for both composites. They share in common decreasing trends at 1050 cm^{-1}, 1028 cm^{-1}, and 998 cm^{-1}, which are peaks primarily associated with cellulose in wood. They also share increasing trends at 1720 cm^{-1}, 1512 cm^{-1}, 1296 cm^{-1}, and 1248 cm^{-1}. The peaks at 1512 cm^{-1} and 1296 cm^{-}

[1] are resin-related peaks, and the peaks at 1248 cm^{-1} and 1720 cm^{-1} are present in both, but much stronger in the resins than in the wood. Infrared analysis of e-beam treated wood showed that the increase of carbonyls (1720 cm^{-1}) was a primary characteristic of the radiation of wood.

There are a few variables of significance on the loadings plot that are unique to each resin. In the R46 composites, the peaks at 1168 cm^{-1} and 1136 cm^{-1} exhibit an increasing trend with increasing dosage, as does the band at 1184 cm^{-1} in the R67 composites. It is interesting to note that the variables associated primarily with wood decrease as dosage increases, and the variables associated only or mostly with the resins increase as dosage increases.

Conclusion

The swelling experiments, along with the suppression of the T_g in the uncured composites and the comparison of theoretical and observed infrared spectra all indicate interaction between the resins and the wood. This interaction indicates the possibility of a better interface between the wood and the resin, resulting in better bonding and a better overall composite.

In studying the R46 composites, the $\Delta E'$ plot indicates that crosslinking increased through 20 kGy, where it leveled off before increasing again around 120 kGy. This suggests a lag in the cure of the resin between 20 and 120 kGy. Similarly, the T_g of the R46 composites increased steadily until 40 kGy before regressing somewhat at the 80 and 120 kGy dosages. At a final dose of 180 kGy, the Tg of the composite approached the T_g of the neat resin, indicating that it had reached final cure. The activation energy of the R46 composites saw its greatest increase between the 40 and 80 kGy doses. After 80 kGy the E_a went into a slight recession. Generally, a peak in a plot such as this indicates the point at which there is the most crosslinking or other factors that inhibit the glass transition. With so many factors to consider from the wood and the resin, it is hard to say if that is exactly what is going on. However, the decrease in E_a at 120 and

180 kGy indicates a freeing up of the molecules in the composite, making the transition from the glassy region to the rubbery region easier to accomplish. This increase in mobility could also be the reason that the cure is finally able to proceed again (as seen in the $\Delta E'$ and T_g plots) from 120 to 180 kGy. The uncured portions of the resin would have a greater degree of freedom to find other unsaturated polymerization sites to bond with.

There was not enough information to calculate $\Delta E'$ for the R67 composites, but the T_g and E_a plots do show some characteristics of their cure. The cure of the R67 composites lagged behind the cure of the neat resin. Unlike the R46 composites, the R67 never seemed to plateau, but generally showed slower curing throughout the range of dosages. The E_a plot indicates a sharp increase between 10 and 40 kGy, and from that point through 180 kGy it very gradually increases. The T_g shows the cure of the composite lagging behind the cure of the neat resin but gradually making up the difference before matching the T_g values of the neat resin at 120 and 180 kGy. Therefore, the R67 composites appear to reach full cure, but not until 120 kGy.

As suspected, the presence of wood in the composites did hinder the cure of both resins, but both were eventually able to reach a level of complete cure. The required dosage for complete cure of the neat resins was 40 kGy for both R46 and R67. The R67 composites reached that level with a dose of 120 kGy. The R46 composites seemed to have reached a level of partial cure with a 40 kGy dose where no more progress was made until around 120 kGy. Complete cure in the R46 composites was finally obtained at 180 kGy.

References

Awal, A., Ghosh, S.B. & Sain, M., 2009. Development and morphological characterization of wood pulp reinforced biocomposite fibers. *Journal of materials science*, 44(11), 2876-2881.

Backman, A.C. & Lindberg, K.A.H., 2002. Interaction between wood and polyurethane-alkyd lacquer resulting in a decrease in the glass transition temperature. *Journal of Applied Polymer Science*, 85(3), 595-605.

Beziers, D., Capdepuy, B. & Chataignier, E., 1990. Electron beam curing of composites. In *Developments in the science and technology of composite materials: Fourth European Conference on Composite Materials, September 25-28, 1990, Stuttgart, FRG*. Kluwer Academic Pub, p. 73.

Bowman, Seth N., 2006. Lignin composites with phenol-acrylates cured by electron beam. Thesis presented for M.S., University of Tennessee, Knoxville.

Chowdhury, M. & Wolcott, M., 2007. Compatibilizer selection to improve mechanical and moisture properties of extruded wood-HDPE composites. *Forest products journal*, 57(9), 46-53.

Ellis, W.D., 2000. Wood-polymer composites: Review of processes and properties. *Molecular Crystals and Liquid Crystals*, 353(1), 75-84.

Garidel, P. & Boese, M., 2007. Mid infrared microspectroscopic mapping and imaging: A bio-analytical tool for spatially and chemically resolved tissue characterization and evaluationof drug permeation within tissues. *Microscopy Research and Technique*, 70(4), 336-349.

Goodman, D.L. & Palmese, G.R., 2001. Curing and Bonding of Composites using Electron Beam Processing. *The Handbook of Polymer Blends and Composites*.

Griffith, W.L. et al., 2006. Electron-Beam Cured Resin Systems for Wood Composites. *ANTEC*.

Ivanov, V.S., 1992. *Radiation chemistry of polymers*, Vsp.

Kazayawoko, M. et al., 1997. Effects of wood fiber surface chemistry on the mechanical properties of wood fiber-polypropylene composites. *International Journal of Polymeric Materials*, 37(3), 237-261.

Kim, J.Y. et al., 2009. Effect of a Novel Polymeric Coupling Agent on the Water Uptake Property and Warp Stability of Poly (vinyl chloride)/Bamboo Flour Composite.

Composite Interfaces, *16*, 7(9), 837-846.

Rekha, N. & Asha, S.K., 2008. Synthesis and FTIR spectroscopic investigation of the UV curing kinetics of telechelic urethane methacrylate crosslinkers based on the renewable resource-Cardanol. *Journal of Applied Polymer Science*, 109(5), 2781-2790.

Sepe, M.P., 1997. Thermal Analysis of Polymers (Rapra Review Report 95). *UK: Rapra*.

Sheikh, N. & Afshar Taromi, F., 1993. Radiation induced polymerization of vinyl monomers and their application for preparation of wood-polymer composites. *Radiation Physics and Chemistry*, 42(1-3), 179-182.

Singh, A., 2001. Radiation processing of carbon fibre-reinforced advanced composites. *Nuclear Instruments and Methods in Physics Research Section B: Beam Interactions with Materials and Atoms*, 185(1-4), 50-54.

Song, Ting, 2005. Eletron beam cured resins for wood composites. Thesis presented for M.S, University of Tennessee, Knoxville.

Stern, M., 2000. Electron-Beam Processing of Plastics: An Alternative to Chemical Additives (15). In *Tecchnical Papers of the Annual Technical Conference-Society of Plastics Engineers Incorporated*. pp. 1772-1776.

Wright, J.R. & Mathias, L.J., 1993. New lightweight materials: Balsa wood-polymer composites based on ethyl -(hydroxymethyl) acrylate. *Journal of Applied Polymer Science*, 48(12), 2241-2247.

Appendix C: DMA Outputs for R46 and R67 Composites

Data outputs from dynamic mechanical analysis are shown in the following section for each sample tested. Sample nomenclature is as follows: R46 or R67 indicates the type of resin used to make the composites; the number indicates the received e-beam dosage (0 – 180 kGy); the final letter identifies individual replicates (A-F). Storage modulus (E') plots are shown in green, loss modulus (E") in red, and the tan δ curves are shown in blue. Where possible, the T_gs are marked as the peak of the tan d curve, and the onset and offset of the glass transition are marked on the E' curves.

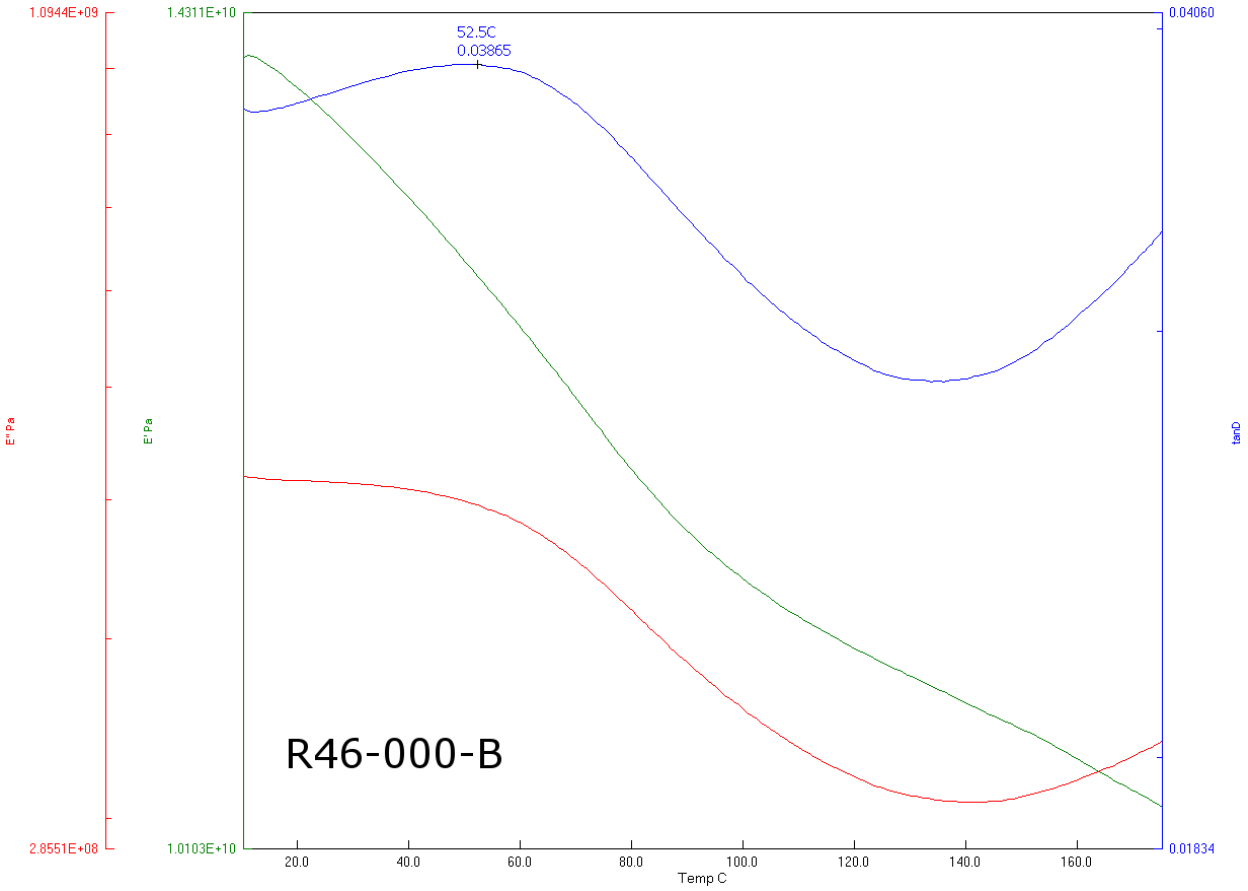

Figure 51: DMA output for R46-000-B

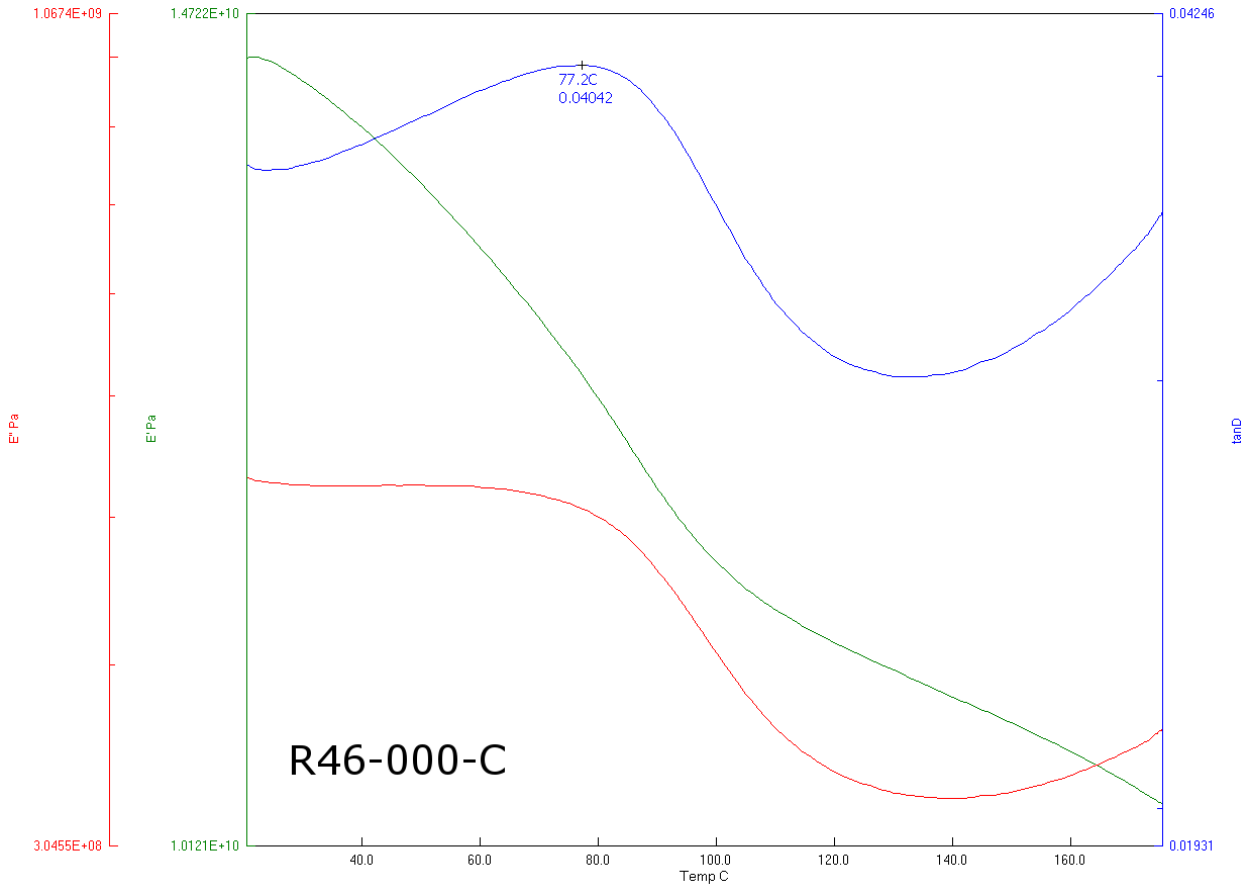

Figure 52: DMA output for R46-000-C

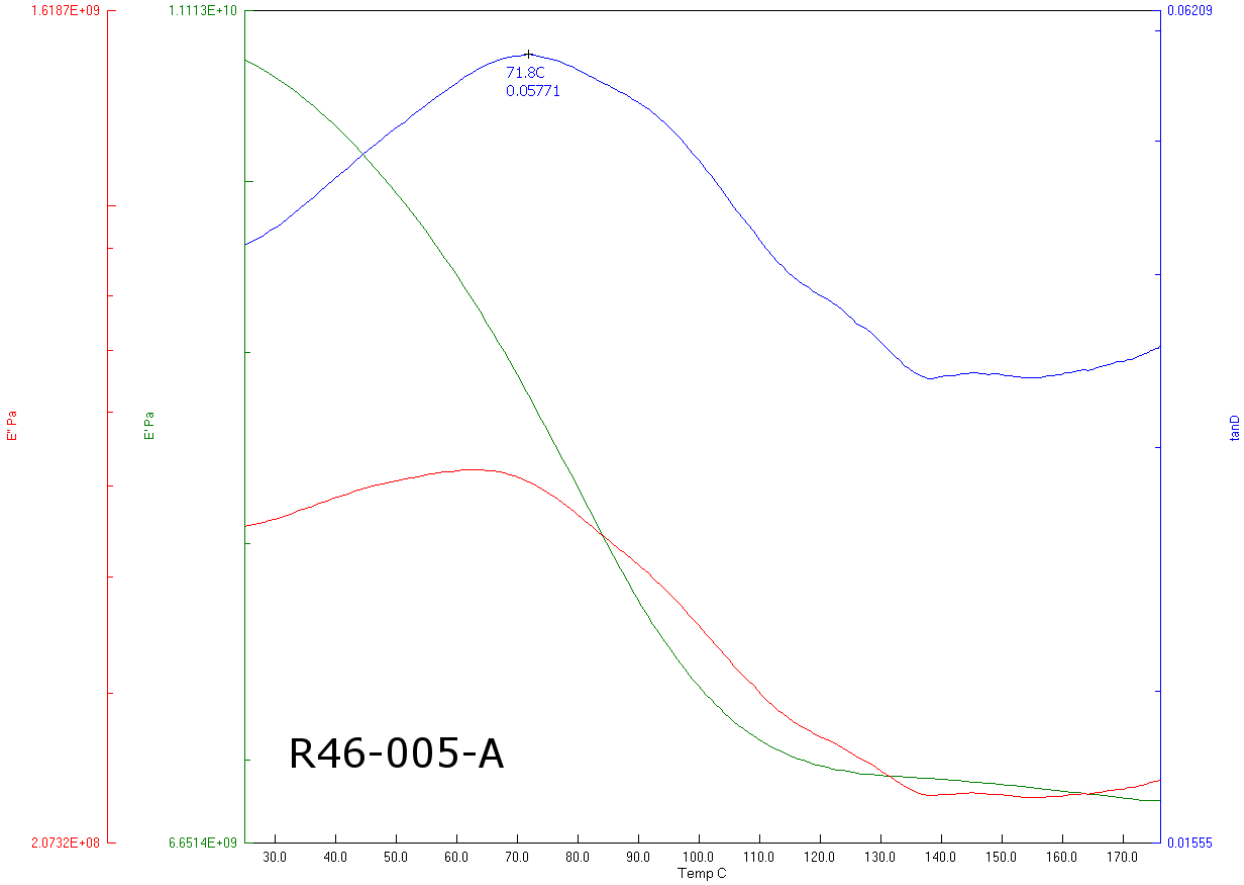

Figure 53: DMA output for R46-005-A

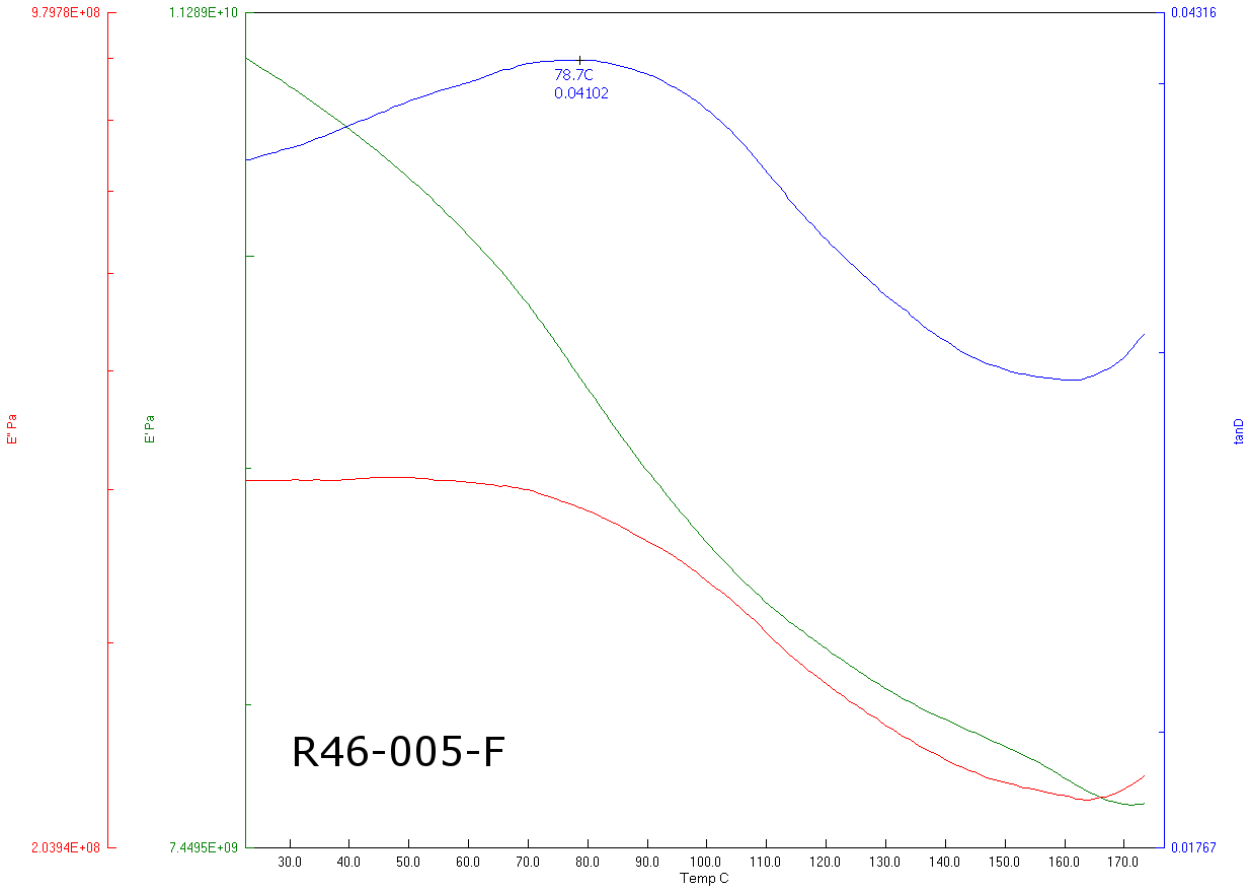

Figure 54: DMA output for R46-005-F

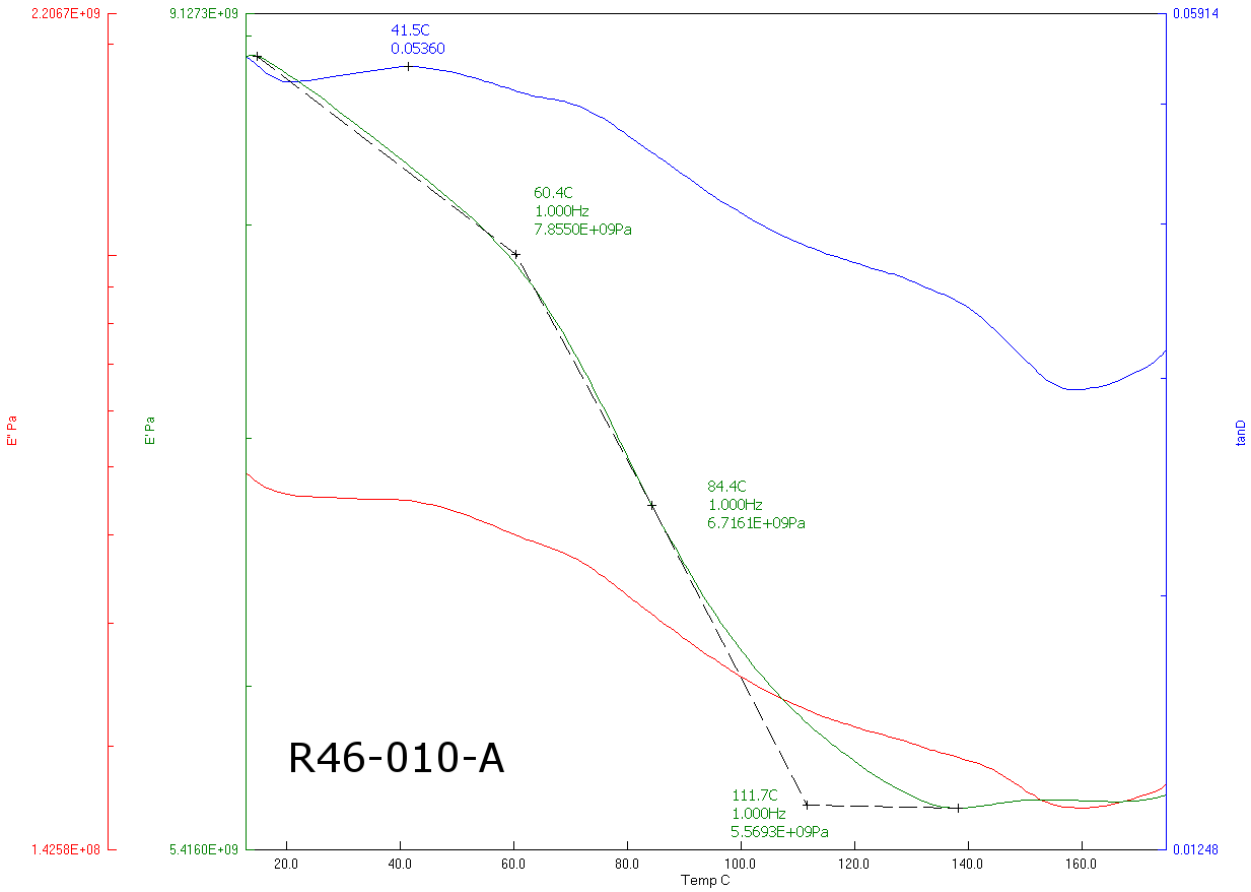

Figure 55: DMA output for R46-010-A

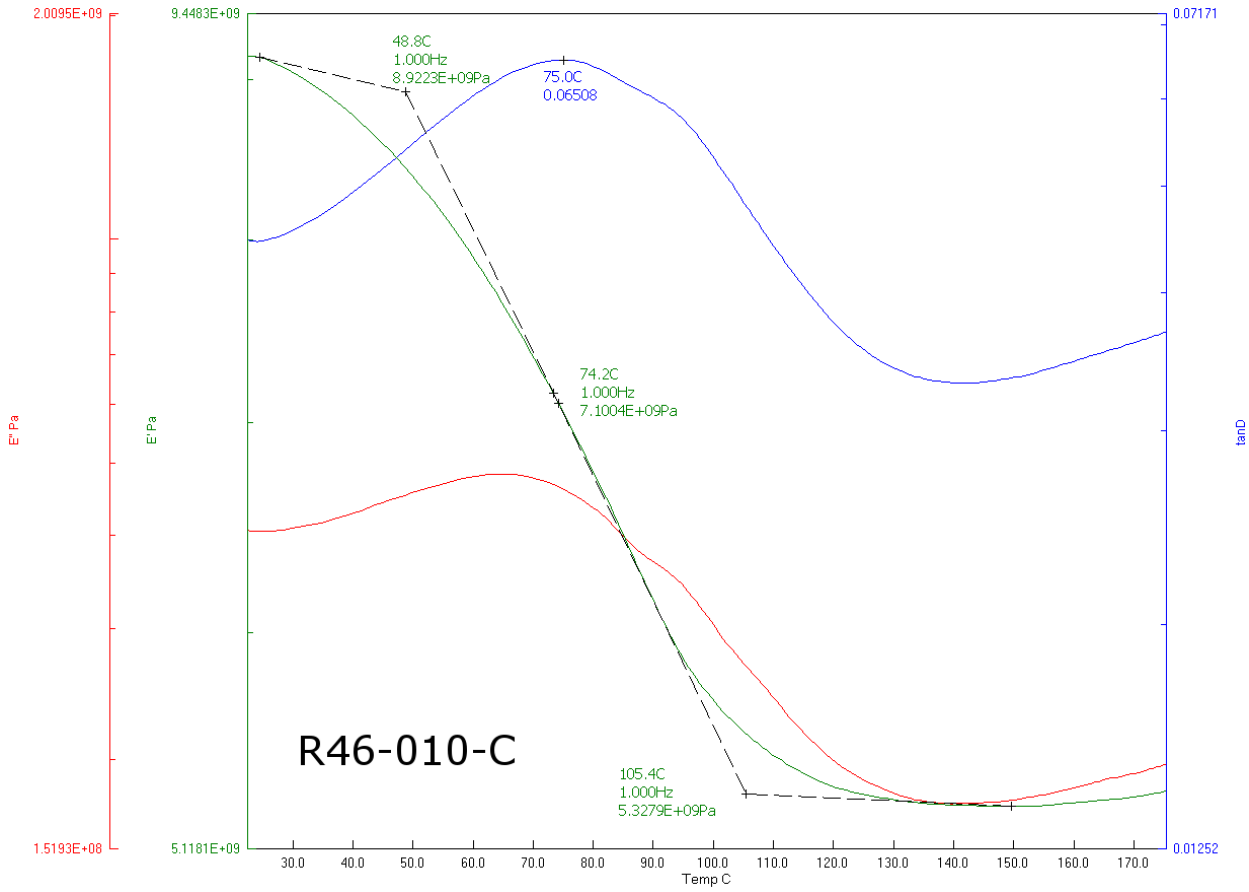

Figure 56: DMA output for R46-010-C

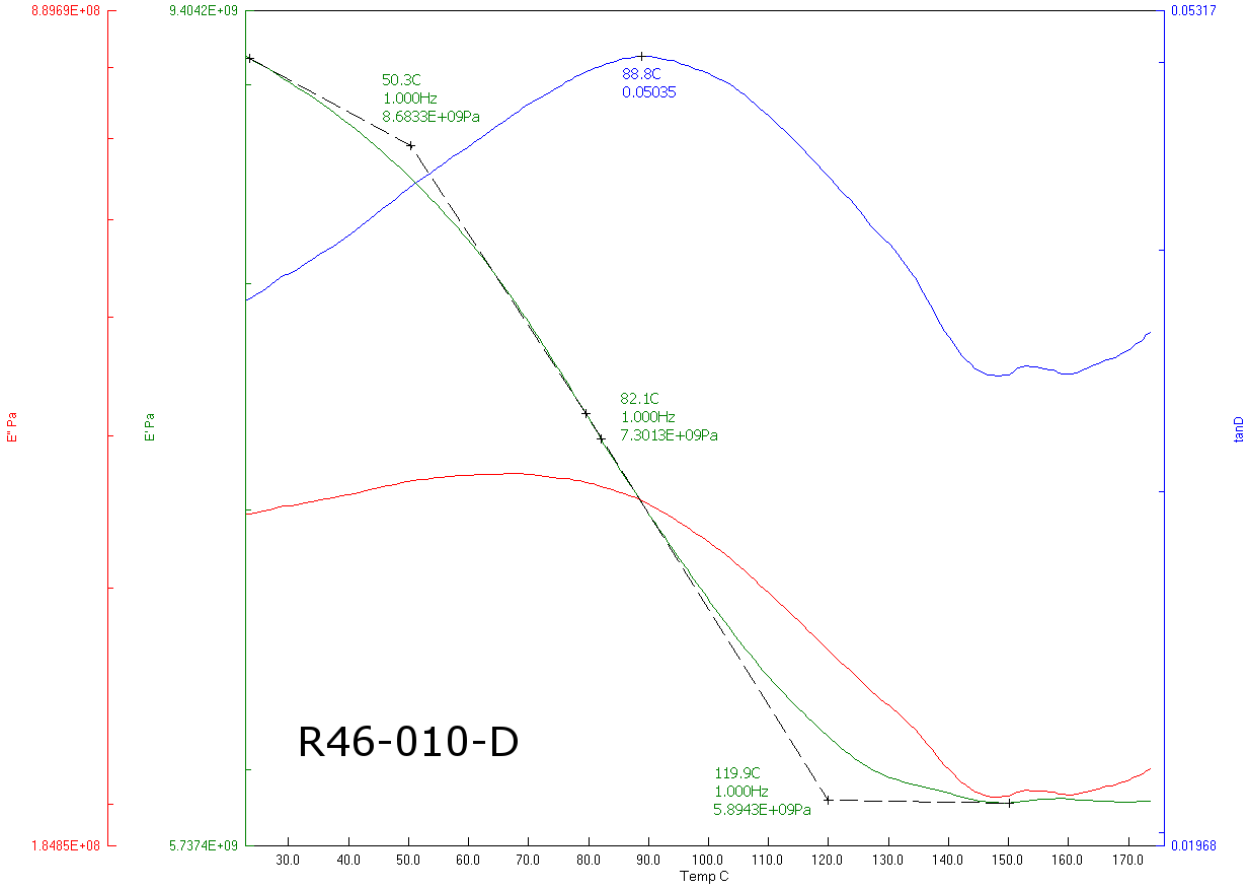

Figure 57: DMA output for R46-010-D

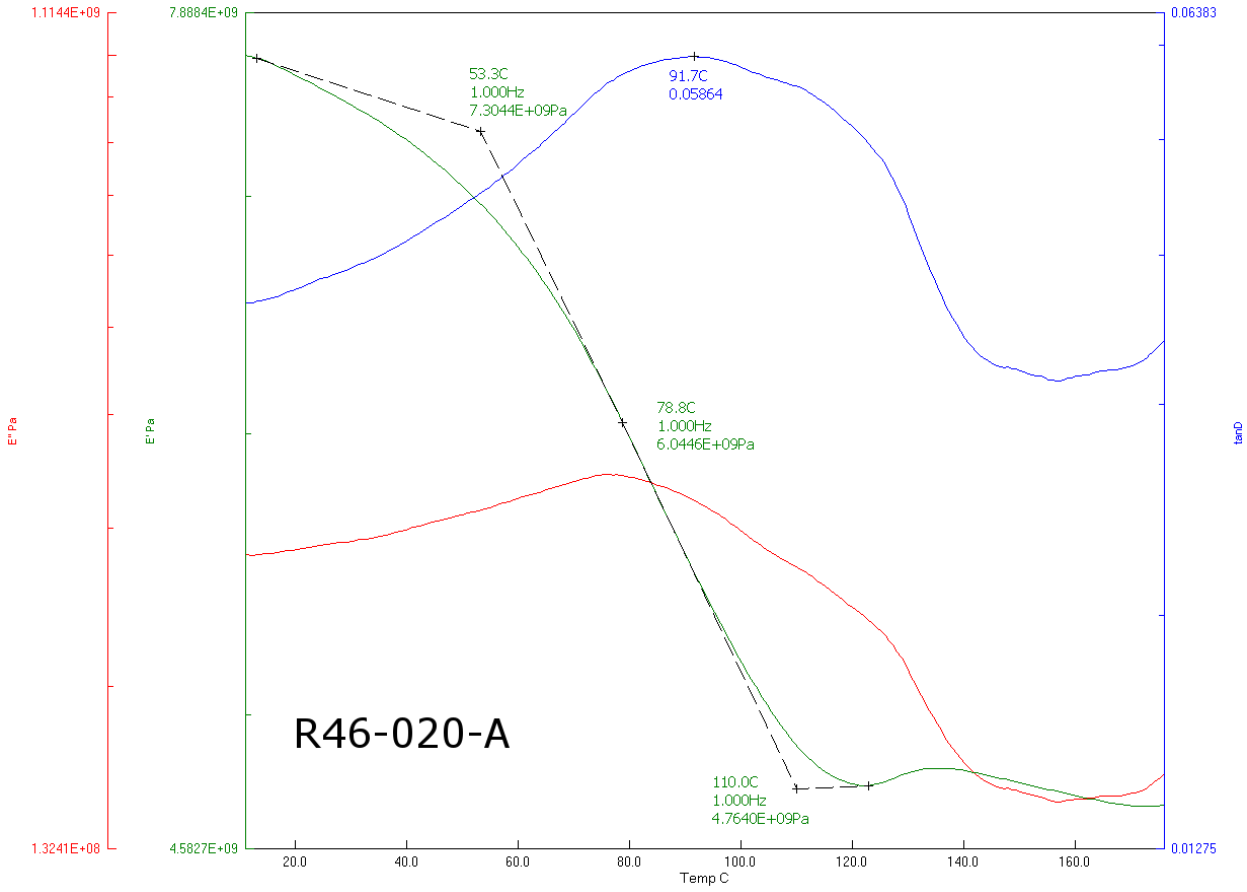

Figure 58 DMA output for R46-020-A

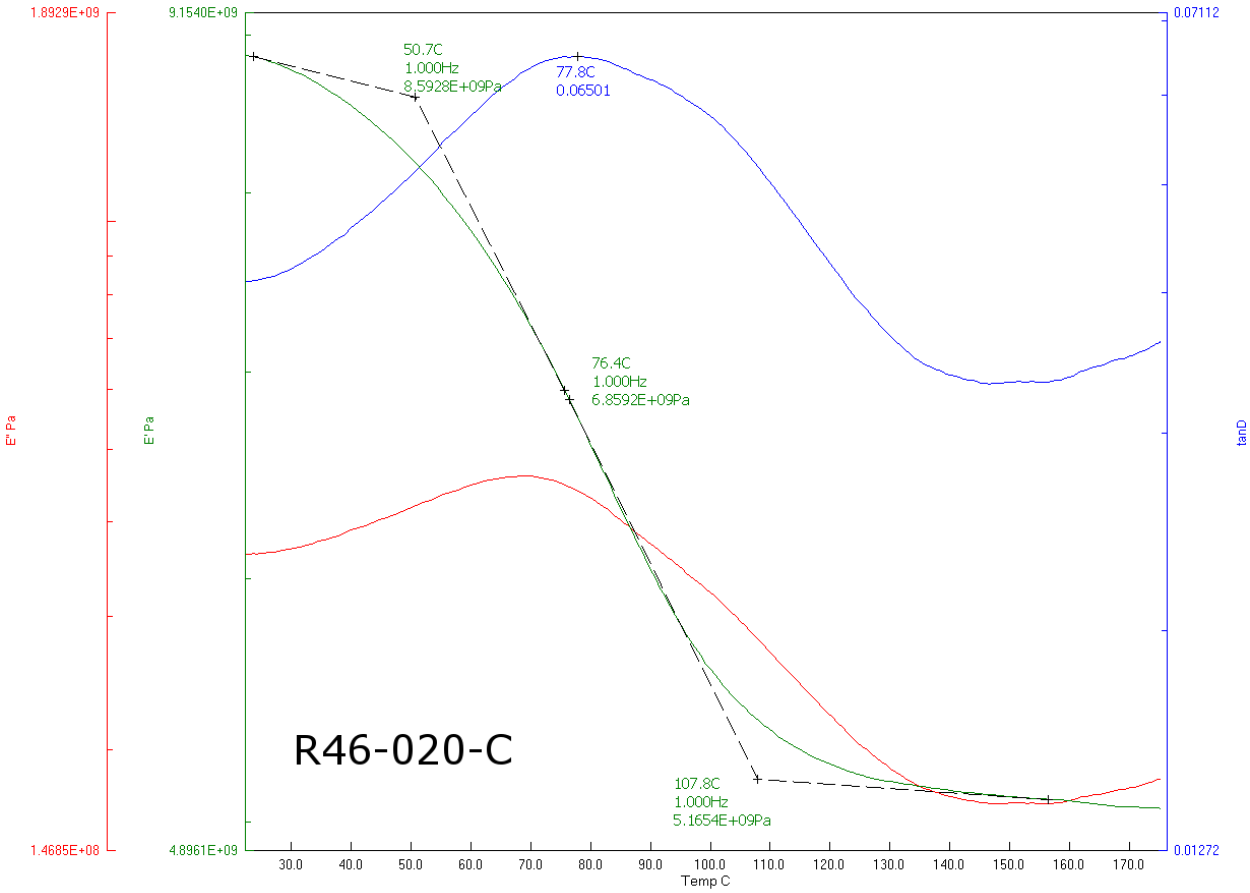

Figure 59: DMA output for R46-020-C

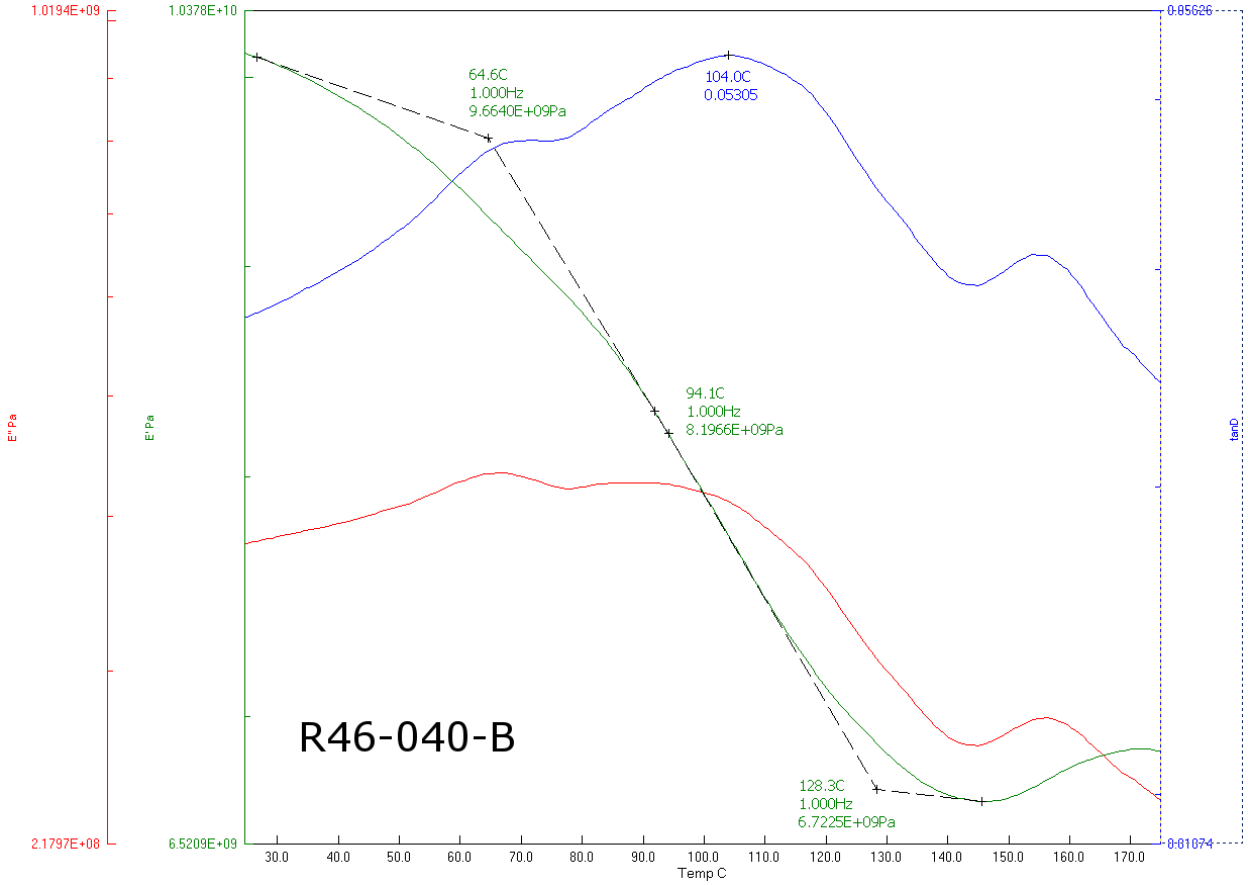

Figure 60: DMA output for R46-040-B

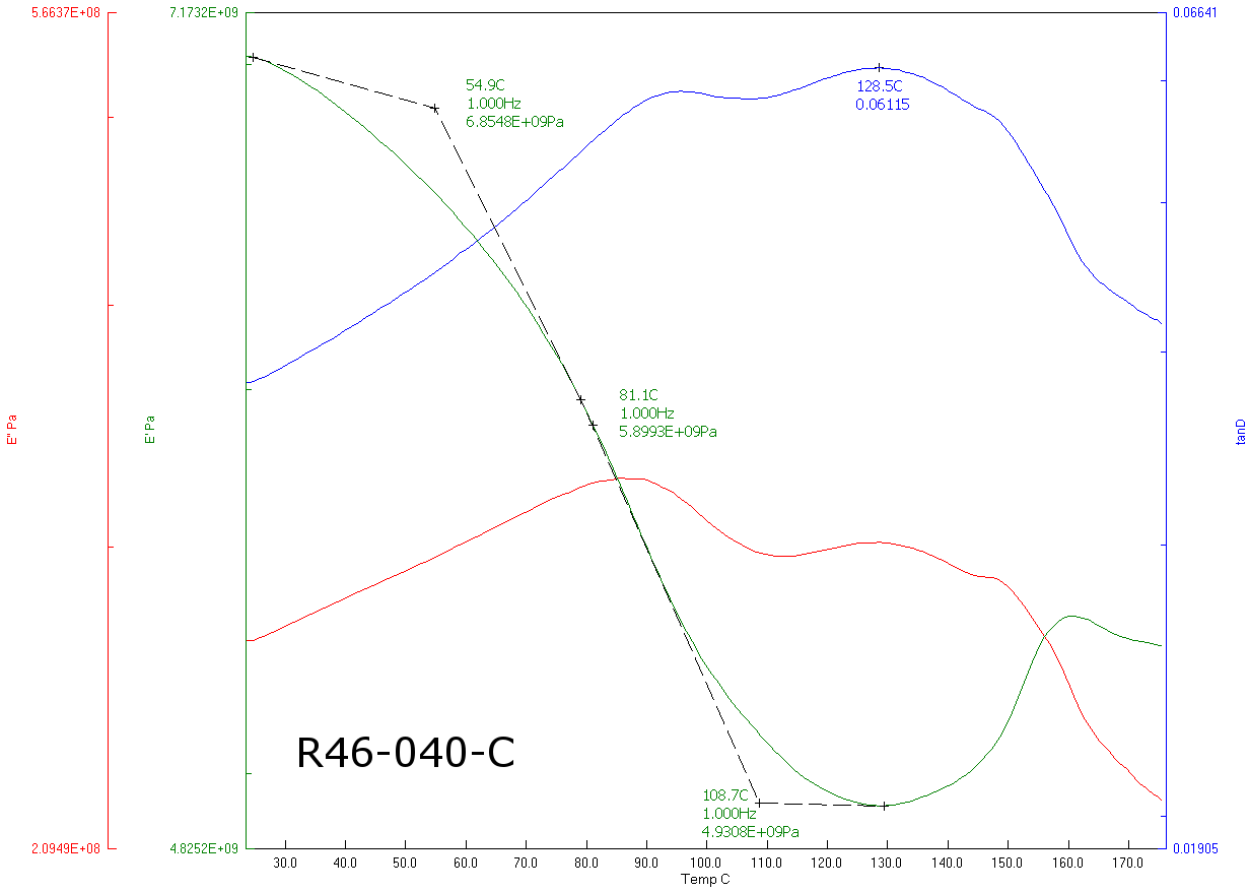

Figure 61: DMA output for R46-040-C

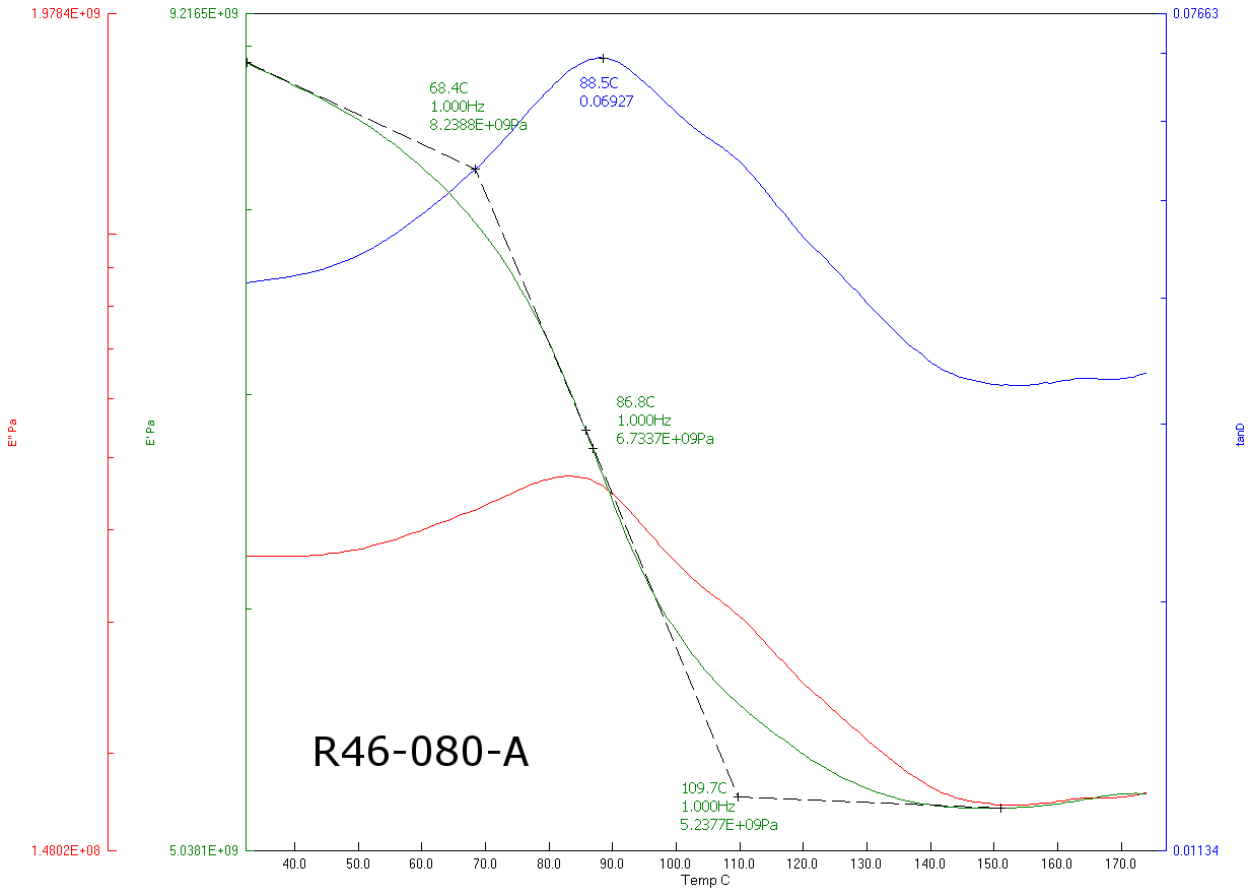

Figure 62: DMA output for R46-080-A

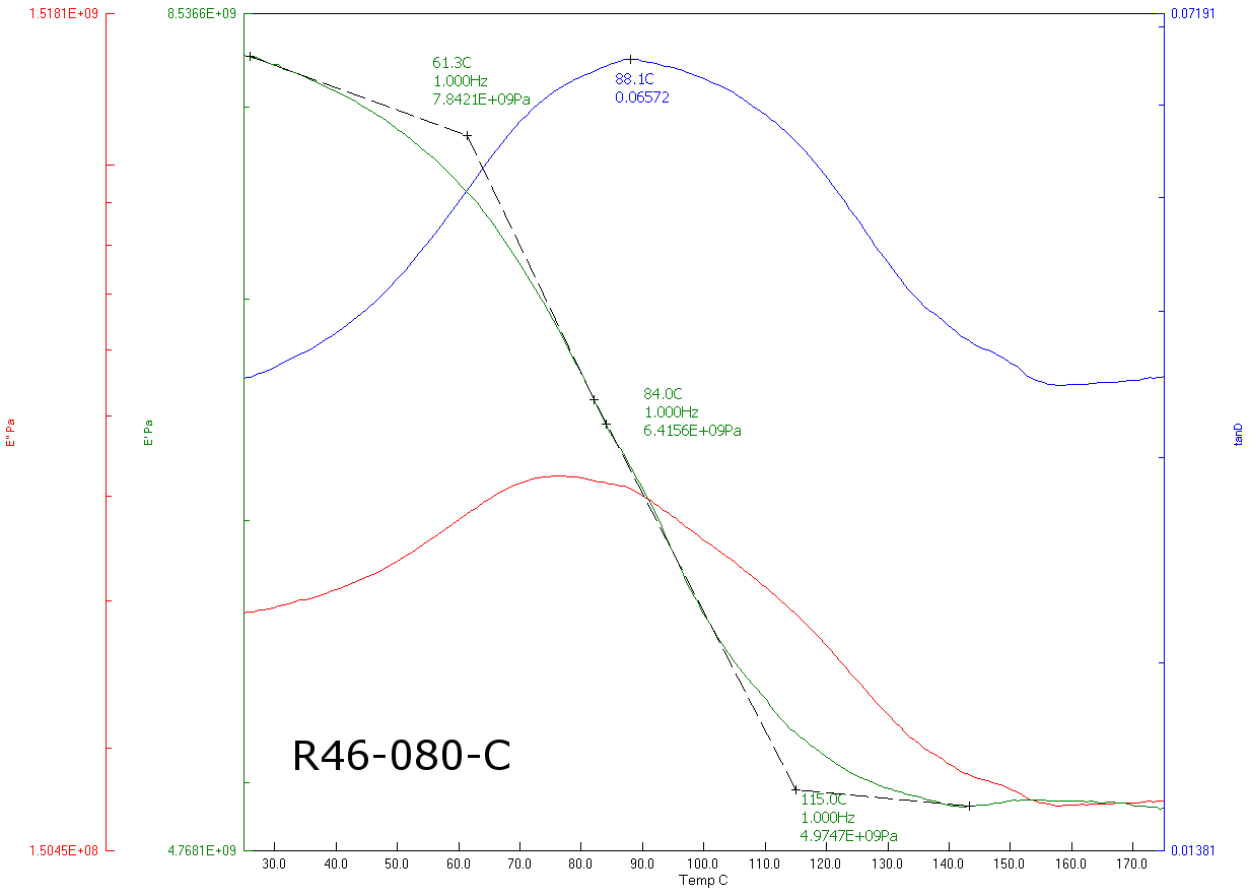

Figure 63: DMA output for R46-080-C

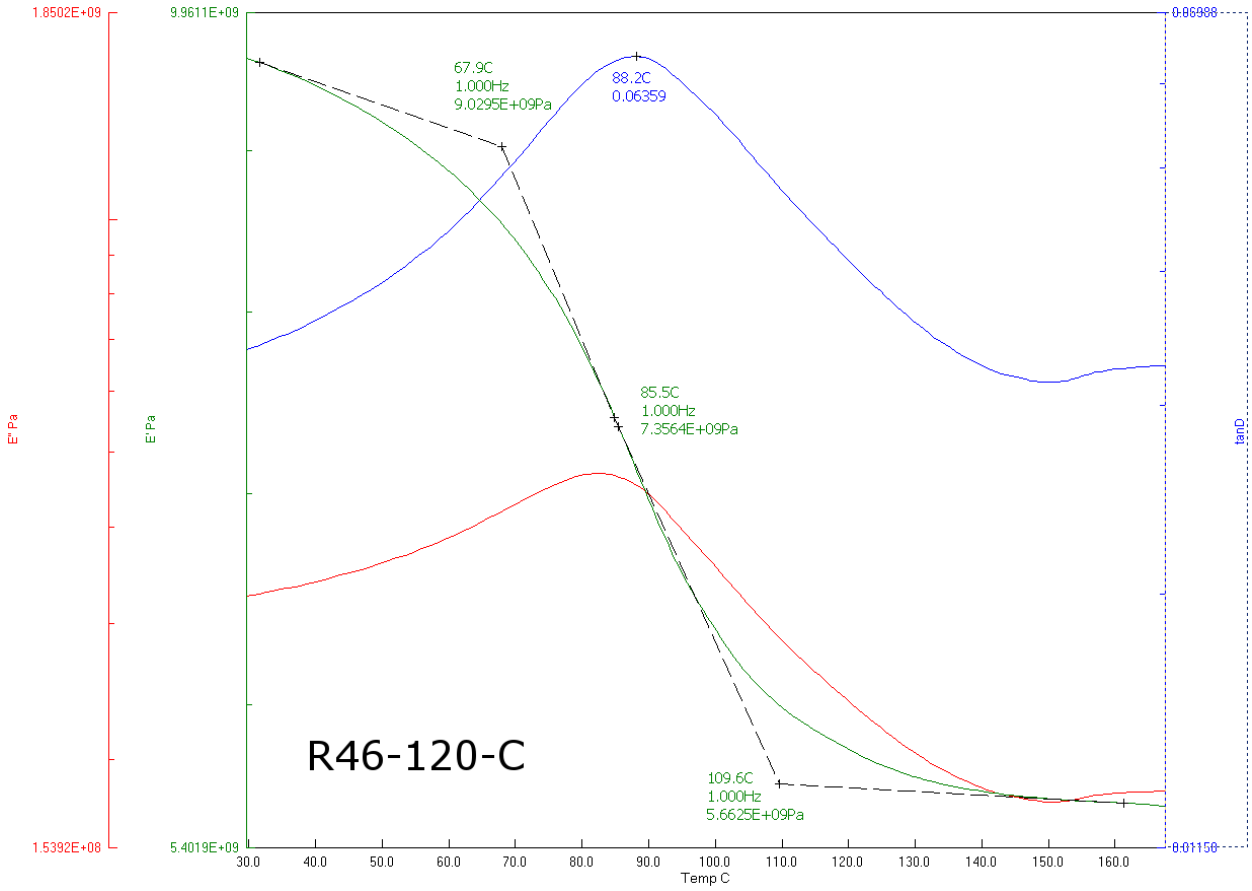

Figure 64: DMA output for R46-120-C

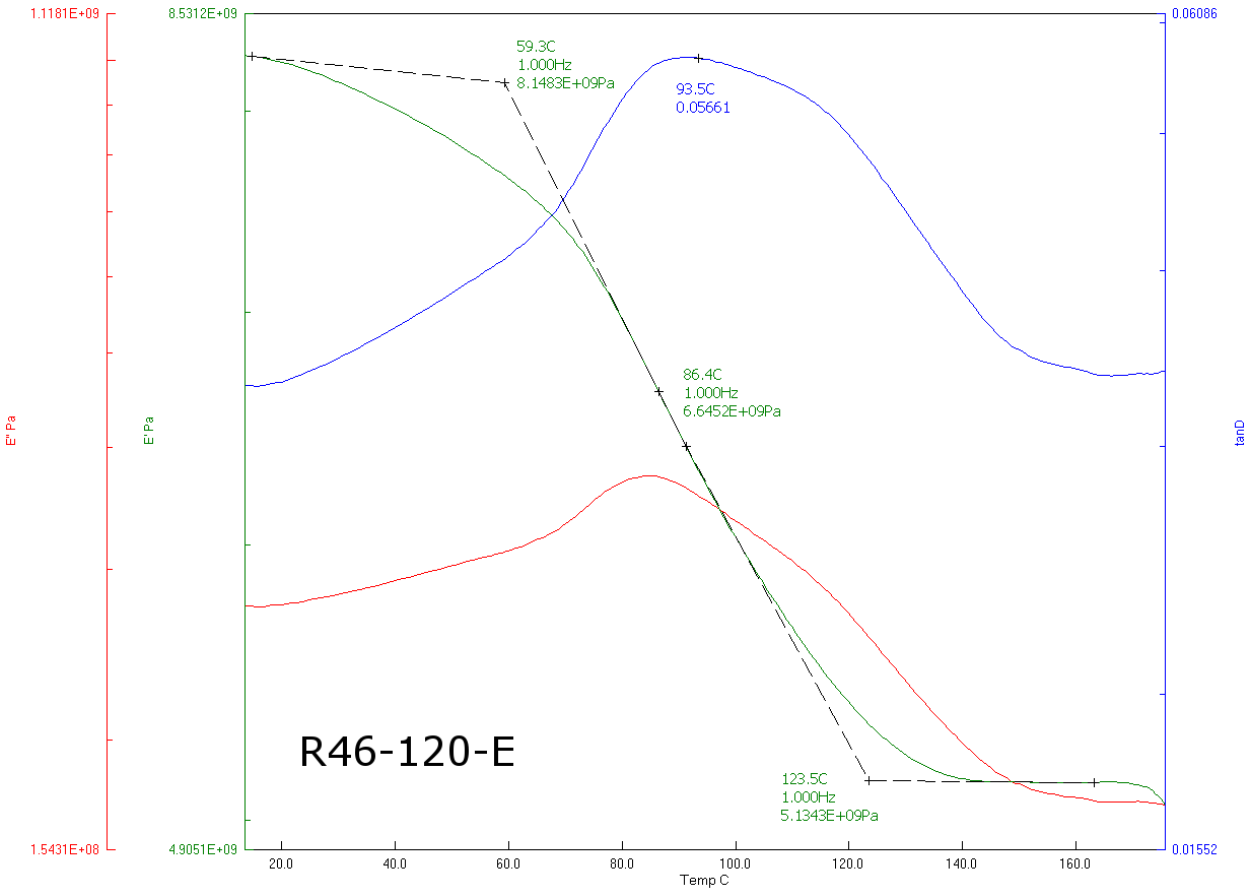

Figure 65: DMA output for R46-120-E

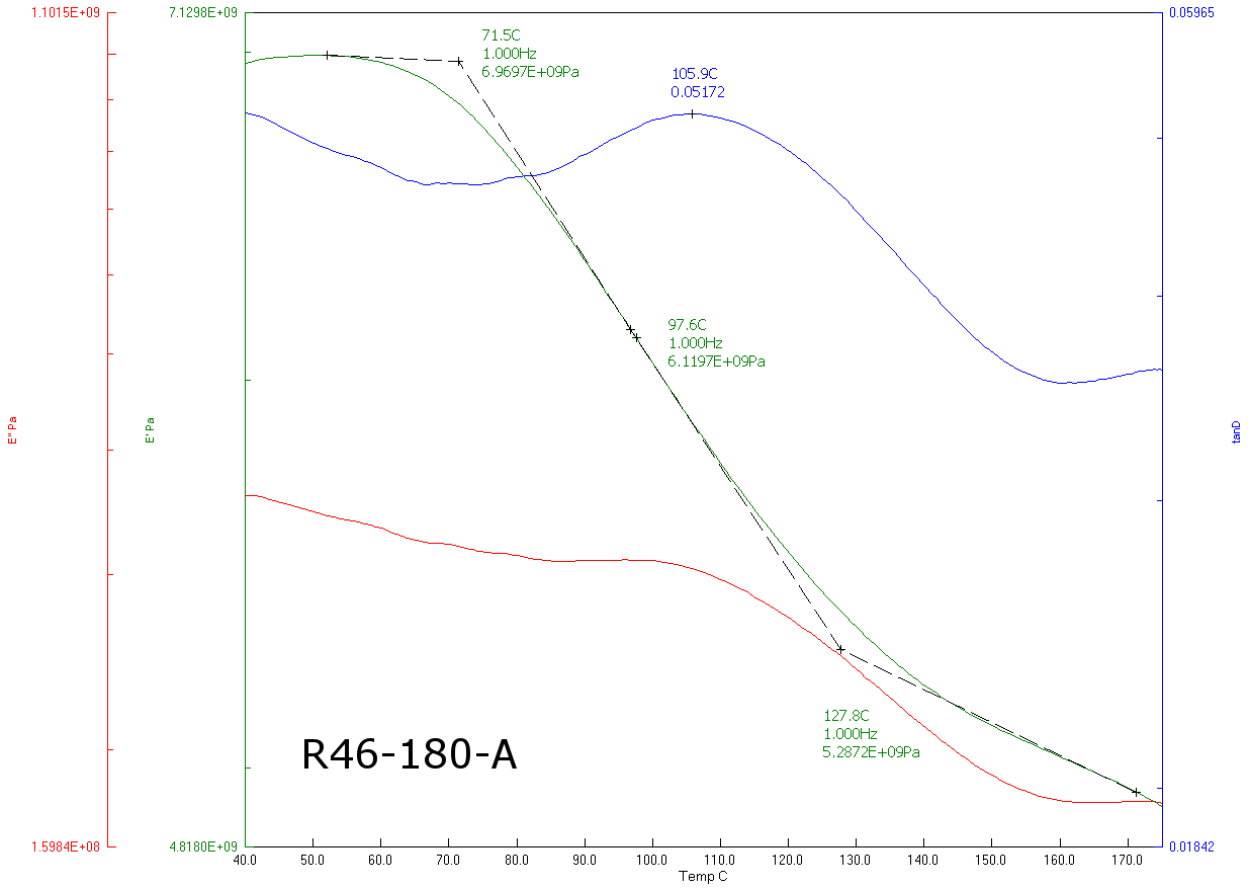

Figure 66: DMA output for R46-180-A

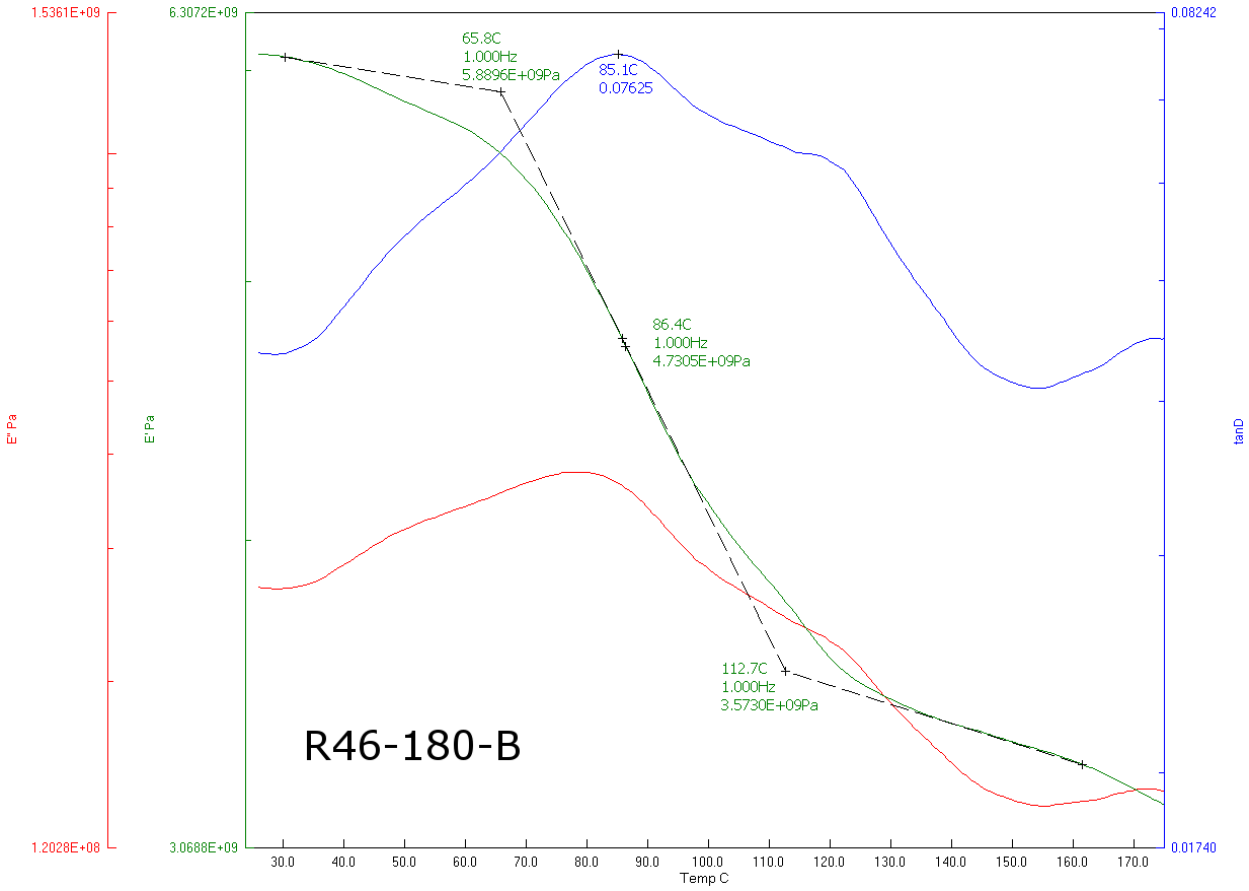

Figure 67: DMA output for R46-180-B

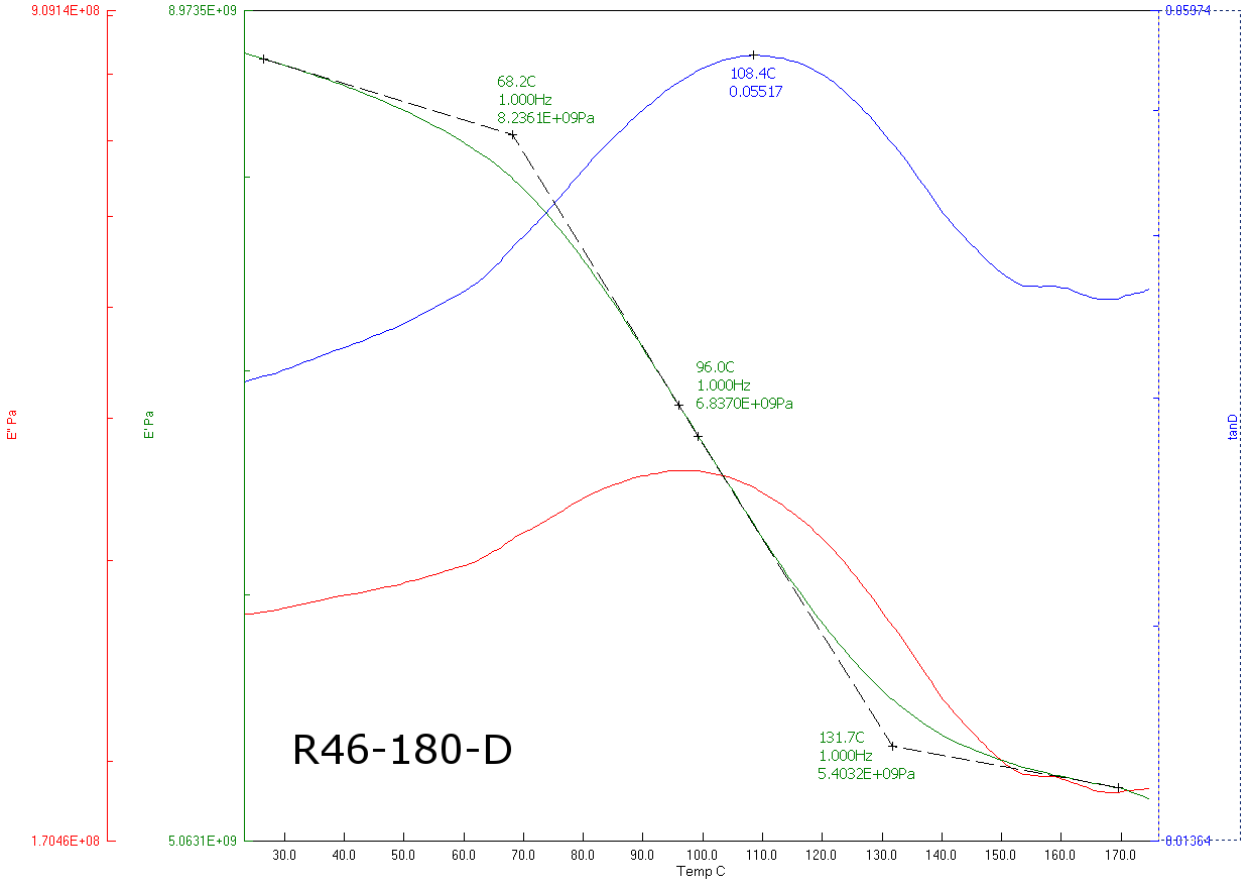

Figure 68: DMA output for R46-180-D

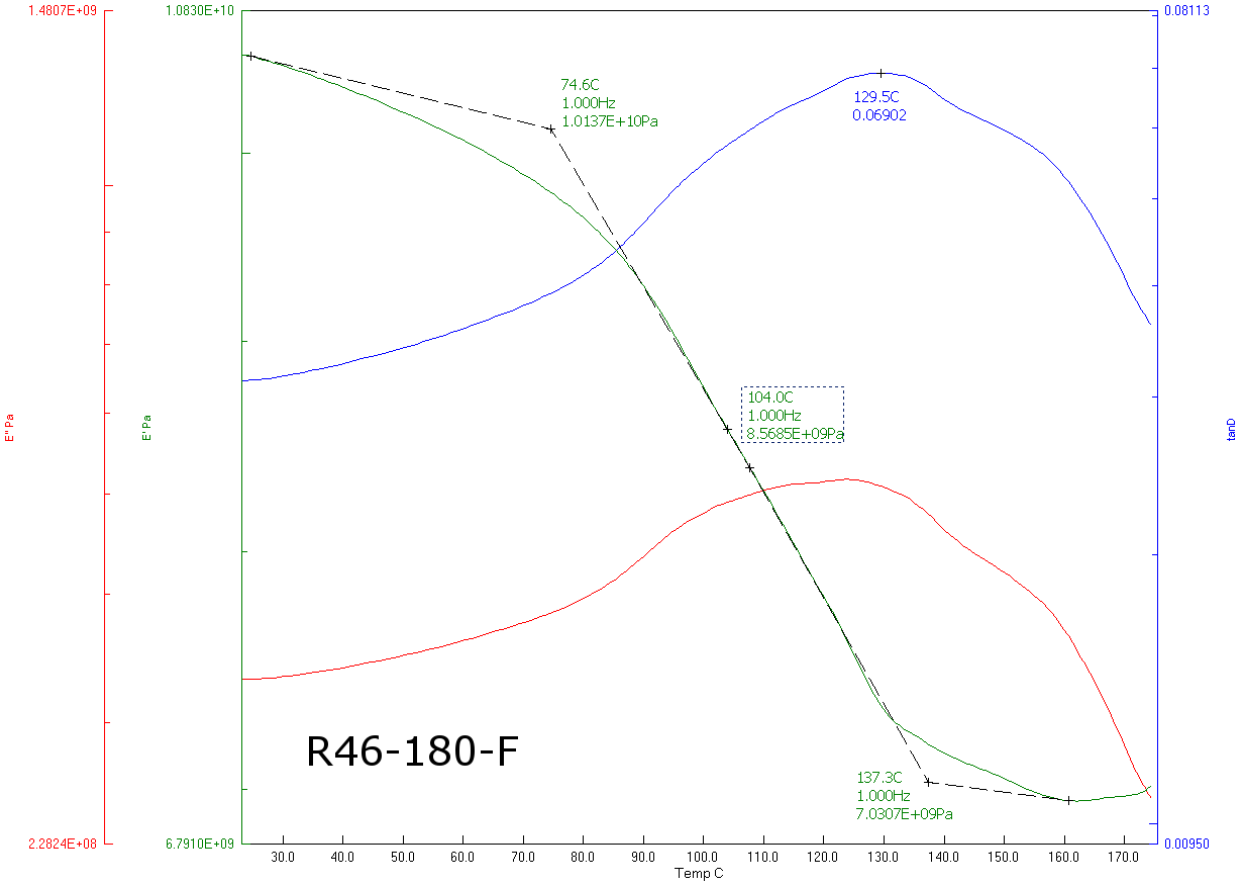

Figure 69: DMA output for R46-180-F

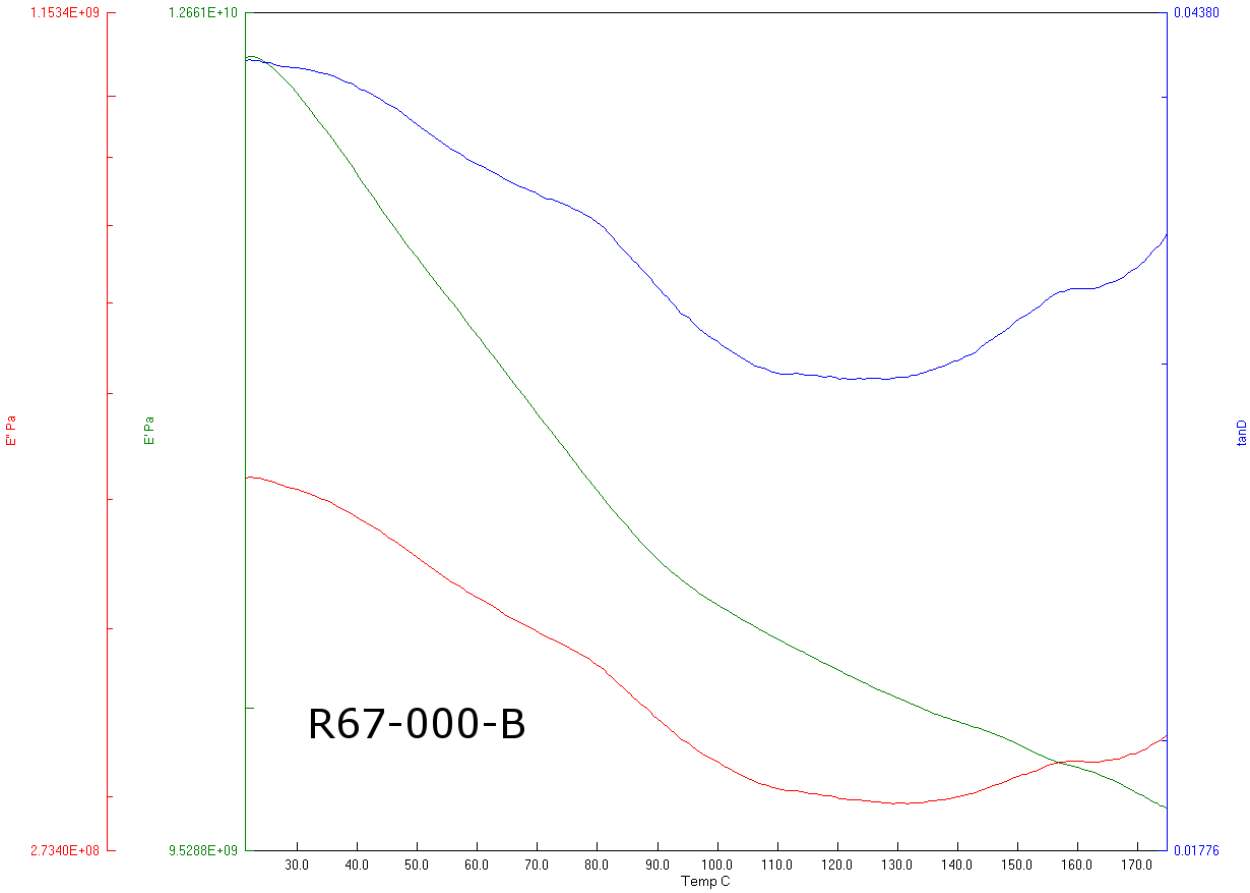

Figure 70: DMA output for R67-000-B

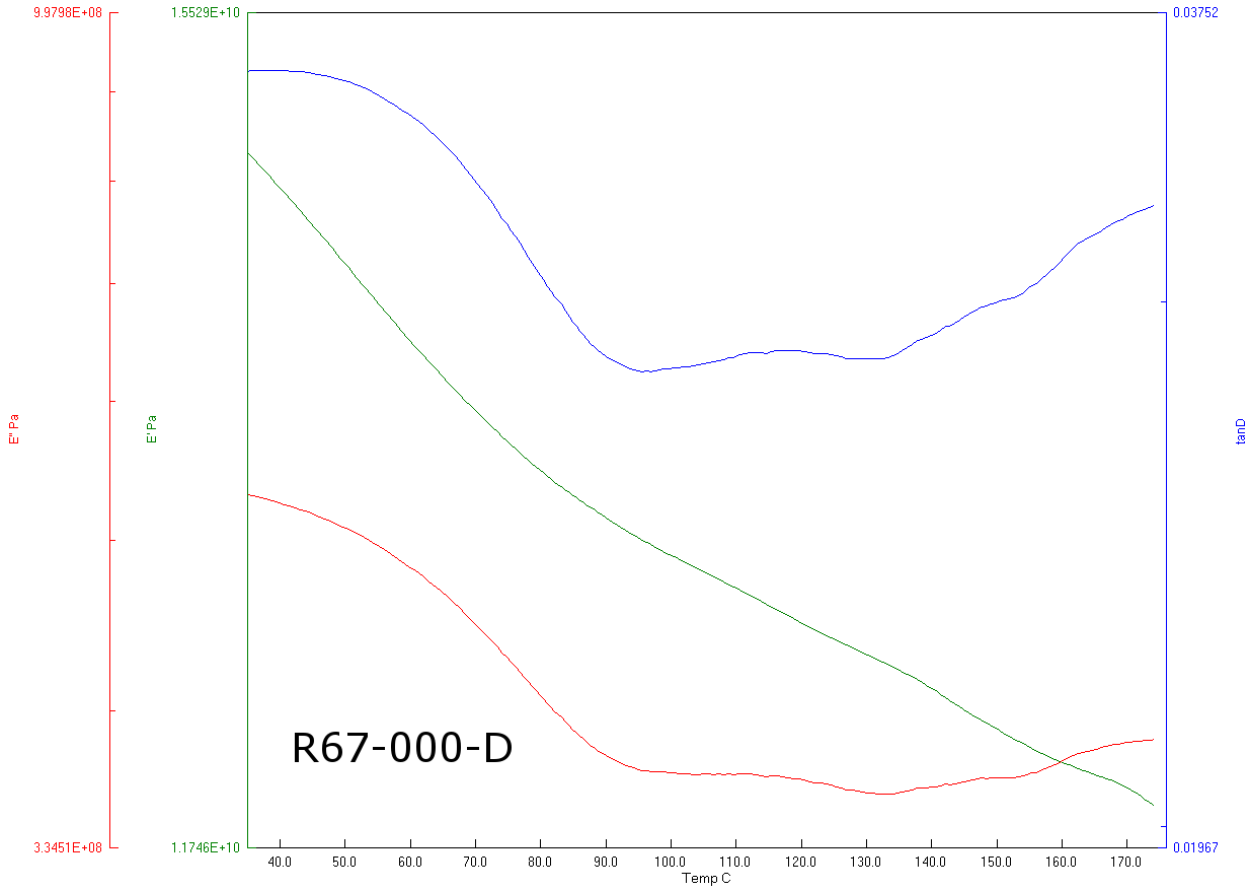

Figure 71: DMA output for R67-000-D

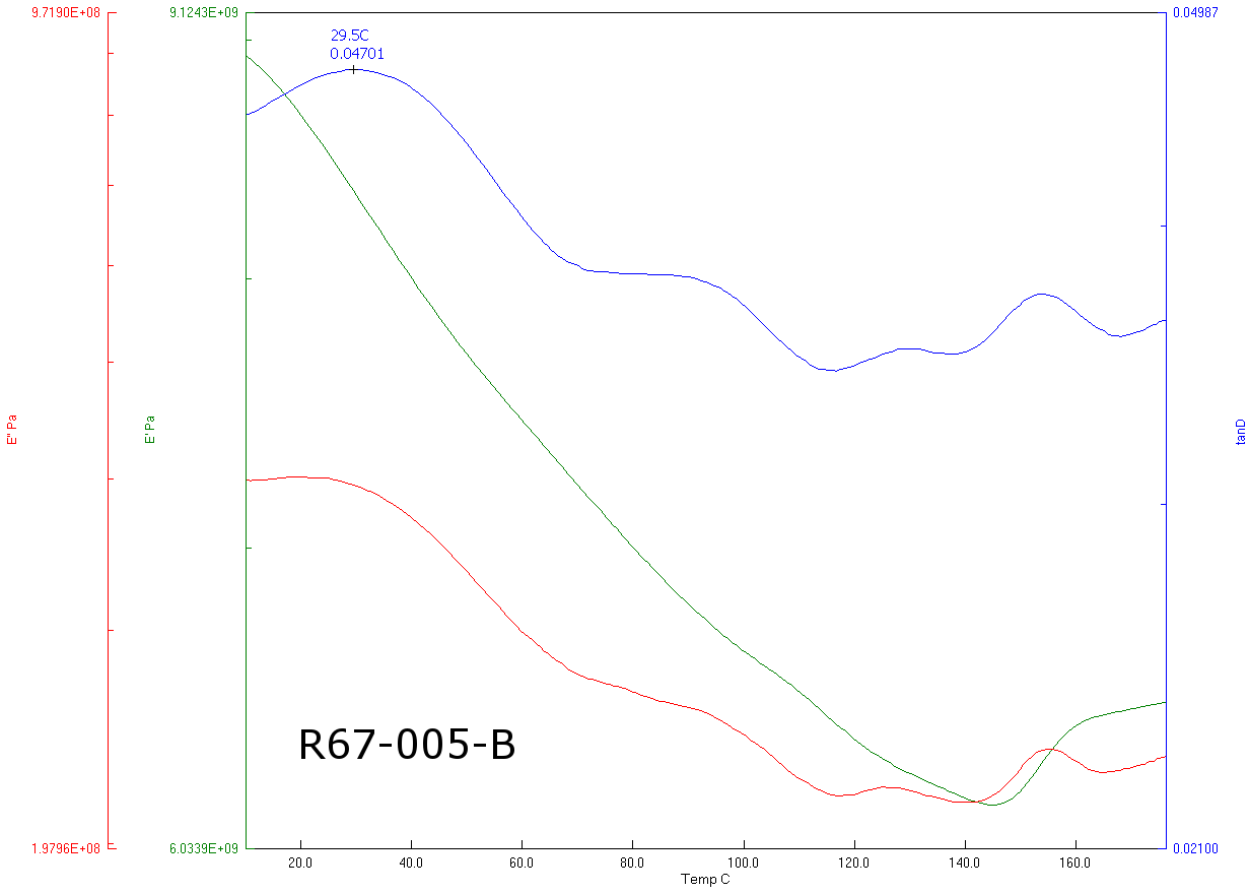

Figure 72: DMA output for R67-005-B

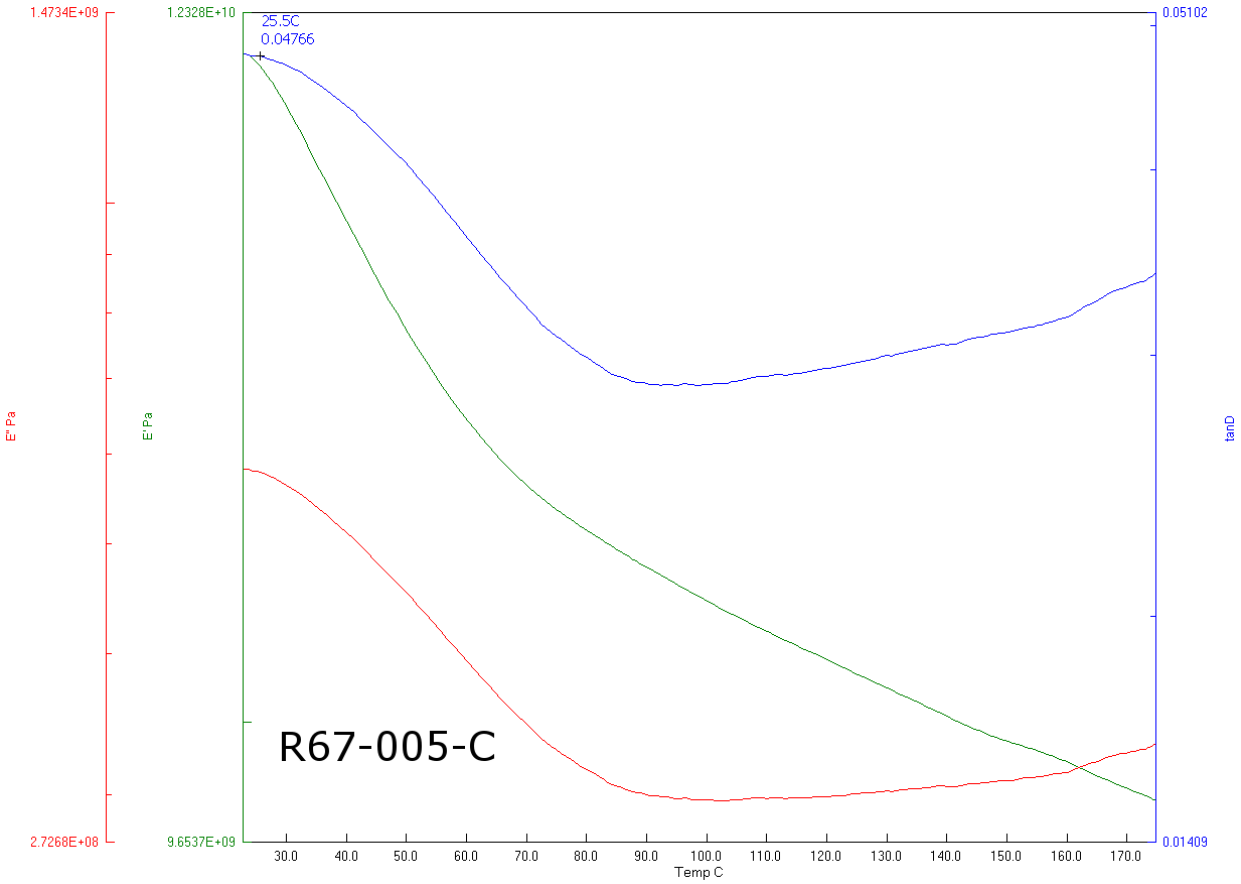

Figure 73: DMA output for R67-005-C

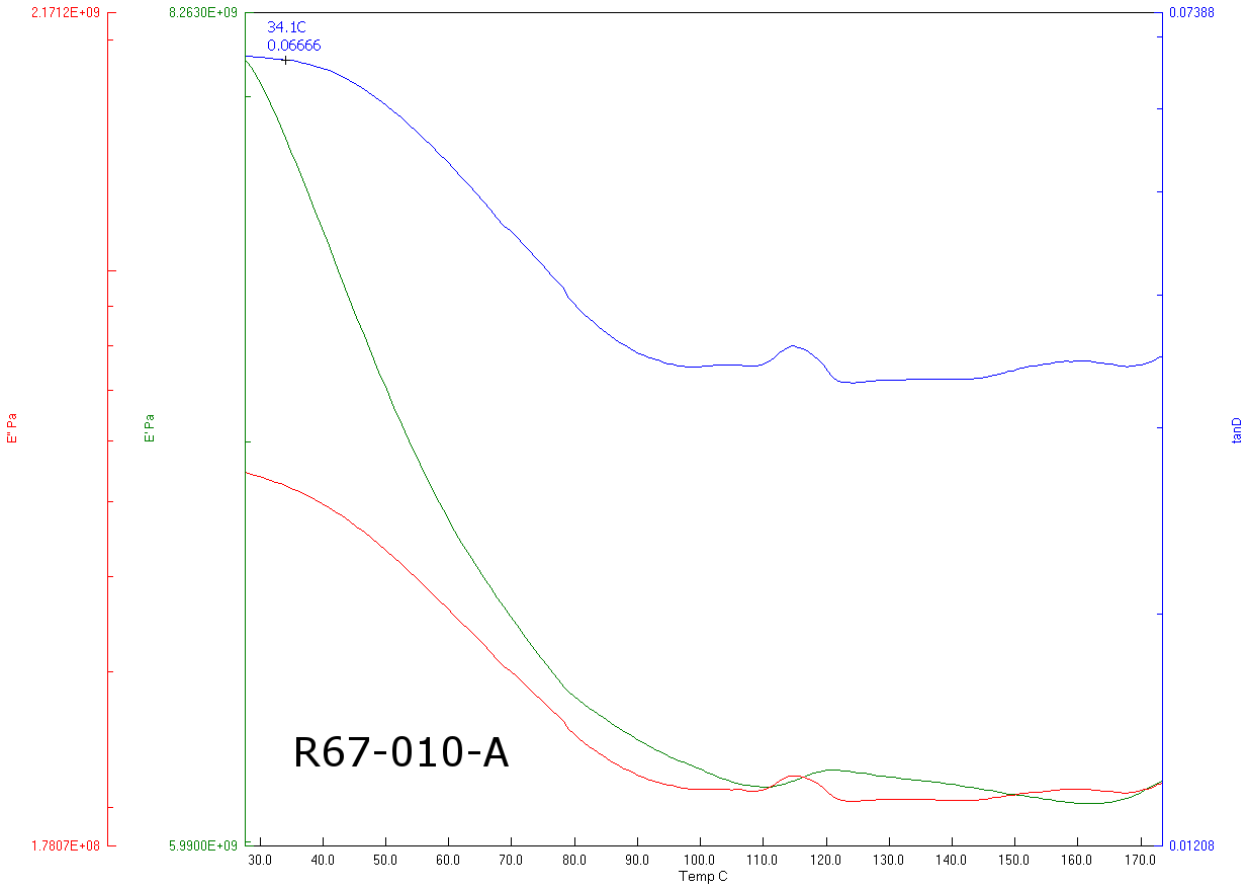

Figure 74: DMA output for R67-010-A

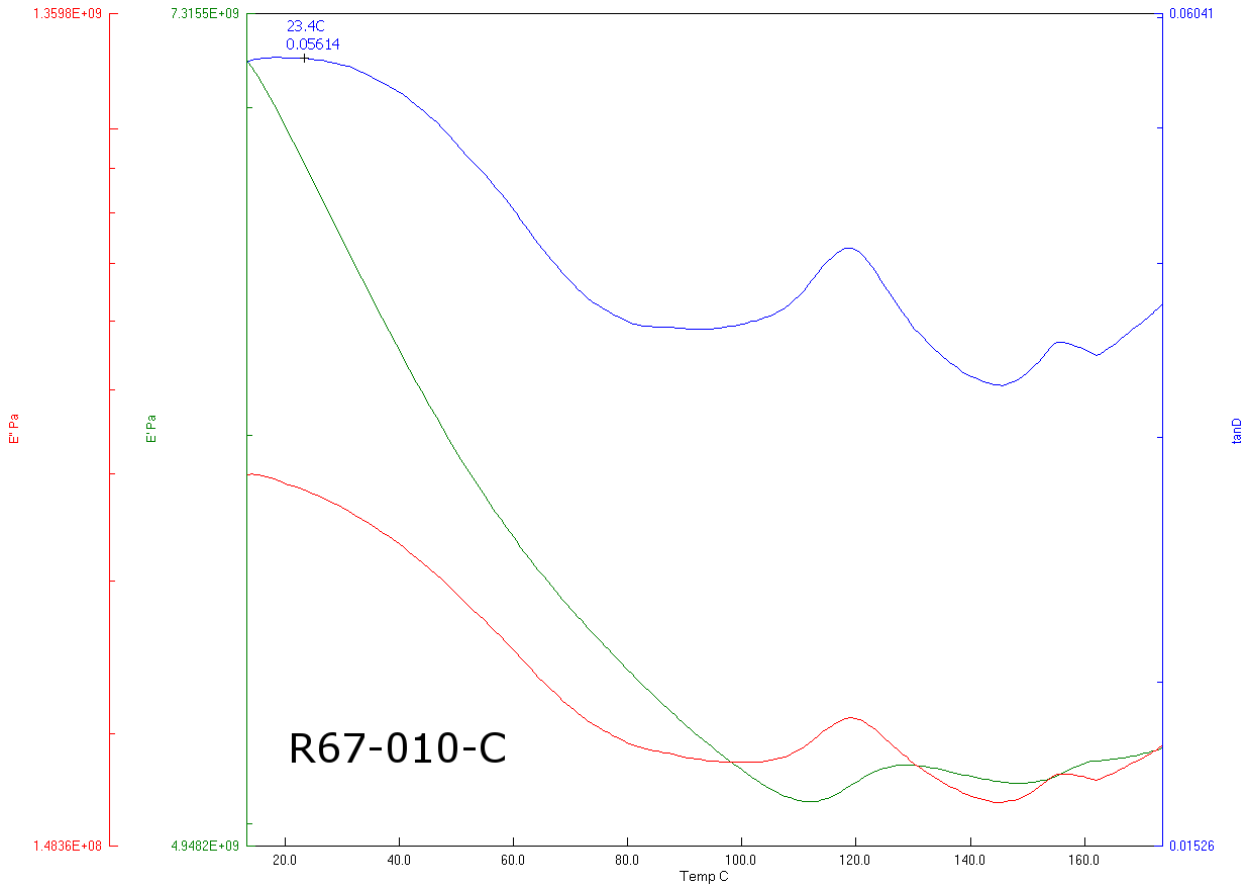

Figure 75: DMA output for R67-010-C

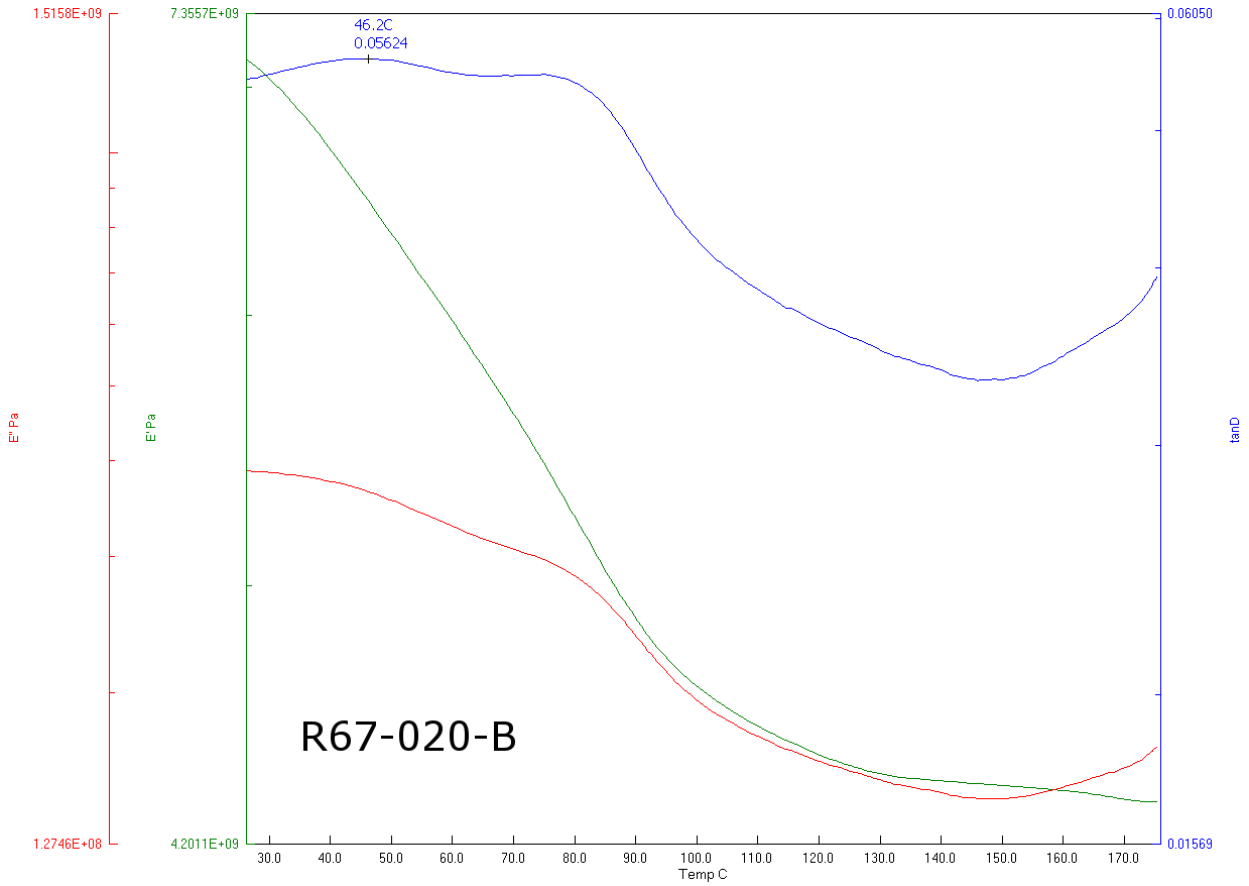

Figure 76: DMA output for R67-020-B

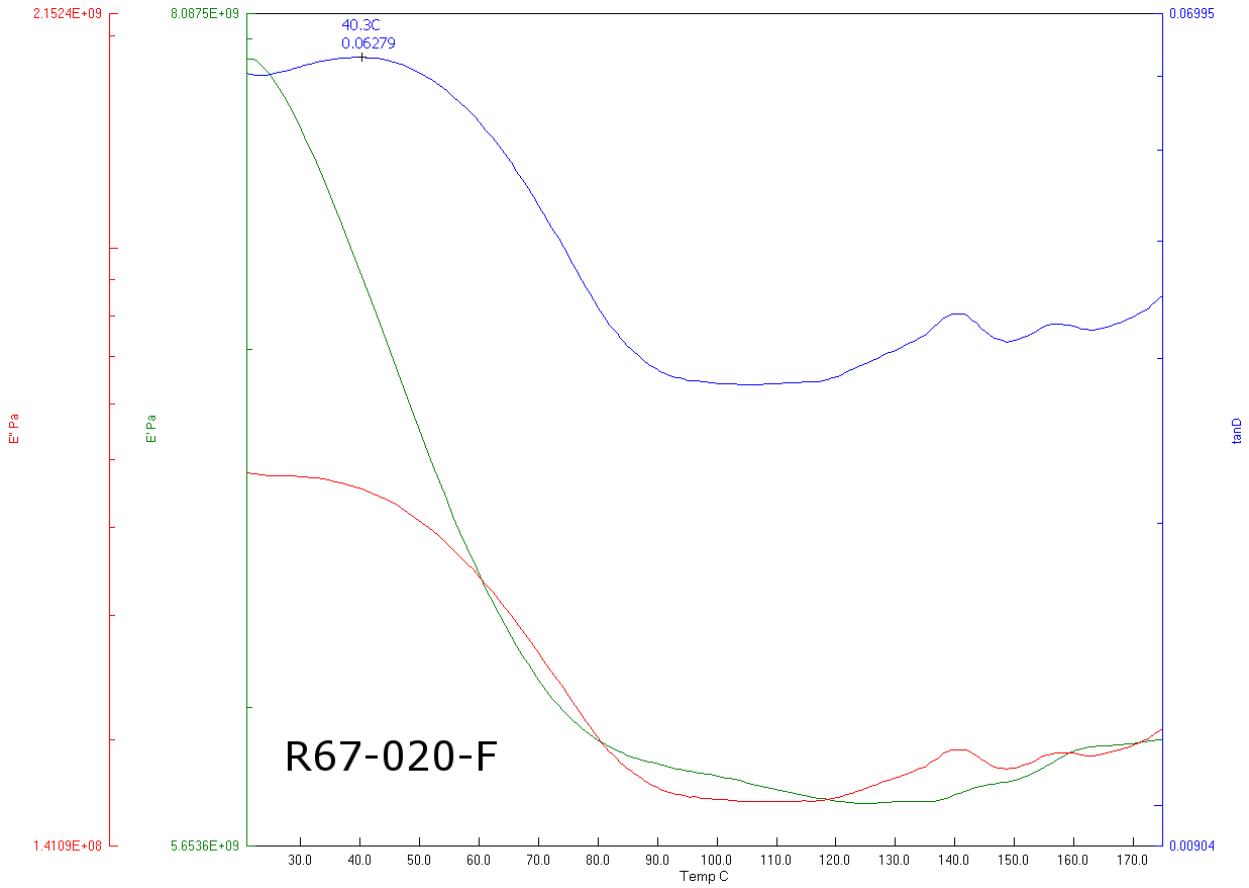

Figure 77: DMA output for R67-020-F

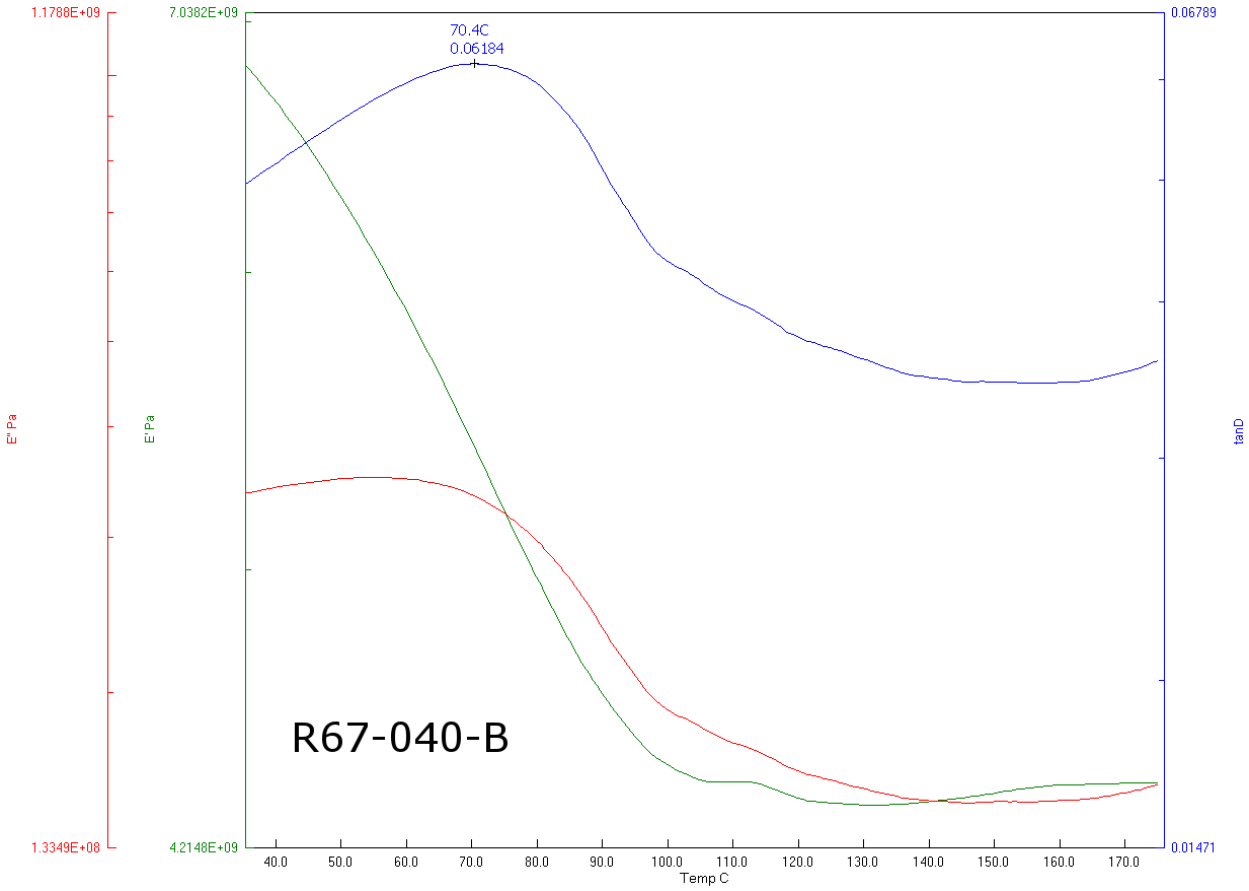

Figure 78: DMA output for R67-040-B

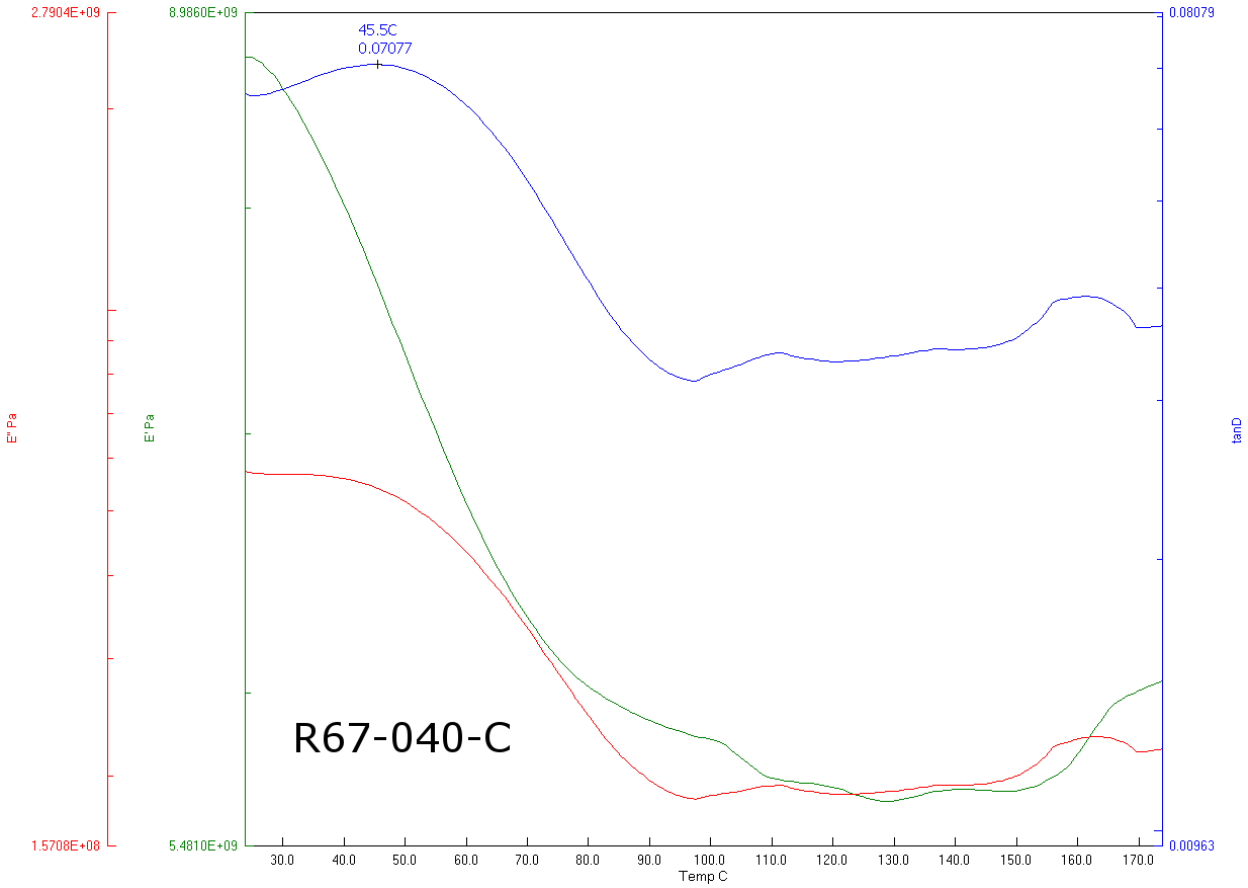

Figure 79: DMA output for R67-040-C

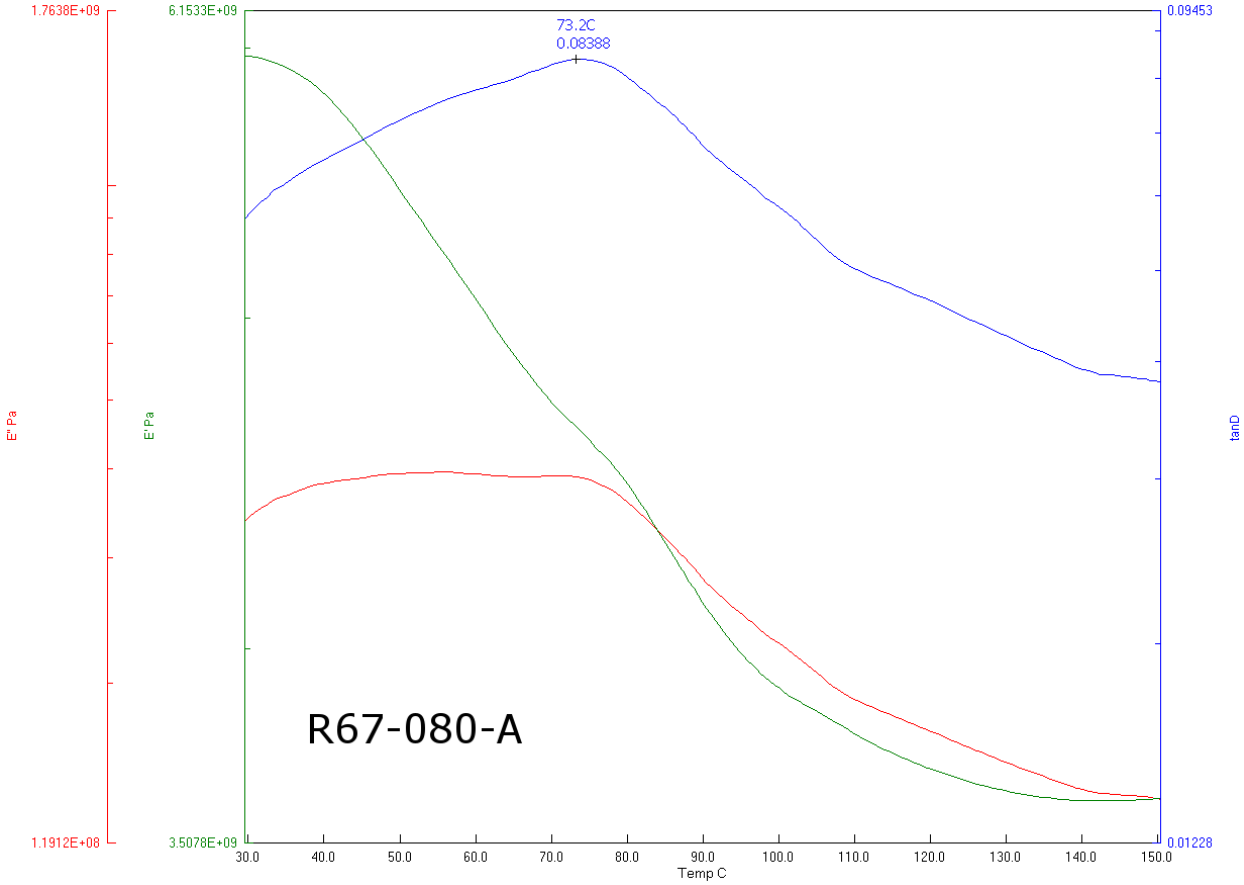

Figure 80: DMA output for R67-080-A

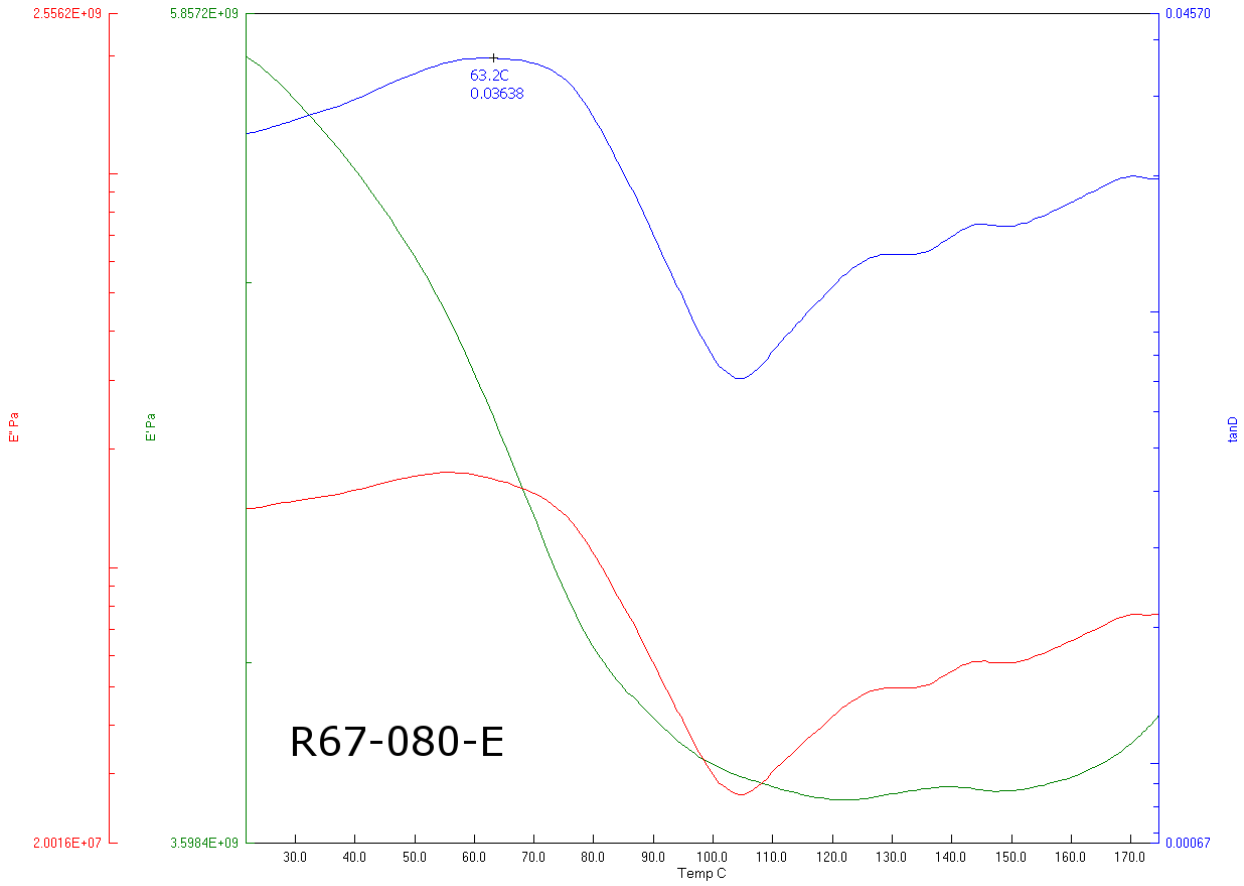

Figure 81: DMA output for R67-080-E

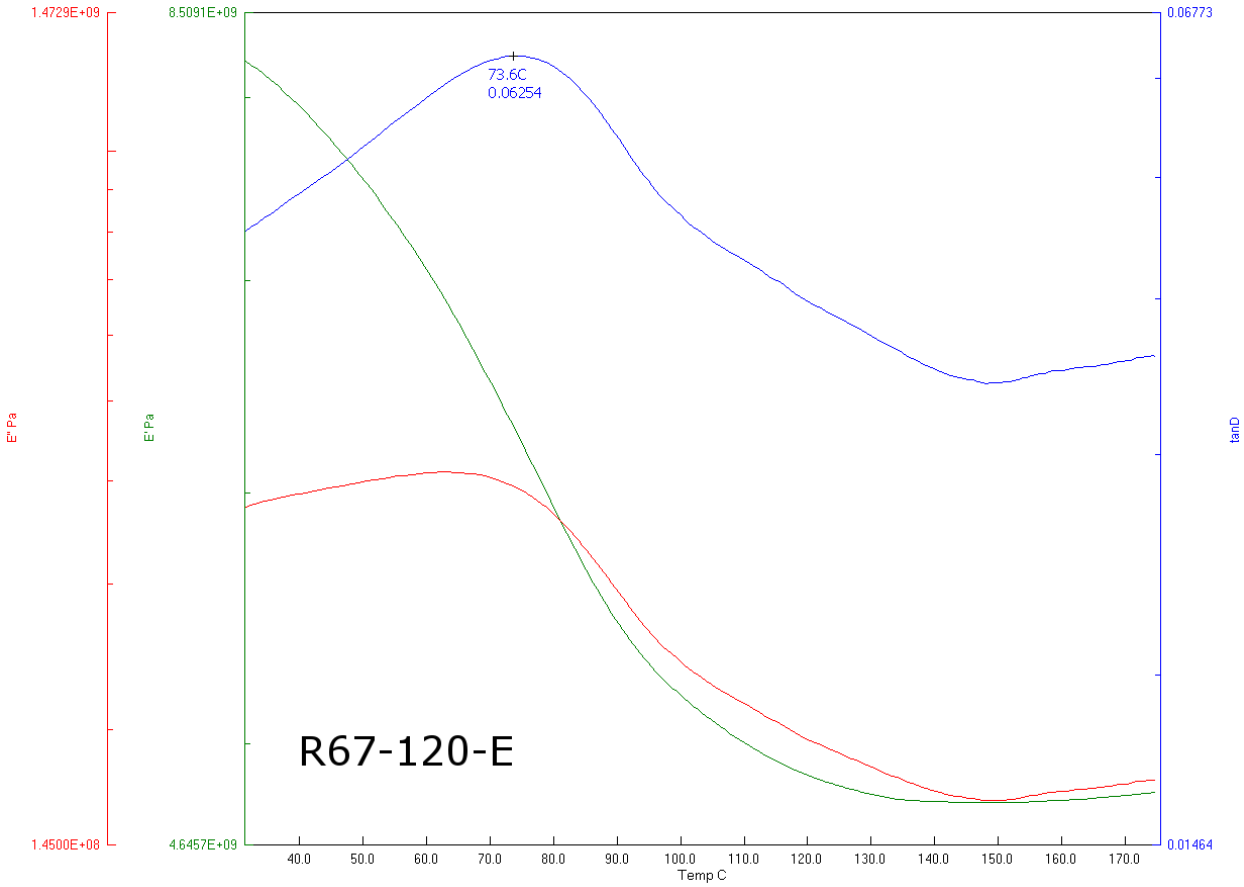

Figure 82: DMA output for R67-120-E

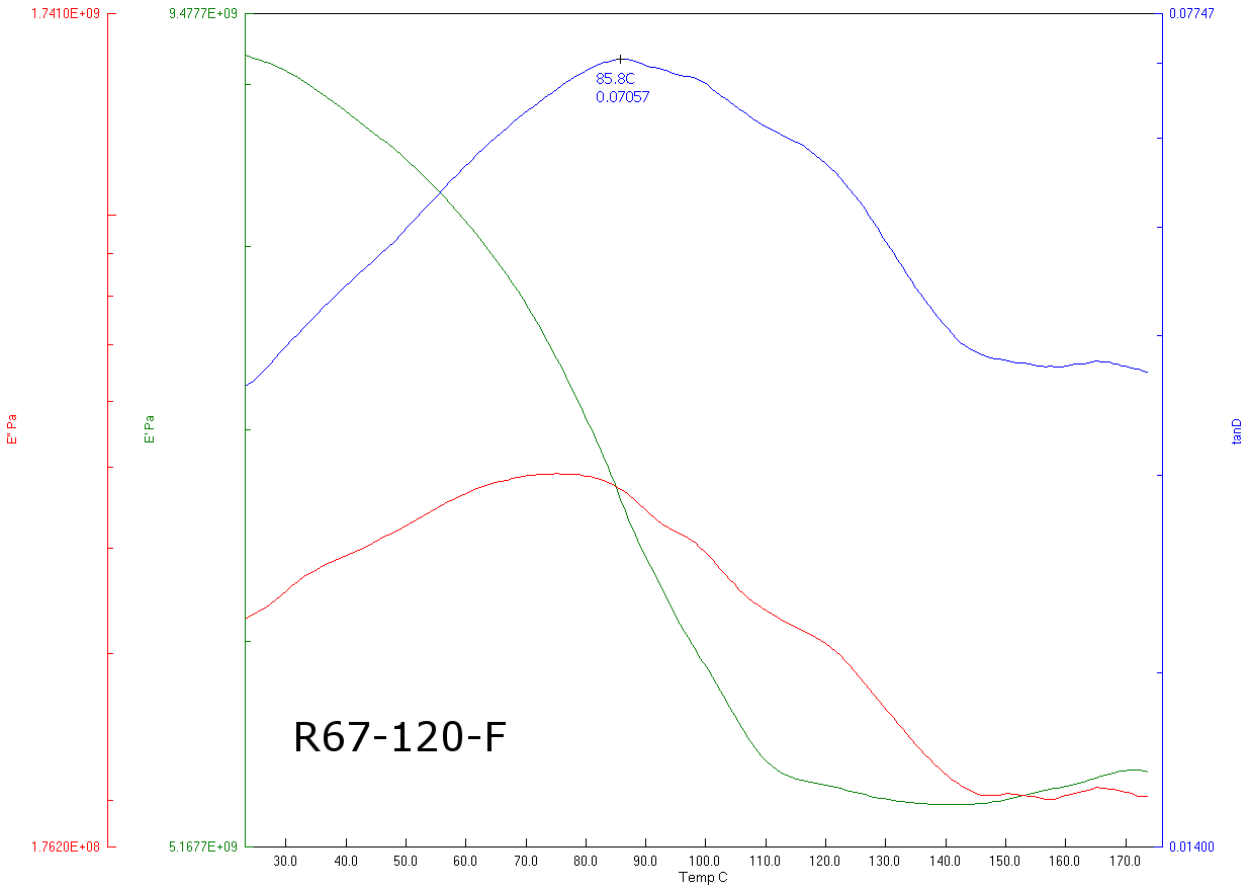

Figure 83: DMA output for R67-120-F

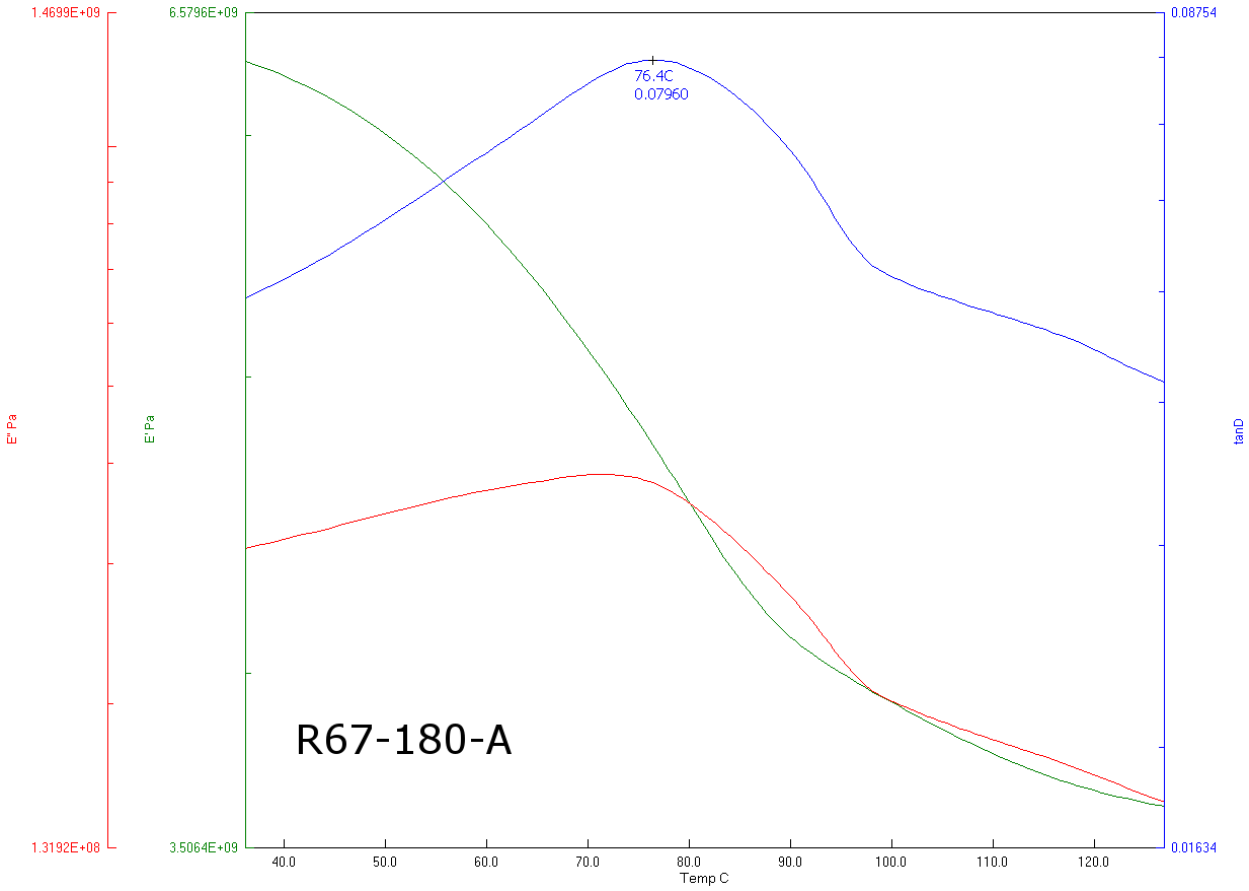

Figure 84: DMA output for R67-180-A

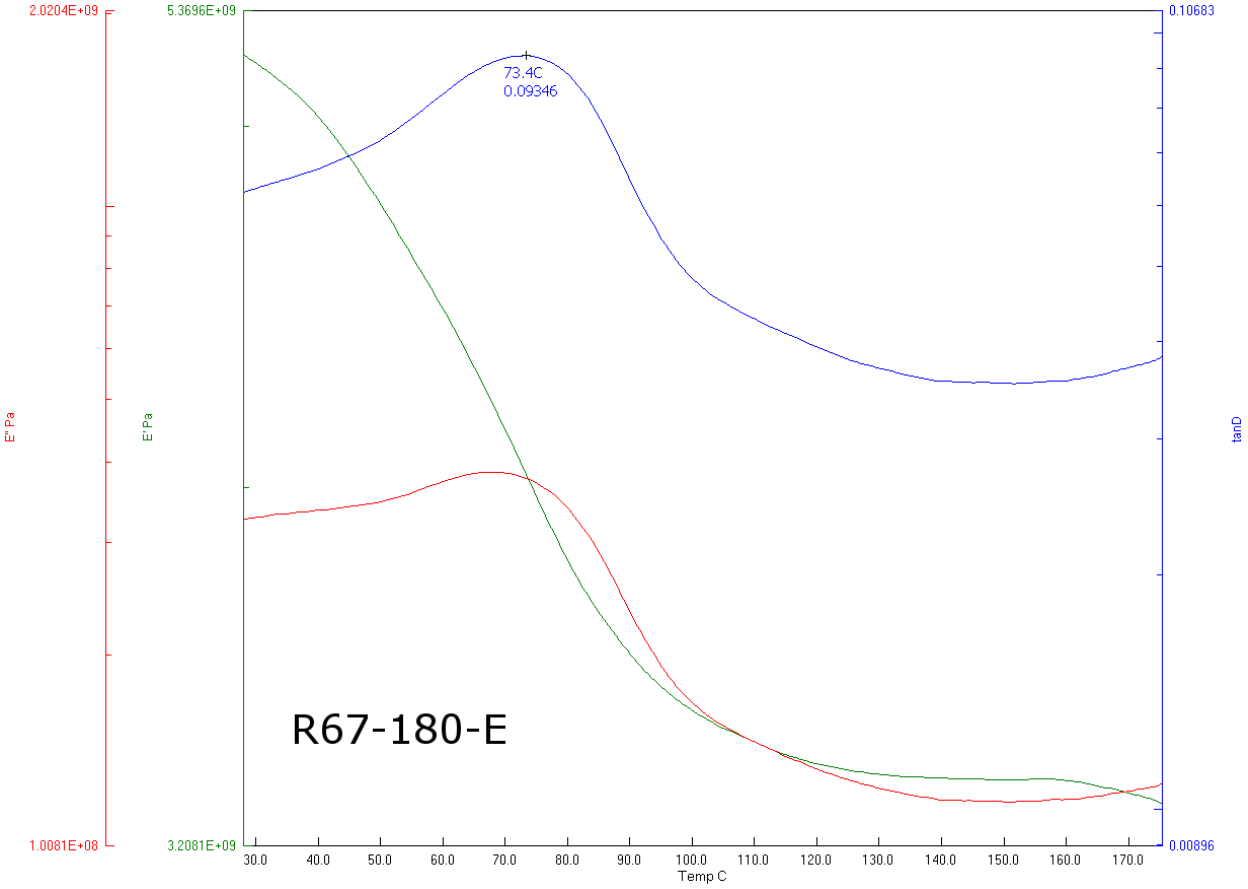

Figure 85: DMA output for R67-180-E

CHAPTER 4: CONCLUSION

CHAPTER 4: CONCLUSION

Maple beams and maple veneers were irradiated with a range of e-beam dosages and were studied with a variety of investigative techniques to determine how the radiation affected the wood. From the three-point bend tests done on the beams, two significant losses of strength were observed, first between 10 and 40 kGy, and then after 120 kGy. Since the radiation-curable adhesives studied require a dose of at least 40 kGy to cure, the first drop in MOR cannot be avoided, but the plateau between 40 and 120 kGy seems like a promising range of operation for curing the resin in a wood composite without further degrading the wood.

The trend of crosslinking at low dosages and chain scission at higher doses, which was observed in other studies, was confirmed in the DMA study through the storage modulus, T_g and E_a plots. The storage modulus plots seemed consistent through all doses except for the 40 kGy samples which showed slightly higher stiffness than the rest, and the 180 kGy samples which were noticeably lower than the others, indicating slight stiffening from 0 to 10 kGy and then weakening beyond 40 kGy, especially at 180 kGy. The 80 and 120 kGy samples had the highest Tg which indicates that at those doses a higher temperature was required to transition from the stiffer region to the more flexible region. The E_a plot shows that the 80 kGy samples required the most energy to induce that transition.

Infrared spectroscopy studies revealed the effect of the radiation in increases in carbonyl groups and decreases in hydroxyls, aromatic skeletal structures of lignin, and ring structures in cellulose, specifically the C_1-H bond where the glucosidic linkage occurs. While these trends were consistent across all dosages, the 180 kGy samples especially stood out in the NIR study, and the high dose grouping (80, 120 and 180 kGy) of samples stood out in the FTIR study.

From all of these studies, it seems that the most destructive radiation effects in wood begin at 80kGy. It is therefore recommended that a dose greater than 80 kGy not be used in wood composites, as this will enter a region of undesired degradation.

When the maple veneers were impregnated with resins, there were several signs that pointed to good interaction between the wood and the resin. The swelling tests showed consistent swelling of the wood similar to that of water, though not to the same degree. A theoretical FTIR spectrum was generated for each composite based on the IR spectra of the neat resins and raw wood. These were compared to the actual spectra taken from uncured composites, and the comparison revealed that some of the peaks associated with the resins were more intense than expected, and some of the peaks associated with wood, specifically the broad hydroxyl band from 3300-3000 cm-1, were shifted to one side on the spectrum. These results indicate interaction between the wood and the resins that could not have been calculated. Finally, the DMA of the uncured composites revealed significant suppression of T_g, which is a sign of plasticization, and associated with interaction between components. Therefore, these tests indicate that the composites will exhibit better interfacial bonding between the wood and the resin, resulting in a stronger more durable composite.

Study of the irradiation of the composites definitely showed that the cure of the resins was hindered by the presence of the wood. The glass transition temperature, which is a common tool for monitoring degree of cure, clearly indicates that the R67 composites did not reach complete cure until 120 kGy and the R46 composites didn't reach complete cure until 180 kGy. Both neat resins only required 40 kGy to attain those levels of cure.

Since both composites need more than 80 kGy to reach complete cure, it appears that the wood will suffer degradation in order to properly manufacture them. However, there are a few

considerations that may help the situation. The R46 composites were curing rapidly before hitting a plateau at about 20 kGy and did not see further cure until 120 kGy. The cure of the R67 composites was generally slower than that of the R46, but never plateaued. The irradiation of the composites was conducted at room temperature, and so it stands to reason that the completion of cure in both cases may be encouraged by an elevation of temperature that would lower the viscosity of the resins, allowing unreacted sites to access other available crosslinking sites. This elevated temperature need not be extreme, to where it approaches the energy, time, and cost problems incurred by thermal curing. Also, just as the presence of the wood hinders the cure of the resins, the presence of the resins may also hinder the degradation of the wood.

VITA

Tim Starr was born in North Providence, RI and lived there with his family – two parents and two older sisters – until he was 22 years old. During that time he gained interest in math from his mother, an appreciation for systematic order from both of his parents, and learned to love science of his own accord. He graduated 13th in his class from North Providence High School, and attended the University of Rhode Island to major in Chemical Engineering. While at URI Tim was fortunate enough to study under Dr. Otto Gregory who taught Thermodynamics and other chemical engineering courses, and eventually began working for him as an undergraduate research assistant in the area of thin films and surface sensors. This exposure to research eventually lead Tim to apply for graduate school, and after graduating from URI he decided to try his hand at southern living when he accepted a graduate research assistantship at the University of Tennessee. Tim was very fortunate to be offered this opportunity, and considers himself even more lucky to have been involved in research at the Forest Products Center. His research involved radiation curable adhesives for wood composites, which is a promising alternative to thermal curing, and a much more interesting topic than he could have ever hoped for. While working on his Master's degree, Tim fell in love with and married April Smelser, and they eventually had a beautiful daughter named Leila. After completing his degree, Tim and his family are looking forward to starting a new chapter of their lives, hopefully finding work in an area closer to their respective families.